UPPSALA
UNIVERSITET

Digital Comprehensive Summaries of Uppsala Dissertations from the Faculty of Science and Technology 2240

GENOME2QUNOME

Interfacing Molecules with Nanomaterials

PRITAM KUMAR PANDA

ACTA
UNIVERSITATIS
UPSALIENSIS
UPPSALA
2023

ISSN 1651-6214
ISBN 978-91-513-1716-8
URN urn:nbn:se:uu:diva-496330

Dissertation presented at Uppsala University to be publicly examined in Häggsalen, 10132, Ångström, Ångströmlaboratoriet Lägerhyddsvägen 1, 752 37 Uppsala, Friday, 31 March 2023 at 09:15 for the degree of Doctor of Philosophy. The examination will be conducted in English. Faculty examiner: Professor Helder Almeida Santos (University Medical Center Groningen (UMCG)).

Abstract

Panda, P. K. 2023. GENOME2QUNOME. Interfacing Molecules with Nanomaterials. *Digital Comprehensive Summaries of Uppsala Dissertations from the Faculty of Science and Technology* 2240. 100 pp. Uppsala: Acta Universitatis Upsaliensis. ISBN 978-91-513-1716-8.

The advent of technological furtherance in the biomedical sector and the renaissance of interdisciplinary science enable us to comprehend human lifestyle, and diseases at molecular and nanoscale levels. Lacking a shared theoretical foundation and terminological lexicon between various scientific domains might impede efforts to incorporate biological principles into nanoscience. In retrospect, it's possible to draw some instructive learnings from the fact that the development of contemporary nanoscience and biology was the consequence of the convergence of fields that had previously been kept separate.

In this Ph.D. thesis, I have given the catchy moniker ***"GENOME2QUNOME"*** (an acronym for "Genetic organization of multicellular organisms and their enzymatic reaction 2 Quantum nanostructured materials for energy scavenging applications"), encompassing a combinatorial approach using computational methodologies in biophysics and nano/materials science. Structure-property correlations, a unifying paradigm based on understanding how nanomaterials behave and what qualities they exhibit at the molecular and nanoscale levels, are now widely acknowledged and are critical in the incorporation of bioinspired materials into nanoscience. Therefore, a unified framework have been elucidated in this thesis for the study of nanoscale materials ranging from 0D to 3D that may be useful in combining various strategies that characterize this interdisciplinary approach.

This thesis is also a part of broader interdisciplinary research strategy aimed at depicting electronic transport in the nanoscale regime, elucidating interface mechanisms for contact electrification, and understanding the complex architectures of nanomaterials. The central hypothesis of this thesis is concentrated on the behavioral transition from the nanoscale regime to macromolecules, which is fascinating in real world scenario but theoretically challenging to bring it in reality or practice. To bridge this gap, I have made an attempt by integrating a wide range of computational methods, ranging from density functional theory (DFT) for systems with few atoms to classical dynamics dealing with billions of atoms.

Keywords: Electronic transport, Contact electrification, Nanomaterials, Zinc Oxide, Tetrapods, 2D-materials, Density functional theory, Non-equilibrium Green's function, Molecular docking, Molecular dynamics simulation

Pritam Kumar Panda, Department of Physics and Astronomy, Materials Theory, Box 516, Uppsala University, SE-751 20 Uppsala, Sweden.

ISSN 1651-6214
ISBN 978-91-513-1716-8
URN urn:nbn:se:uu:diva-496330 (http://urn.kb.se/resolve?urn=urn:nbn:se:uu:diva-496330)

Dedicated To

My Grandfather Late. Shri. Saranga Dhar Tripathy

&

my wife Suman and son Ayaan

A: Avoid negative sources, people, and bad habits
B: Believe in yourself
C: Consider thing from every angle
D: Don't give up and don't let bad things get you down
E: Enjoy life today, yesterday is gone and tomorrow will never come
F: Family and friends are hidden treasures
G: Give more than you plan to give each day
H: Hang onto your dream
I: Ignore the bad, think good
J: Just do it
K: Keep on trying no matter how hard it seems
L: Love yourself first
M: Make it happen
N: Never let them see you sweat
O: Open your eyes and see everything around you
P: Practice make perfect
Q: Quitters never win, and Winners never quit
R: Read, learn, and study about everything important in your life
S: Stop procrastinating
T: Take control of your own destiny
U: Understand yourself first so that you can better understand others
V: Visualise it
W: Want it more than anything
X: You already marked your spot in the world
Y: You are unique. No one can replace you
Z: Zero in on your target. GO FOR IT!

Cover Page

The cover page represents the overall schema of my thesis. I have given a catchy moniker "GENOME2QUNOME", an acronym for "Genetic organization of multicellular organisms and their enzymatic reaction 2 Quantum nanostructured materials for energy scavenging applications". The artwork represents a perspicacious approach comprised of both scientific domains i.e., biophysics/bioinformatics and nano/materials science. The artwork is by Alexandr Mitiuc/ Alamy Stock Photo, licensed for presentations and newsletters.

List of Papers

This thesis is based on the following papers, which are referred to in the text by their Roman numerals.

I. **2D g-C_3N_4 monolayer for amino acids sequencing**
X. Zhao*, P. K. Panda*, D. Singh, X. Yang, Y. K. Mishra, R. Ahuja
Appl. Surf. Sci., 146609 (2020)

II. **Van der Waals induced molecular recognition of canonical DNA nucleobases on a 2D GaS monolayer**
D. Singh, P. K. Panda, Y. K. Mishra, R. Ahuja
Phys. Chem. Chem. Phys., 22, 6706-6715 (2020)

III. **Two-Dimensional Bismuthene Nanosheets for Selective Detection of Toxic Gases**
P. Panigrahi, P. K. Panda, Y. Pal, H. Bae, H. Lee, R. Ahuja, T. Hussain
ACS Appl. Nano Mater. 5, 2984–2993 (2022).

IV. **Gas sensing by conjugate molecules in hybrid nanodevices**
O. Sher, H. Xu, T. Duan, P. K. Panda, T. Jarrosson, F. Serin, A. Grigoriev, W. Luo, R. Ahuja, H. M Jafri and K. Leifer
(Manuscript)

V. **Contact electrification through interfacial charge transfer: a mechanistic viewpoint on solid–liquid interfaces**
P. K. Panda, D. Singh, M. H. Köhler, D. D. de Vargas, Z. L. Wang, R. Ahuja,
Nanoscale Adv. 4**,** 884-893 (2022).

VI. **Molecular nanoinformatics approach assessing the biocompatibility of biogenic silver nanoparticles with channelized intrinsic steatosis and apoptosis**
P. K. Panda, P. Kumari, P. Patel, S. K. Samal, S. Mishra, M. M. Tambuwala, A. Dutt, K. Hilscherova, Y. K. Mishra, R. S. Varma
Green Chem. **24**, 1190-1210 (2022).

VII. **Enhancement of antiviral drug efficacy through multimodal mechanism of Au nanoparticles decorated ZnO tetrapods**
R. K. Suryawanshi, C.D. Patil, L. Koujah, P. K. Panda, S.K. Singh, A. Agelidis, I. Volety, L.Siebert, R. Adelung, R.Ahuja, Y.K. Mishra, D. Shukla
(Manuscript)

**Equal contribution*

Papers not included in the thesis but are correlated to the aforementioned papers which are included in the thesis.

I. **Structure-based drug designing and immunoinformatics approach for SARS-CoV-2**
P. K. Panda, M. N. Arul, P. Patel, S. K. Verma, W. Luo, H.-G. Rubahn, Y. K. Mishra, M. Suar, R. Ahuja
Science Advances., eabb8097 (2020)

II. **Degradation of Alzheimer's amyloid-β by a catalytically inactive insulin-degrading enzyme**
B. R. Sahoo*, P. K. Panda*, W. Liang, W.-J. Tang, R. Ahuja, A. Ramamoorthy
J. Mol. Biol. **433**, 166993 (2021)

III. **Carbon-Phosphide Monolayer with High Carrier Mobility and Perceptible I-V Response for Superior Gas Sensing**
D. Singh, V. Shukla, P. K. Panda, Y. K. Mishra, H.-G. Rubahn, R. Ahuja
New J. Chem., 44, 3777-3785 (2020)

IV. **Analysis of molecular ligand functionalization process in nano-molecular electronic devices containing densely packed nano particle functionalization shells**
O. Sher, Y. Han, H. Xu, H. Li, T. Daun, S. Kumar, A. Grigoriev, P. K. Panda, A. Orthaber, F. Serein-Spirau, T. Jarrosson, S.H. M Jafri, K. Leifer
Nanotechnology. 33, 255706 (2022)

V. **Putative targeting by BX795 causes decrease in protein kinase C protein levels and inhibition of HSV1 infection**
R. K. Suryawanshi, C. D. Patil, D. Wu, P. K. Panda, S.K. Singh, I. Volety, R. Ahuja, Y.K. Mishra, D. Shukla
Antiviral Research, 208,105454, (2022)

VI. **Crystallinity modulation originates ferroelectricity like nature in piezoelectric selenium.**
N. R. Alluri, N. P. M. J. Raj, G. Khandelwal, P. K. Panda, A. Banerjee, Y. K. Mishra, R. Ahuja, S.-J. Kim
Nano Energy, 107008 (2022).

VII. **Investigation of Nd3+ incorporation in Ce-Rhabdophane: Insight from structural flexibility and occupation mechanism**.
H. Liu, X. Zhao, Y. Teng, Y. Li, X. Zheng, S. Wang, L. Wu, P. K. Panda, R. Ahuja
J. Am. Ceram. Soc. (2022).

VIII. **One dimensional Au-ZnO hybrid nanostructures based CO2 detection: Growth mechanism and role of the seed layer on sensing performance.**
M. González-Garnica, A. Galdámez-Martínez, F. Malagón, C. D. Ramos, G. Santana, R. Abolhassani, P. K. Panda, A. Kaushik, Y. K. Mishra, T. V. K. Karthik
Sensors Actuators B Chem. **337**, 129765 (2021).

IX. **Rational Design of 2D h-BAs Monolayer as Advanced Sulfur Host for High Energy Density Li-S Batteries**.
N. Khossossi, P. K. Panda, D. Singh, V. Shukla, Y. K. Mishra, I. Essaoudi, A. Ainane, R. Ahuja
ACS Appl. Energy Mater. (2020), doi:10.1021/acsaem.0c00492.

X. **Hydrogen storage characteristics of Li and Na decorated 2D Boron Phosphide.**
N. Khossossi, Y. Benhouria, S. R. Naqvi, P. K. Panda, I. Essaoudi, A. Ainane, R. Ahuja
Sustain. Energy Fuels (2020).

XI. **Molecules versus Nanoparticles: Identifying a Reactive Molecular Intermediate in the Synthesis of Ternary Coinage Metal Chalcogenides.** S. Gahlot, E. Jeanneau, D. Singh, P. K. Panda, Y. K. Mishra, R. Ahuja, G. Ledoux, S. Mishra
Inorg. Chem. (2020).

XII. **Impact of edge structures on interfacial interactions and efficient visible-light photocatalytic activity of metal–semiconductor hybrid 2D materials.**
D. Singh, P. K. Panda, N. Khossossi, Y. K. Mishra, A. Ainane, R. Ahuja
Catal. Sci. Technol. **10**, 3279–3289 (2020).

XIII. **Strain-Engineered Metal-Free h-B2O Monolayer as a Mechanocatalyst for Photocatalysis and Improved Hydrogen Evolution Reaction .**
Zhao, X. Yang, D. Singh, P. K. Panda, W. Luo, Y. Li, R. Ahuja, *J. Phys. Chem. C* (2020), doi:10.1021/acs.jpcc.0c00834.

XIV. **Necklace-like Nitrogen-Doped Tubular Carbon 3D Frameworks for Electrochemical Energy Storage.**
R. Yuksel, O. Buyukcakir, P. K. Panda, S. H. Lee, Y. Jiang, D. Singh, S. Hansen, R. Adelung, Y. K. Mishra, R. Ahuja, R. S. Ruoff
Adv. Funct. Mater. (2020)

XV. **Bio-acceptable 0D and 1D ZnO nanostructures for cancer diagnostics and treatment.**
B. Ortiz-Casas, A. Galdámez-Martínez, J. Gutiérrez-Flores, A. B. Ibañez, P. K. Panda, G. Santana, H. A. de la Vega, M. Suar, C. G. Rodelo, A. Kaushik,
Mater. Today. (2021)

XVI. **Progress in supercapacitors: roles of two dimensional nanotubular materials.**
P. K. Panda, A. Grigoriev, Y. K. Mishra, R. Ahuja
Nanoscale Adv. **2**, 70–108 (2020).

XVII. **Core-shell nanostructures: perspectives towards drug delivery applications.**
R. Kumar, K. Mondal, P. K. Panda, A. Kaushik, R. Abolhassani, R. Ahuja, H.-G. Rubahn, Y. K. Mishra
J. Mater. Chem. B. **8** (2020)

XVIII. **Data-Driven Machine Learning Approaches for Advanced Battery Modeling.**
P. K. Panda, N. Khossossi, R. Ahuja
AIP Publ., 4–1–4–18 (2021).

XIX. **Background of Computational and Experimental Investigations for Next-Generation Efficient Battery Materials.**
P. K. Panda, D. Singh, R. Ahuja
AIP Publ., 1–1–1–34 (2021).

XX. **Computational and Experimental Techniques to Envisage Battery Materials.**
P. K. Panda, R. Ahuja
AIP Publ., 2–1–2–22 (2021).

XXI. **Organic Batteries: the Route Toward Sustainable Electrical Energy Storage Technologies**
P. K. Panda, D. Singh, R. Ahuja
AIP Publ., 3–1–3–22 (2021).

XXII. **Future Outlook and Direction of Next-Generation Battery Materials**.
P. K. Panda, R. Ahuja
AIP Publ., 11–1–11–22 (2021).

XXIII. **Antibodies Against Phosphorylcholine Among 60-Year-Olds: Clinical Role and Simulated Interactions.**
S. K. Samal, P. K. Panda, M. Vikström, K. Leander, U. de Faire, R. Ahuja, J. Frostegård
Front. Cardiovasc. Med. **9**, 618 (2022).

XXIV. **Effects of Atorvastatin on T-Cell Activation and Apoptosis in Systemic Lupus Erythematosus and Novel Simulated Interactions With C-Reactive Protein and Interleukin 6**
J. Sun, P. K. Panda, S. Kumar Samal, R. Ahuja, S. Ajeganova, I. Hafström, A. Liu, J. Frostegård
ACR Open Rheumatol. (2021).

XXV. **Network analysis reveals that the tumor suppressor lncRNA GAS5 acts as a double-edged sword in response to DNA damage in gastric cancer.**
S. Gupta, P .K. Panda, W. Luo, R. F. Hasimoto, R. Ahuja
Sci Rep 12, 18312 (2022).

XXVI. **Dynamical modeling of miR-34a, miR-449a, and miR-16 reveals numerous DDR signaling pathways regulating senescence, autophagy, and apoptosis in HeLa cells.**
S. Gupta, P. K. Panda, R. F. Hashimoto, S. K. Samal, S. Mishra, S. K. Verma, Y. K. Mishra, R. Ahuja
Sci. Rep. **12**, 1–13 (2022).

XXVII. **Investigation of the Factors That Dictate the Preferred Orientation of Lexitropsins in the Minor Groove of DNA.**
H.Y. Alniss, I.I. Witzel, M.H Semreen, P.K. Panda, Y.K.Mishra, R. Ahuja, J.A Parkinson
J. Med. Chem. **62**, 10423–10440 (2019).

XXVIII. **Nanoparticle–biological interactions: the renaissance of bionomics in the myriad nanomedical technologies.**
P. K. Panda, S. K. Verma, M. Suar
Nanomedicine (2021).

XXIX. **Intrinsic atomic interaction at molecular proximal vicinity infer cellular biocompatibility of antibacterial nanopepper.**
E. Jha, P. K. Panda, P. Patel, P. Kumari, S. Mohanty, S. K. S. Parashar, R. Ahuja, S. K. Verma, M. Suar
Nanomedicine. **16**, 307–322 (2021).

XXX. **Determining factors for the nano-biocompatibility of cobalt oxide nanoparticles: Proximal discrepancy in intrinsic atomic interaction at differential vicinage.**
S. K. Verma, P. K. Panda, P. Kumari, P. Patel, A. Arunima, E. Jha, S. Husain, R. Prakash, R. Hergenröder, Y. K. Mishra
Green Chem. (2021).

XXXI. **Zebrafish (Danio rerio) as an ecotoxicological model for Nanomaterial induced toxicity profiling.**
S. K. Verma, A. Nandi, A. Sinha, P. Patel, E. Jha, S. Mohanty, P. K. Panda, R. Ahuja, Y. K. Mishra, M. Suar
Precis. Nanomedicine. **4**, 750–782 (2021).

XXXII. **Clinical evolution, genetic landscape, and trajectories of clonal hematopoiesis in SAMD9/SAMD9L syndromes**
S. S. Sahoo et.al.
Nature Medicine. 27, 1806–1817 (2021).

Details of my contributions

All the works presented in the **Papers I to VII** have been performed in the close collaboration with the co-authors, senior authors, mentors and under the guidance of my supervisors. A brief description of my contribution to the works is summarized as follows. In paper I – VII, I took the central responsibility for designing the project. I was involved in the conceptualisation, development of the methodology, performing theoretical calculations simulation, validation, formal analysis, visualisation, writing the original draft

manuscript. The papers which are not included in this thesis are also correlated to the papers included. [1]–[24]

In paper **V**, the project was supervised by Prof. Zhong Lin Wang, Georgia Institute of Technology, USA. The paper **VII**, the work has been performed in collaboration with University of Illinois at Chicago, USA.

Paper I: I helped in conceptualization, designing of the project, performed transport calculations, molecular docking analysis, and molecular dynamics simulations and in writing the original draft manuscript. **Paper II:** I was involved in performing transport calculations using Siesta. **Paper III:** I participated in designing the research and performed the transport calculations, analyzed data, and wrote the manuscript. **Paper IV:** The conceptualization was done by Prof. K. Leifer and all the computational calculations involving transport calculations, binding energy estimations, molecular docking analyses and molecular dynamics simulations have been performed by me. **Paper V:** I have designed and performed all the computational analyses and wrote/edited/reviewed the original draft. **Paper VI:** I helped in performing binding energy estimations and molecular dynamics simulations. **Paper VII:** I have been involved in performing molecular docking analyses of ZnO tetrapods with macromolecules.

Contents

List of Figures

All the figures depicted in this thesis are reprinted with permission from Royal Society of Chemistry, Elsevier, and Copyright @ American Chemical Society.

Abbreviations

GENOME	Genetic organization of multicellular organisms and their enzymatic reaction
QUNOME	Quantum nanostructured materials for energy scavenging applications
CE	Contact electrification
DFT	Density Functional Theory
NEGF	Nonequilibrium Green's Functions
MD	Molecular Dynamics
TF	Thomas-Fermi
TDDFT	Time-dependent density functional theory
KS	Kohn-sham
LDA	Local-density approximation
Ψ	Wavefunction
SCF	Self-consistent field
GGA	Generalized gradient approximation
PAW	Projector augmented wave)
HOMO	Highest occupied molecular orbital
LUMO	Lowest unoccupied molecular orbital
MO	Molecular orbitals
GROMACS	Groningen machine for Chemical Simulation
LAMMPS	Large-scale Atomic/Molecular Massively Parallel Simulator
NMR	Nuclear magnetic resonance
PDB	Protein data bank
BPDT	Biphenyl-4,4′-dithiol
TPDT	*p*-Terphenyl-4,4′′-dithiol
AuNPs	Gold nanoparticles
AlN	Aluminium nitride
GaN	Gallium nitride
Si	Silicon

AgNPs	Silver nanoparticles
ZnO	Zinc oxide
vdW	Van der Waals
NEB	Nudged elastic band
MM	Molecular mechanics
QM	Quantum mechanics
LJ	Lennard-jones
NVT/NPT	No. Of Particles, Volume, Temperature, Pressure
VMD	Visual molecular dynamics
AIMD	Ab-initio molecular dynamics
EWG	Electron withdrawing groups
AA	Amino acid
ppb	Parts per billion
ss	Single stranded
FET	Field-effect transistor
ATGC	Adenine, thymine, guanine, cytosine
NH_3	Ammonia
NO_2	Nitrogen dioxide
H_2S	Hydrogen sulfide
SO_2	Sulfur dioxide
0D/2D/3D	Zero/Two/Three-dimensional
NDR	Negative differential resistance
zbt	Zero-bias transmission
NanoMoED	Nano-molecular electronic devices
MEP	Minimum-energy profile
TENG	Triboelectric nanogenerator
CE	Contact electrification
HS	Heparan sulfate
HSV	Herpes simplex virus
ZOTEN	Tetrapod-like zinc oxide microparticles
ANZOT	ZOTEN with gold nanoparticles
VLDL	Very low-density lipoprotein
LDL	Low density lipoprotein
PEX	Peroxisomal biogenesis receptor protein family

1 Introduction

“We will never be able to investigate or comprehend human diseases/lifestyles without the chance to merge materials science and biology”. It is crucial to comprehend interface science, or bio-interactions due to the intricacy of these interactions and their importance in controlling activity at the molecular and atomic levels. Understanding how nanomaterials interact with biomacromolecules to change their function requires knowledge from both domains. My thesis, which I've given the catchy moniker **“GENOME2QUNOME”** (an acronym for "Genetic organization of multicellular organisms and their enzymatic reaction 2 Quantum nanostructured materials for energy scavenging applications"), is an umbrella term encompassing a combinatorial approach using scientific domains, i.e., bioinformatics, nanoinformatics, biophysics, and materials science.

In order to better understand how materials, behave and what qualities they exhibit at the molecular and nanoscale levels, materials science and biophysics have established a fruitful relationship. Researchers can now investigate biological systems and materials with an accuracy and level of detail that was previously unattainable because of advancements in quantum physics and nanoscience, leading to a deeper understanding of the underlying mechanisms that govern the behavior of these systems. Quantum physics provides a theoretical framework for understanding the interactions between atoms and molecules, which is essential for comprehending the activities of biological systems and nanomaterials, including protein structural conformation and electron transport in two-dimensional materials. The ability to produce and control materials at the nanoscale, made possible by nanoscience, however, paved the way for the development of new materials with hitherto unanticipated characteristics and applications. Quantum physics and nanoscience are providing exciting new insights into the fundamental processes that govern the behaviour of materials and biological systems, paving the way for the development of new materials and technologies with a wide range of applications in fields as diverse as energy storage and conversion, biomedicine, and diagnostics.

Lacking a shared theoretical foundation and terminological lexicon between fields might impede efforts to incorporate biological principles into materials science and engineering. In retrospect, it's possible to draw some instructive

lessons from the fact that the development of contemporary materials science and engineering was the consequence of the convergence of fields that had previously been kept separate by the categorization of materials into different types. A unifying paradigm based upon processing-structure-property correlations is now widely acknowledged and has been crucial in the incorporation of bioinspired materials (mimicking nature) into materials science and engineering. Therefore, a unified framework for the study of biomaterials, biological materials, and biomimetic materials may be useful in bringing together the many divergent approaches and obstacles that characterize this field. To better understand the adaptive and hierarchical character of biological materials, the standard materials science and engineering paradigm have to be adjusted. This raises some intriguing questions that need to be addressed with the help of interface or interdisciplinary science[25].

Can researchers characterize the diverse behaviors of nanomaterials before using them in any biological applications? Is it conceivable to develop a diagnostic tool that can recognize and differentiate between healthy and cancerous cells, then use nanotechnology to eliminate the latter? When will the nanotechnologists and materials scientists who are working on genetic technology projects to enable us to live in a disease-free condition be considered in the brainstorming sessions? How does sophisticated modern science progress in the university setting? These are some of the fascinating issues or directions for research that might occur to a young researcher who wishes to explore nanoscience, materials science, or both. The development of intelligent nanomedicines for numerous diseases, including cancer, has advanced significantly, but there are still many obstacles to overcome in this young sector. Nano-bio interactions, which can address some of the intrinsic atomistic and mechanistic interactions at the atomic level, are the most important complex challenges in this developing field. Other complex challenges include active sites, molecular structures, surface modifications, doping, nanoparticle toxicity, physiochemical properties, and many other aspects. The collaborative research of nanoscience and biology can aid in the formulation of nanomedicine designs by combining different physicochemical variables applicable to nano–bio interactions. Because of this, the discovery and prediction of the fundamental processes of nano-bio interactions may be facilitated by the use of in silico methods and high-throughput selection, such as the nano-quantitative structure-activity relationship approach and nanoinformatics. Once these barriers are eliminated, we will have a clearer picture of what nano, biomedicine, and biodynamics look like.[13].

The state of human health will never stop being discussed. Human life expectancy has increased dramatically thanks to the vast body of information we currently possess, the astounding development in medical technology, and the enormous progress in the quality of our living environments in terms of

cleanliness. Major medical and healthcare advancements in the modern period are pulled in opposite directions by the increasing desire for a better quality of life and the approaching aging problem in society. The notion of precision medicine has been stoked by its promising possibilities [26]. Precision medicine proposes a new medical paradigm in which treatment is based on a patient's specific genetic makeup and requires two major prospects in medicine: improved diagnostics at the molecular level and personalized pharmaceuticals, medical devices, prosthetics, and other medical aids. As a result of this shift in thinking, molecular biology technologies are in high demand, and several types of biological sensors are being called for in applications ranging from individual diagnosis to the development of medical products. In addition, the union of biological methods and electronic sensors has produced a plethora of inexpensive portable medical gadgets that make it possible to put our lofty ideas into practice in areas like telemedicine, the Internet of Things, smart healthcare, big data-based diagnostics, and so on.

At the molecular level, life is crafted by a dynamic network of chemical entities that develop through time. Proteins and nucleic acids, for instance, fold (taking on a structure appropriate to their function), ions are transported across membranes, enzymes set off chains of events, and so on. There has been a rise in the importance of computational approaches in the life sciences as researchers try to deal with the complexity of biological systems incorporating various scientific domains. Researchers now have the ability to study matter at a scale of one billionth of a meter, allowing them to break down traditional boundaries between the physical, chemical, and biological sciences. By manipulating their dimensions on the nanoscale scale, we as scientists in the field of nanoscience are able to create useful structures, gadgets, and systems for a wide range of applications. In his talk titled "there is plenty of room at the bottom," delivered at the California Institute of Technology, prominent physicist Richard Feynman laid the groundwork for what would later become nanotechnology in the minds of many professionals in the area[27]. Feynman envisioned a method of creating objects at the nanoscale, both atomically and molecularly. Instead of using phrases like tiny size, little objects, and miniaturization, Feynman instead introduced the contemporary notions of nanoscale, nanotechnology, nanoengineering, and nano-object. The practice of manipulating materials at the atomic and molecular levels; a potentially paradigm-shifting innovation that might alter our current way of life.

1.1 Scope of the thesis

The theoretical frameworks/computational approaches that served as the foundation of this thesis are part of an overall research strategy that aims to depict the genesis of **"GENOME2QUNOME"**. The work in this thesis is concerned with the transition from the nanoscale regime to macromolecules, and I classified it accordingly based on the chapters that follow, namely,

Chapter 1: **Electronic transport at the nanoscale**
Chapter 2: **Contact electrification (Interface mechanisms)**
Chapter 3: **Nanomaterials with complex architectures**

For personalized medicine to become a reality, it is necessary to identify a large panel of diagnostic markers[28]. Due to its comprehensive, simultaneous detection of many target indicators for use in biological and medical applications, a single-molecule electrical measuring technique utilizing nanodevices is gaining interest as a sensor to execute such tailored medicine. High sensitivity, low cost, high throughput detection, simple mobility, low-cost availability through mass manufacturing methods, and the flexibility to integrate many functionalities and numerous sensors are benefits of single-molecule electrical measurement employing nanodevices like nanopores. **Chapter 1** deals with the domain "Molecular electronics," which is a multidisciplinary discipline that relies on physics, biochemistry, and materials science to solve a variety of problems. Scientists are primarily concerned with answering the question, "how does current travel through molecules? How can a miniature device detect biological molecules that helps in identifying disease biomarkers or sequencing patterns? In this chapter, I try to address the aforementioned queries using theoretical quantum physics techniques and in-silico methods **(Paper I, II).** A brief introduction to theoretical methods has been described in **Combinatorial approach (section2). Paper III & IV** deal with detection of harmful gases using 2-dimensional materials and hybrid nano-devices, respectively.

Chapter 2 deals with a complicated phenomenon requiring mechanical contact/sliding of two materials including various physio-chemical processes, but the scientific understanding of contact electrification (CE) (triboelectrification) remains a mystery. The interfacial charge transfer between the two materials at contact is the most crucial component in understanding the contact electrification. The hypothesized phenomena, which includes the experimental examples of Wang et al., can only be understood by experimental verification[29]. However, with the help of sophisticated theoretical assumptions, one may foresee the tribology of the materials, which is useful in many fields, such as the manufacturing, transportation, and energy sectors. **Paper V** deals with the mechanistic viewpoint of the solid-liquid interface.

Nanomaterials with complex architectures are generating a lot of research interest in an interdisciplinary community because they offer a lot of flexibility, from simple and efficient applications to hybridizing their surfaces with desired functional organic or biomolecules. These nano- and microscale structures' unique properties make them suitable for a wide range of interesting technological applications, particularly in the field of green energy, such as bioelectronics, biofuel cells, and so on. The 3rd chapter discusses the unique potentials of tailored interfaces using novel nanomaterials such as zinc oxide tetrapods and biogenic nanoparticles, which have programmable operations in response to structural morphologies. At a given stimulus, unique physical, structural, or morphological features of hybrid nanomaterials can provide changes in physical insights related to volume-phase transitions, electrical conductivity, zeta potential, dielectric constant, mechanical flexibility, permeability, wettability, and biocompatibility, etc. **Papers VI and VII** depict the nanoinformatics approach taken to decipher the biocompatibility, anti-bacterial, and anti-viral properties of biogenic silver nanoparticles and complex 3-dimensional ZnO tetrapods.

As we know, quantum physics provides a theoretical framework for understanding and manipulating the behavior of matter and energy at the molecular and subatomic levels. While my thesis addresses translational research, as the title suggests, I try to incorporate combinatorial techniques integrating bioinformatics into my research works because it involves the use of computational methods to analyze and interpret large amounts of biological data.

Together, this combinatorial approach allows for a deep understanding of the individual differences in a person's genetics, physiology, and biochemistry, which can inform the development of targeted and effective medical treatments. By combining the insights from quantum physics and bioinformatics, personalized medicine promises to deliver more precise, efficient, and personalized healthcare solutions, transforming the way we approach medical treatment. The central mystery of contemporary biology using theoretical biophysical techniques is addressed in this thesis. How a nanomaterial interacting with macromolecules—the quantum of life—embodies the behavior of a vast number of molecules whose actions are determined only by physical law! The advent of high-powered computing in the sciences has made it possible to examine single cells, proteins, and DNA at every level of organization, from the molecular to the organismal. By linking experimental data on structure to that on dynamics, molecular dynamics simulations provide unprecedented insight into biological events. Several cellular activities lie in the million-to-billion-atom realm, which is becoming increasingly described by simulations at atomic resolution. It deals with macromolecular biophysics, where I examine the developments in the study of macromolecules, all of which have been propelled by large-scale molecular dynamics simulations that demonstrate the

value of molecular dynamics simulations, which cannot be accomplished by smaller-scale simulations or current DFT methodologies alone, in the crucial task of linking atomic detail to the function of supramolecular complexes.

The aforementioned topics depicted in the chapters are fascinating in the real world, but to assume (real-time calculations) theoretically is a difficult challenge. That's why I use a combination of different computational methodologies, starting from DFT (which deals with a few atoms) to classical dynamics (which deals with billions of atoms). To bridge the concepts of biophysics and quantum physics, the topic **GENOME2QUNOME** has been interagted to impersonate the real-world scenarios. DFT tools such as VASP, Siesta, and Transiesta were used to calculate ab initio quantum mechanical calculations, whereas Autodock4, Vina, and GROMACS, LAMMPS were used to obtain conclusive based evidence of my research works for computational approaches such as molecular docking and molecular dynamics simulations.

2 Combinatorial approach

This chapter provides a high-level summary of the theoretical underpinnings of this thesis. The ab *initio* and in *silico*-based methods have been utilized throughout my research works. In the context of computational simulations, the ab initio methods that I have used are based on quantum mechanical models to calculate properties of materials or molecules based on their underlying quantum mechanical interactions, whereas, In silico simulations are based on either experimental data or first principles and were used to study a wide range of scientific and engineering problems, such as the behavior of materials, the design of drugs, and the behavior of biological systems. First principles (ab-initio) define the electronic structure of an atomic system without using any parameters obtained from experimentation. Beginning with the many-body issue, this chapter will provide an outline of the key methods. The electronic structure computations in this thesis make use of density functional theory, and the following part provides a brief review of some of the most essential features of this method's implementation in the atomic-scale simulations. An introduction to the theory of electron transport across a scattering zone is provided, relying on the nonequilibrium Green's functions (NEGF) theory.

DFT (density functional theory) methods can be used for large scale simulations, but their computational cost increases rapidly with system size, which can limit their practical applicability for very large systems. The use of efficient algorithms, parallel computing, and approximations such as hybrid functionals can help reduce the computational cost, making DFT methods more feasible for large-scale simulations. However, alternative methods such as classical molecular dynamics may be more suitable for simulating very large systems. Classical simulations, such as molecular dynamics (MD), do not suffer from the same computational cost limitations as DFT methods because they do not require explicit evaluation of the electronic wave function. Instead, classical simulations treat the electrons as point charges that interact with the nuclei through classical force fields. These force fields are parameterized based on quantum mechanics calculations or experimental data and can be used to efficiently calculate the interactions between the particles in a system.

One advantage of classical simulations is that they can easily be extended to very large systems, as the computational cost of classical simulations

increases only linearly with the number of particles. Additionally, classical simulations can be used to study systems over long-time scales, making them well-suited for investigating slow processes such as structural relaxation and phase transitions. However, classical simulations have limitations compared to quantum mechanical methods, as they do not accurately describe quantum mechanical effects such as tunnelling and zero-point energy. Additionally, the parameters used in classical force fields are often based on limited data and may not accurately describe the interactions in all systems. Nevertheless, classical simulations are a powerful tool for understanding the behavior of many physical and biological systems. That's why dealing with millions and billions of atoms such as protein structures requires classical dynamics approach which I have introduced in my work **(Figure 2.1).**

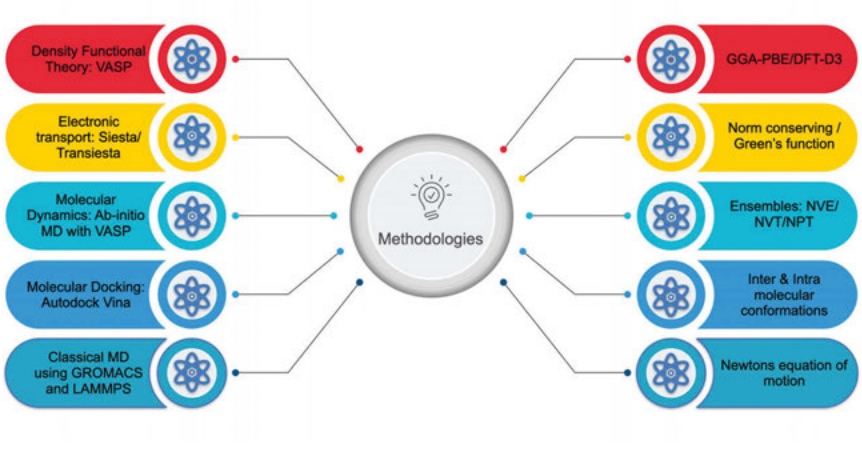

Figure 2.1: Methodologies used by using combinatorial approach in this thesis.

I have also made use of computational methods, such as molecular docking, that may be used to predict how a tiny molecule would interact with a protein. This data is helpful for predicting the preferred orientation of one molecule to another when a small molecule and a protein target are bonded to create a stable complex, which has applications in both drug design and the study of the molecular basis of biological processes. The degree of association or binding affinity between two molecules may be estimated using this data, which can also be used to calculate scoring functions like shape complementarity and conformational space. The majority of scoring functions are based on molecular mechanics force fields, which are in turn based on physics and are energy estimations of poses inside a binding site for another macromolecule.

2.1 DFT formalism

Density functional theory has dominated the field of quantum mechanical modeling of periodic systems for the past 30 years. Recently, it has also gained popularity among quantum chemists, who use it to model molecular energy surfaces. Density-functional theory is used to study the electronic structure of many-body systems, specifically the ground state of atoms, molecules, and condensed phases. To forecast and calculate material behavior based on quantum mechanical considerations, computational materials scientists can use ab initio (from first principles) DFT computations, which do not require higher-order factors like fundamental material characteristics. A potential operating on the electrons in the system is used to assess the electronic structure in modern DFT methods. This DFT potential is made up of the effective potential V_{eff}, which depicts atom-to-atom interactions, and the external potentials V_{ext}, which are determined solely by the system's structure and elemental composition. Studying an issue for a typical supercell of an n-electron material, then, may be done as an analysis of n sets of Schrödinger-like equations, often known as Kohn-Sham equations, each involving the behavior of a single electron.

With their two HK theorems, Walter Kohn and Pierre Hohenberg laid the theoretical groundwork for density functional theory. The theoretical basis of DFT is the Thomas-Fermi (TF) model of the electronic structure of a material. The HK theorems were initially only applicable to degenerate ground states, but they have now been expanded to encompass them even in the absence of a magnetic field. The first HK theorem demonstrates that the ground-state properties of a many-electron system are uniquely described by an electron density that requires just three spatial coordinates. It established the groundwork for reducing the many-body problem of N electrons with 3N spatial coordinates to three spatial dimensions by the use of the functionals of the electron density. Since that time, the time-dependent density functional theory (TDDFT), which may be used to describe excited states, has been created by extending this theorem to the time-dependent domain. In the second HK theorem, it is proven that the system has an energy functional, and it is demonstrated that this functional is minimized by the ground-state electron density.

Walter Kohn and Lu Jeu Sham, who later won the Chemistry Nobel Prize for their work on the HK theorem, enhanced it even more. The Kohn-Sham DFT was the outcome of this (KS DFT). The framework reduces a complex many-body problem involving interacting electrons in a fixed external potential to a considerably more straightforward issue with noninteracting electrons moving in a useful potential. The electrons' Coulomb interactions, including the exchange and correlation interactions, are considered when calculating the effective potential in addition to the external potential. The final two interactions

appear to be difficult to represent with the KS DFT. The Thomas-Fermi model may be used to compute the precise exchange energy for a uniform electron gas, and the local-density approximation (LDA), which is derived from fits to the correlation energy for a uniform electron gas, is the most basic approximation. Since the wavefunction of a system with non-interacting particles can be expressed as a Slater determinant of orbitals, its solution is simple. Additionally, the precise function of kinetic energy in such a system is understood. It is yet unknown and approximative to calculate the exchange-correlation portion of the total energy functional.

The “many-body problem” refers to the challenge of understanding the collective behavior of a large number of interacting particles. In physics, the many-body problem arises in a variety of contexts, including quantum mechanics, solid-state physics, and chemical physics. In these fields, the many-body problem involves predicting the behavior of a system of many particles that are interacting with each other through various forces, such as electromagnetic or van der Waals forces. The many-body problem is difficult because the interactions between the particles are often complex and non-linear, making it challenging to find a general solution that describes the behavior of the entire system. This difficulty is compounded by the fact that the number of particles in the system can be very large, making it computationally intensive to perform simulations.

To tackle the many-body problem, physicists and scientists use a variety of approximation methods, including perturbation theory, mean-field theory, and numerical simulations. These methods allow us to make predictions about the collective behavior of the particles and to understand how the interactions between the particles influence the properties of the system as a whole. Overall, the many-body problem remains a central challenge in physics and related fields, and its solution has important implications for our understanding of a wide range of physical and chemical phenomena, including the behavior of materials, the structure of molecules, and the behavior of subatomic particles. I am interested in calculating the properties using DFT methods by utilizing the Schrödinger equation. It is a mathematical formula that describes how particles, such as atoms and molecules, behave in the quantum world. It is used to calculate how these particles change and move over time.

In simple terms, the Schrödinger equation shows how the probability of finding a particle in a certain place changes over time. The equation considers the effects of quantum mechanics, which is a theory that explains the behavior of matter and energy at a very small scale. The Schrödinger equation helps us understand the "wave-like" behavior of particles and how they can exist in multiple states or locations at the same time. It is a fundamental tool in quantum physics and is used to make predictions about the behavior of particles

and develop new technologies in areas such as electronics, materials science, and medicine. It is an essential tool for understanding the behavior of particles in the quantum world and making predictions about their behavior.

It is standard practice in many-body electronic structure studies to assume that the nuclei of the molecules or clusters being treated are immobile (the Born-Oppenheimer assumption), so creating a constant external potential V through which the electrons must propagate. Then, a wavefunction Ψ(r1,..., rN) meeting the many-electron time-independent Schrödinger equation will characterize the electronic state as stationary.

$$\hat{H}\Psi = \left[\hat{T} + \hat{V} + \hat{U}\right]\Psi = \left[\sum_{i=1}^{N}\left(-\frac{\hbar^2}{2m_i}\nabla_i^2\right) + \sum_{i=1}^{N} V(\mathbf{r}_i) + \sum_{i<j}^{N} U(\mathbf{r}_i, \mathbf{r}_j)\right]\Psi = E\Psi \qquad (2.1)$$

where Ĥ is the Hamiltonian; E is the total energy; T̂ is the kinetic energy; V̂ is the potential energy from the external field owing to positively charged nuclei; and Û is the electron-electron interaction energy for the N-electron system. While V is independent of the system, T̂ and Û are universal operators since they are constants in any N-electron system. This complex many-particle equation cannot be decomposed into simpler single-particle equations because of the interaction term Û. To simplify, the Hamiltonian Ĥ described as

$$\begin{aligned}\hat{H} = &-\frac{\hbar^2}{2}\sum_{k}^{N_{\text{nucl}}}\frac{\nabla^2}{M_k} - \frac{\hbar^2}{2}\sum_{i}^{N_{el}}\frac{\nabla^2}{m_e} \\ &+\frac{1}{2}\sum_{k\neq l}^{N_{\text{nucl}}}\frac{Z_k Z_l e^2}{|\mathbf{R}_k - \mathbf{R}_l|} + \frac{1}{2}\sum_{i\neq j}^{N_{el}}\frac{e^2}{|\mathbf{r}_i - \mathbf{r}_j|} - \sum_{i,k}^{N_{el},N_{nucl}}\frac{Z_k e^2}{|\mathbf{r}_i - \mathbf{R}_k|}\end{aligned} \qquad (2.2)$$

where the first two components are the kinetic operators for the nucleus and the electrons. The second row contains terminology describing the interaction between nuclear- nuclear, electron-electron and nuclear-electron respectively. The hydrogen atom presents the simplest situation in which this issue may be handled exactly. Approximations like the Born-Oppenheimer approximation are necessary for more complex systems like solids, where a large number of particles must be considered.

The Born-Oppenheimer approximation is a method used in quantum mechanics to separate the motion of the heavy, slowly moving nuclei in a molecule from the motion of the rapidly moving electrons. This separation allows for a simpler treatment of the electronic structure and energies of a molecule. In essence, the approximation says that the nuclei can be considered to be fixed in space while the electrons move around them, and thus the electronic and nuclear motions can be treated as separate and independent.

The core concept behind density-functional theory is to substitute a simpler system for the more difficult many-body problem (as given by Eq. 2.1 and

2.2). Although DFT is an accurate theory, in reality it requires approximations to the Hamiltonian due to the lack of knowledge of the precise functional describing the interactions between electrons in the system. The Hohenberg-Kohn theorems are the cornerstone of DFT.

The main theorems of DFT are:

1. Hohenberg-Kohn theorem: This states that the total density of a many-body system determines its external potential and the system's ground-state energy uniquely.
2. Kohn-Sham theorem: This states that for a given total density, there exists a set of non-interacting particles (referred to as Kohn-Sham orbitals) that yield the same total density as the actual interacting system and whose energies can be used to determine the total energy of the system.
3. The Variational principle: According to this, the ground-state energy of a many-body system is the minimum of the energy functional over all possible densities.

These theorems provide the foundation for DFT and allow for efficient and accurate calculations of the electronic structure and properties of complex systems in physics, chemistry, and materials science.

To obtain the ground-state density, the Kohn-Sham equations can be solved iteratively until self-consistency is achieved. Self-consistency means that the density obtained from the solution of the Kohn-Sham equations is equal to the total density of the system. This is an important requirement in DFT, as the ground-state energy and other properties of a system depend on the accurate representation of its density. In practice, the Kohn-Sham equations are solved using numerical methods, such as the self-consistent field (SCF) iteration or matrix diagonalization techniques. The process starts with an initial guess for the density, and the Kohn-Sham equations are solved for this density to obtain the corresponding Kohn-Sham orbitals. The new density is then calculated from these orbitals, and the process is repeated until the density converges to a self-consistent solution. Once self-consistency is achieved, the ground-state energy and other properties of the system can be calculated using the density and the Kohn-Sham orbitals. The use of iterative, self-consistent procedures makes DFT a highly efficient and versatile tool for studying the electronic structure of complex systems.

To be able to solve the Kohn-Sham equations, we can use Exchange-correlation functionals that are mathematical functions used in Density Functional Theory to describe the exchange and correlation interactions between the electrons in a many-body system. These interactions cannot be described exactly

by a single function and are a major source of approximations in DFT. The exchange-correlation energy of a system is defined as the difference between the exact energy of the system and the sum of the kinetic energy of the electrons and the electrostatic energy of the interaction between the electrons and the nuclei. The exchange-correlation functional maps the total electron density of a system to its exchange-correlation energy. There are several types of exchange-correlation functionals, ranging from simple models based on physical intuition to more sophisticated models based on numerical and empirical data. Some of the most commonly used functionals are the Local Density Approximation (LDA), the Generalized Gradient Approximation (GGA), and hybrid functionals, which combine the strengths of different types of functionals. The choice of exchange-correlation functional has a significant impact on the accuracy of DFT calculations. While simple functionals are relatively inexpensive to use, but they often provide poor accuracy for some systems. More sophisticated functionals are generally more accurate but also more computationally expensive. Since the difference between the functionals is modest compared to the approximations in the transport calculations, this thesis makes use of both GGA and LDA. However, the choice between the functionals should not be as significant as dealing with the transport calculations or, in general for structural optimization.

In order to reduce the computing cost of the simulations, the influence of the mobility of the core electrons of an atom and its nucleus might be replaced by an effective potential. A pseudopotential is a simplified representation of the interaction between electrons and nuclei in a many-body system. In quantum mechanics, the interaction between electrons and nuclei is described by the Coulomb potential, which is computationally demanding to solve for large systems. The pseudopotential replaces the interaction between electrons and the full nucleus with a simpler interaction between electrons and a core region of the nucleus, represented by a so-called "pseudo-atom."

The idea behind pseudopotentials is to describe the core electrons (which are tightly bound to the nucleus and do not contribute much to the electronic properties of the system) with a simplified, computationally efficient potential, while accurately describing the valence electrons (which determine the chemical and physical properties of the system). This allows for much more efficient and accurate calculations of the electronic structure and properties of large, complex systems. Pseudopotentials are commonly used in first-principles calculations, such as those based on Density Functional Theory (DFT), to study the electronic structure and properties of materials, molecules, and nanostructures. They are also used in quantum chemistry and solid-state physics, among other areas of research. There are different types of pseudopotentials, including Norm-Conserving, Ultrasoft, and PAW (Projector Augmented Wave) pseudopotentials. The choice of a pseudopotential depends on the

accuracy required for a given calculation and the computational resources available.

2.2 DFT methods

In my research works, I have used several DFT programs for numerical calculations in which several approximations are made. I do not intend to introduce mathematical formulae or derivations as the resources for derivation of exact functionals, pseudopotentials, basis sets, transport properties, conductance, and technical details can be found here in Refs. [30]–[59] And also intended for non-experts who can easily understand my research works.

1. SIESTA (Spanish Initiative for Electronic Simulations with Thousands of Atoms)[56]which are based on first-principles simulation code that uses Density Functional Theory to study the electronic structure and properties of materials, molecules, and nanostructures. Some of the main aspects of the implementation of DFT in SIESTA.

2. VASP (Vienna Ab initio Simulation Package)[60] is a first-principles simulation code that uses Density Functional Theory to study the electronic structure and properties of materials, molecules, and nanostructures. It is widely used in the scientific community for its accuracy, efficiency, and versatility, and has been applied to a wide range of systems and problems, including solid-state materials, surfaces, and interfaces, as well as molecules and nanostructures.

3. TRANSIESTA (Transport In Electronic Structure Calculations)[61] is a first-principles simulation code that uses Density Functional Theory to study the electronic transport properties that is based on the SIESTA code, which is used to perform self-consistent electronic structure calculations.

4. The Non-Equilibrium Green's Functions (NEGF)[62] formalism is a quantum mechanical method for simulating the transport of electrons through nanoscale electronic devices such as transistors and diodes. NEGF considers the device as an open quantum system in which electrons are allowed to flow in and out, and it models the interactions between the electrons and the device in a non-equilibrium state. The method provides a powerful tool for predicting and understanding the electronic behavior of these systems and for optimizing the performance of nanoscale electronic devices.

As mentioned before, Kohn-Sham DFT [51] is one of the most effective approaches to defining equilibrium characteristics of materials. Because of this, it has become the standard for use in calculating electron transport. The two together proved to be particularly effective in characterizing open-boundary systems under nonequilibrium conditions. In the same way that DFT faithfully reproduces patterns in relative energy, here trends in the amplitude of electron transport between identical systems are also recreated. This enables us to develop predictions that can be used as a guide for future experiments and quantitative estimates that can be compared with trials.

However, caution is warranted since the Kohn-Sham (KS) wavefunctions are not the "actual" single-particle wavefunctions and certain less well-founded approximations are incorporated when the current is computed. This indicates that the generally employed XC-functionals are believed to be capable of describing the non-equilibrium scenario we are dealing with, and that the KS-wavefunctions adequately represent the genuine electron wave functions (which we know is not always the case). The many-body effects that are often present in transport processes are not described by this approach since we are just utilizing the single-particle wavefunctions. For instance, it is well-known that the conductance of many molecules weakly coupled to the electrodes is overestimated by commonly used DFT-methods and functionals due to an underestimate of the gap between the highest occupied molecular orbital (HOMO) and the lowest unoccupied molecular orbital (LUMO). In many cases, this may be fixed by factoring in correlation effects, as in the case of GW or self-interaction correction.

Since the Kohn-Sham (KS) wavefunctions are not the "real" single-particle wavefunctions, and because the current is calculated using some less well-founded assumptions. Therefore, the KS-wavefunctions are a good approximation to the true electron wave-functions, and the commonly used XC-functionals are thought to be able to describe the non-equilibrium situation we're dealing with. Using just the wavefunctions of a single particle, this method cannot account for the many-body effects that are often present in transport processes. Examples include the fact that many molecules with weak coupling to the electrodes have their conductance overestimated by commonly used DFT-methods and functionals because the gap between the highest occupied molecular orbital (HOMO) and the lowest unoccupied molecular orbital (LUMO) is not properly accounted for (LUMO). In many instances, consideration of correlation effects, as in the case of GW or self-interaction correction, may be all that's needed to resolve the issue.

As was previously said, defining convergence of the basis set may be a tricky business, and it may be much more so for transport computations. In order to standardize transport computations, there have been several efforts to create a

benchmark of basis sets. The most important takeaway is that similar to structural convergence in DFT, a DZP-basis is frequently sufficient for transport, and that increasing the number of basis functions may produce an even "better" result compared to plane-wave computations. Since the form of the transmission function is duplicated, a SZ or a SZP may be used to provide a satisfactory qualitative outcome. The Fermi level and some molecular orbitals (MO) have been found to be extremely sensitive to the size of the basis set, with a change in basis having the potential to move the Fermi level into or out of the HOMO-LUMO gap and reorder MOs, thereby causing a change in transmission on the order of orders of magnitude. What this means for the interpretation of conductance between, say, molecule conformers, is up for debate. These challenges may be mitigated to a large extent, however, by using the same basis sets, functionals, and other characteristics when comparing systems of a similar kind. To sum up, in this thesis, we model the electron transport using the nonequilibrium Green's function technique (NEGF) in conjunction with density functional theory, which allows us to explain from first principles several systems that might be employed in molecular electronics devices.

2.3 In-*silico* methods

In order to get more insight into my study, I have combined the ab-inito first principles DFT and quantum transport in the non-equilibrium Green's functions formalism (NEGF) with in-silico approaches such as molecular modeling, molecular docking, and molecular dynamics simulations. Full description of codes and implementation of the methods can be found here in Refs. [63]–[72]

1. Molecular docking is a computational method used to predict the binding of a small molecule to a target protein. Autodock4 and Autodock Vina are two popular software programs for performing molecular docking simulations.

    a. Autodock4 uses a genetic algorithm to search for the optimal binding conformation of the ligand to the target protein, while considering the protein's flexible side chains and the ligand's rotatable bonds.
    b. Autodock Vina, on the other hand, is a faster and more efficient version of Autodock4, using a faster search algorithm and an improved scoring function to predict the binding of the ligand to the protein. Both Autodock4 and Autodock Vina are widely used in drug discovery and in the design of new therapeutic compounds, as they provide valuable information on the

binding affinity and specificity of candidate drugs to their target proteins.

c. Hex is the first Fourier transform (FFT)-based protein docking service to be powered by graphics processors. When using two graphics processors simultaneously, a typical 6D docking run takes 15 s, which is up to two orders of magnitude quicker than conventional FFT-based docking methods with equivalent resolution and scoring functions. Utilizing SPF shape-density representations to polynomial order N=20, All Hex Docking Correlations quickly provide a list of up to 25 000 potential solutions. Near-native orientations are almost always present in the top 3000 orientations, while a wider list is used to avoid disqualifying meritorious candidates in exceptional cases. These potential solutions are then re-scored using higher order shape-only or shape plus electro-static correlations (using, for instance, polynomials to order N=25 or N=30), depending on the user's preferences. In comparison to the typical order N=25 polynomials, which are somewhat soft, order N=30 polynomials produce significantly crisper representations of each protein.

2. Molecular Dynamics (MD) simulation is a computational method used to study the behavior of molecular systems over time. GROMACS and LAMMPS are two widely used open-source software packages for conducting MD simulations.

    a. GROMACS (GROningen MAchine for Chemical Simulations) is a highly optimized and versatile software that can handle large and complex molecular systems, making it well suited for studies of protein-protein interactions, protein-ligand binding, and other large-scale molecular systems. It features a wide range of integrators and force fields, as well as efficient parallel computing capabilities.

    b. LAMMPS (Large-scale Atomic/Molecular Massively Parallel Simulator) is a highly scalable and parallel molecular dynamics simulation software that can handle large molecular systems and perform simulations of complex physical processes, such as reactive dynamics and material deformation. LAMMPS is designed to work well on large-scale parallel computing platforms and can perform simulations of large molecular systems, such as proteins and nanomaterials. Both GROMACS and LAMMPS are widely used by researchers in a variety of scientific disciplines, including biophysics,

materials science, and condensed matter physics, for the study of complex molecular systems and their interactions.

3. Molecular modeling is the process of creating computer-based representations of molecules and their interactions.

    a. AlphaFold2 [73] is a deep learning-based protein structure prediction tool developed by OpenAI that can accurately predict the three-dimensional structure of proteins from their amino acid sequences. This technology represents a major breakthrough in the field of protein structure prediction and has numerous applications in drug discovery and the study of biological systems.

    b. Protein structures established by various experimental methods, such as X-ray crystallography and Nuclear Magnetic Resonance (NMR) spectroscopy, are stored in the Protein Data Bank (PDB). Protein Data Bank is an invaluable tool for scientists since it has an abundance of data on protein structures and their interactions.

    c. Visualization of molecular models is also an important aspect of molecular modeling. Discovery Studio Visualizer is a molecular visualization and analysis software developed by Biovia that provides a range of tools for visualizing and analyzing molecular structures and interactions.

    d. ChimeraX [74] open-source molecular visualization and analysis program that provides a wide range of features for the visualization and manipulation of molecular structures. It is widely used by researchers for a variety of purposes, including the visualization of protein structures and their interactions, as well as for the preparation of figures for scientific publications.

2.4 Implementation of methods

The study of basic 2D materials is frequently thought of as a contemporary field of study, yet it is really reawakening. The pioneering work of Langmuir, who studied the deposition of alkali metal atoms on metal films and laid the groundwork for the area of surface science, can be credited with launching the study of elemental monolayers in the 1930s. Fifty years ago, it was anticipated that three technical elements—materials, energy, and knowledge—would be principally responsible for sustaining and governing our contemporary

civilization. The fast expansion of new material research and development not only considerably enhanced contemporary living, but also made the other two technologies possible. Surface scientists studied the formation and (chemical, electrical, and optical) characteristics of several metal monolayers on a variety of metal substrates in the years that followed. While studies of elemental monolayers and 2D materials have traditionally focused primarily on surface science, recent advances in effective separation techniques and the examination of monolayer graphene's intriguing electronic and thermal characteristics have sparked renewed interest in 2D layered materials like transition metal oxides, chalcogenides, and MXenes. This excitement has been brought about by the discovery of novel and intriguing physics, such as non-trivial high-temperature ballistic transport topology, valleytronics, and other optoelectronic properties, primarily because of their 2D nature; these have recently been examined in a number of excellent reviews. Nanomaterials are therefore designed for a variety of possible purposes in next-generation technology, including spintronics, sophisticated nanoelectronics, nanosensing, and many more. Although there are many ways to respond to difficult challenges, such as the increasing global need for energy or the development of medical applications, material science nevertheless plays a crucial role in reaching ambitious goals. It has historically contributed significantly to improvements in the safe, dependable, and effective utilization of energy and utilizable natural resources. Materials science is anticipated to become more important in sustainable energy production, conservation, and savings technologies as a result of the development of nanomaterials.

A deeper understanding of this plan will have a long-term effect on scientific, commercial, and environmental research viewpoints. The relevant and interesting problems that will emerge during the development of the project will provide a wide range of topics for future research projects and partnerships in the field of interdisciplinary science, which will be of value to all collaborators. Research findings of our group, to which I have significantly contributed, have been summarized in this thesis via various chapters and papers, and it can therefore be thoroughly explained that a varied, yet complementary collection of contributions will be made further, illustrating the latest developments in the utilization of these emerging 2D materials for various applications.

For **chapters 1-3,** the nano materials, and macromolecules (proteins) used are listed below:

Chapter 1: An analog of graphene, graphitic carbon nitride (g-C_3N_4); single-layer gallium sulfide (GaS); Bismuthene (bBi); phenyl-based molecules of 4,4’-biphenyldithiol (BPDT) and p-ter-phenyl-4,4"-dithiol (TPDT) with functionalized gold nanoparticles (AuNPs)

Chapter 2: Aluminium nitride (001), Gallium nitride (001) and Silicon (001) surfaces
Chapter 3: Silver nanoparticles (AgNPs), Zinc Oxide (ZnO) Tetrapods

2.5 First-principles based DFT methods

For papers **I-VI in chapters 1-3**, I have used first-principles density functional theory computations inside the VASP framework to determine ground-state structures and associated electronic properties. Generalizing the pseudopotential in the linear augmented plane wave (PAW-PBE) approach allowed us to account for the ion-electron interaction in the Hamiltonian. The Perdew-Burke-Ernzerhof (PBE) parameterization, on the other hand, relied on an approximation of the exchange and correlation functional inside the generalized gradient approach (GGA). Because the dispersive forces cannot be captured by the normal DFT and semi-local approximation for the exchange-correlation, a nonlocal correction term has been employed to characterize them; for instance, the DFT-D3 correction approach of Grimme's dispersion.
The DFT-D3 method determines the self-consistent total energy obtained from Kohn–Sham DFT (KS-DFT) additionally corrected by the E_{disp} term, as given by:

$$E_{\text{DFT-D3}} = E_{\text{KS-DFT}} + E_{\text{disp}} \qquad (2.3)$$

where the underlying E_{disp} is a pairwise term accounting for the long-range van der Waals (vdW) interactions and is defined as

$$E_{\text{disp}} = -\frac{1}{2}\sum_{i=1}^{N_{at}}\sum_{j=1}^{N_{at}}\sum_{L}{}'\left(f_{d,6}\left(r_{ij,L}\right)\frac{C_{6ij}}{r_{ij,L}^{6}} + f_{d,8}\left(r_{ij,L}\right)\frac{C_{8ij}}{r_{ij,L}^{8}} \right), \qquad (2.4)$$

Where $C_{6ij} = \sqrt{C_{6ii}C_{6jj}}$ is the dispersion coefficient, $R_{0ij} = \sqrt{\frac{C_{8ij}}{C_{6ij}}}$ is the vdW radius and $f(r_{ij})$ is the damping function.

The valence electrons have been described using a plane-wave basis set with an approximation to an energy cutoff (in eV). Depending on the materials, the Brillouin zone has been sampled using different k-meshes for a unit cell and for supercells. Each electronic structure employed in the analysis was fine-tuned until Hellman-Feynman forces were less than 0.001 eV. Approximately 20-25 Å along the z-direction of the materials surfaces were employed to avoid the interactions between the periodic images of the surfaces.

Since adsorption is crucial to many surface processes, it is necessary to accurately anticipate its characteristics from both a theoretical and practical

perspective. In particular, it has been a long-standing objective in surface research to pinpoint the underlying factors that determine adsorption energy. Many activities, including catalysis, gas sensors, molecular electronics, biomedical applications, and so on, rely on molecules' adsorption to solid surfaces. Although bond formation and breaking occur throughout the processes, the adsorption energy is crucial in establishing their underlying mechanisms. Therefore, one of the most important aims in these areas has been to identify the physical and chemical factors that determine adsorption energy.

The adsorption energy can be calculated using the following equation:

$$E_{ads} = E_{\text{system (molecule + substrate)}} - [E_{\text{substrate (slab/sheet/monolayer)}} - E_{\text{molecule}}] \quad (2.5)$$

where E_{system} is the total energy of adsorbed system, $E_{molecule}$ is the energy of an isolated molecule, and $E_{substrate}$ is the energy of clean substrate.

Important physical quantities, such as the charge density, may be calculated from first principles using density functional theory. It's possible to learn a lot about the materials under investigation, including their chemical bonds, charge transfers, and orbital hybridizations, from this data. By deducting the charges of the substrate and the molecule from the system's total charge, we may get charge density difference maps/plots.

$$\Delta\rho_{system} = \rho_{system} - [\rho_{substrate} + \rho_{molecule}] \quad (2.6)$$

where ρ_{system}, $\rho_{substrate}$, and $\rho_{molecule}$ are the electron charge distribution of the whole system, slab, and molecule, respectively.

Both classical physics and quantum mechanics may provide an interpretation of the work function notion. According to classical physics, a metal surface always retains a positive picture of an escaping electron. The negative electron is attracted to the positive image, but it always ends up back at the metal's surface, preventing it from ever being able to exit the crystal. However, an electron needs extra energy, generally in the form of light, to overcome this attractive pull. The work function is the minimal amount of energy an electron needs to leave a metal's surface. The work function is defined as the minimal amount of energy needed to eject an electron from a solid surface. According to this description, the work function is determined using the following equation,

$$\Phi = E_{\infty} - E_{F} \quad (2.7)$$

where E_{∞} denotes the electrostatic potential of electrons far from the surface and E_F depicts the electrostatic potential of electrons at the Fermi level, respectively.

Nudged elastic band (NEB) calculations, which provide saddle points and lowest energy routes between known reactants and products, have been used in several of my investigations. This technique is effective because it optimizes a sequence of intermediate pictures along the chemical pathway. Each picture determines the minimum energy required to keep its distance from others the same. Specifically, the spring forces are added along the band between the pictures, and the component of the force owing to the potential perpendicular to the band is projected out, all in an effort to achieve this restricted optimization.

2.6 Quantum transport based on NEGF methods

The study of electron transport in nanoscale devices is a primary focus of this thesis which can be inferred from **Chapter 1**. Applications like this entail coupling a molecular system or nanojunction to 2D electrodes or facilitating transport in a periodic 2D system. Detailed description of quantum transport theory using TRNASIESTA can be found here in these Refs. [59], [61], [62], [75]–[105]

The electronic transport properties of the 2D materials with and without the molecules adsorption were calculated using the non-equilibrium Green's function (NEGF) in the TranSiesta module of Siesta code in order to examine the sensing performance of the 2D materials (monolayer/slab) as a nanoelectronics sensor. According to the Landauer-Buttiker formulae, we may determine the magnitude of the electric current flowing through the atomic scale system.

$$I(V_b) = G_0 \int_{\mu_L}^{\mu_R} T(E, V_b)[f(E-\mu_L) - f(E-\mu_R)]dE, \qquad (2.8)$$

where V_b shows the applied bias voltage, μ_L and μ_R, are the two electrochemical potentials of left and right electrodes, respectively. T(E, V_b) is the transmission coefficient at energy E and applied bias voltage V_b, f(E) is the Fermi–Dirac distribution function, and $G_0=2e^2/h$ is the quantum conductance. As seen from the above equation, the current is the integral of the transmission coefficient over the applied bias window. The transmission probability *T (ε)* of electrons with incident energy E, which are to be transmitted from left electrode to right electrode, were estimated as Eq. 2.9

$$T(\varepsilon) = T_r\left\{\Gamma_R(\varepsilon)\zeta^R(\varepsilon)\Gamma_L(\varepsilon)\zeta^A(\varepsilon)\right\} \qquad (2.9)$$

Here, $\Gamma_R(\varepsilon)$ and $\Gamma_L(\varepsilon)$ are the broadening matrix for the left and right electrodes of the designed device respectively $\zeta^R(\varepsilon)$ and $\zeta^A(\varepsilon)$ present the

retarded and advanced green's function, respectively. The conductance in the zero bias case will be evaluated as,

$\zeta = \zeta_o T(\varepsilon_F)$ where, $\zeta_o = 2e^2/h$ is the quantum conductance and e & h are charges of the electron and Planck's constant, respectively.

Schematic illustrations of 2D electronic device setup with left and right electrodes and a scattering region have been depicted here based on the papers I-IV. **(Figure 2.2-2.5)**

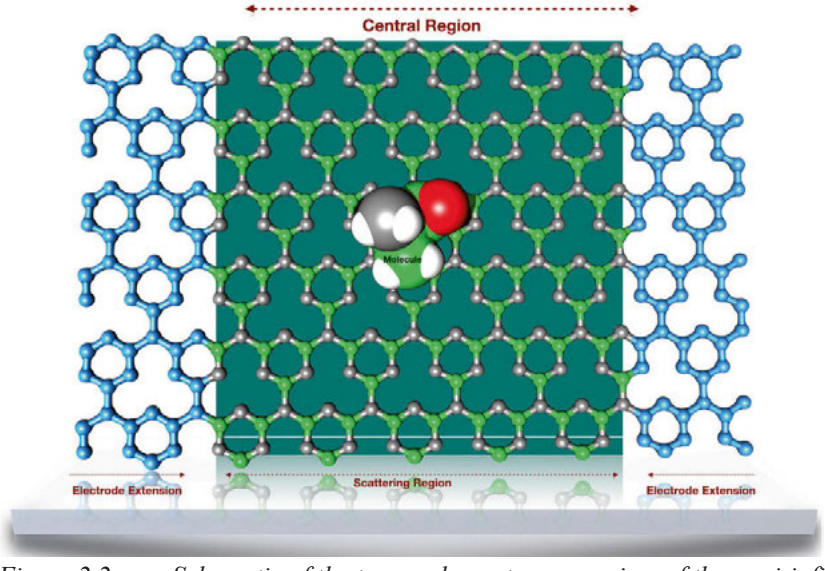

Figure 2.2: Schematic of the two-probe system comprises of the semi-infinite left and right electrode regions of g-C_3N_4 and the central scattering region consisting of amino acid molecules. (Adapted from Paper I)[106]

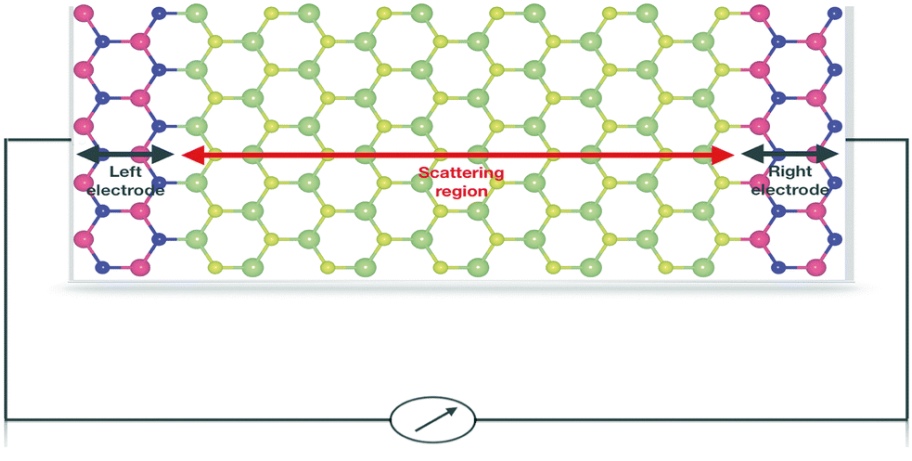

Figure 2.3: Illustration of the proposed device setup with left and right GaS electrodes, and a central scattering region containing the same material, the target nucleobase pairs AT and GC molecules, and a portion of the semi-infinite GaS electrodes. The blue (S atom) and red (Ga atom) atoms on both side in the device modelling represents the size of the left/right electrode. The light green and yellow colour atoms represent the scattering region. (Adapted from Paper II) [107]

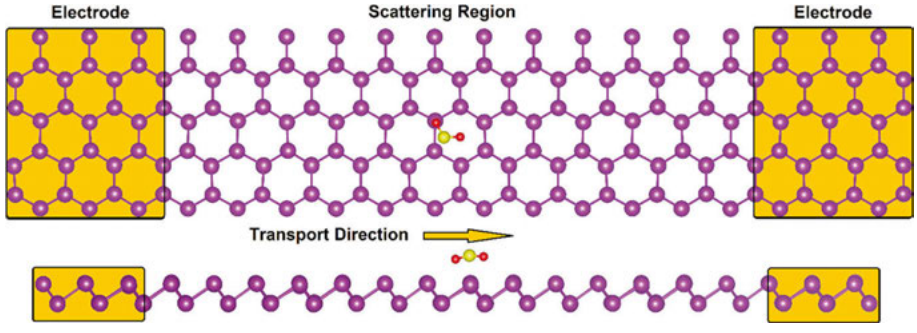

Figure 2.4: Top and side views of the schematic presentation of a transport device to measure I vs V characteristics of the bBi sheet adsorbed with the gas molecules. The left and right boxes (orange-shaded area) present semi-infinite electrodes, and the central part where the gas molecule is adsorbed (here SO_2 gas) presents the scattering region (purple: Bi, yellow: sulfur, red: oxygen). (Adapted from Paper III) [108]

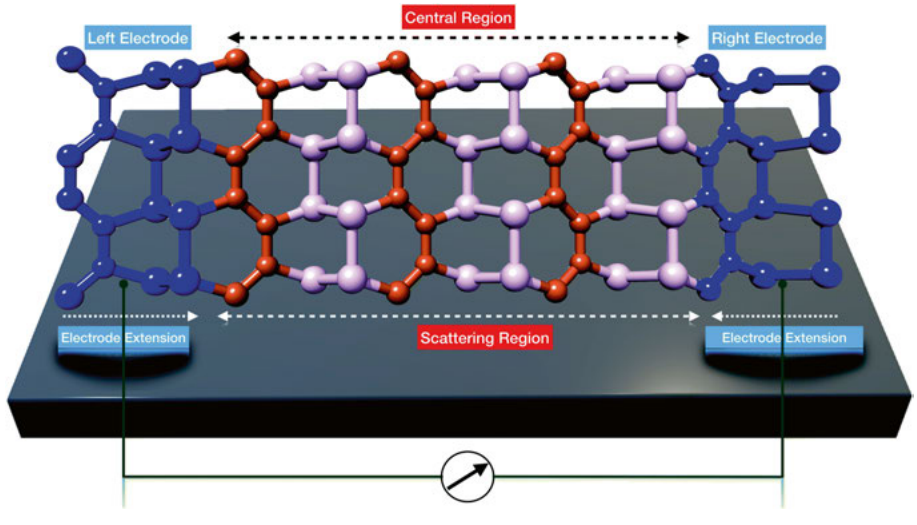

Figure 2.5: Schematic representation of the model device top and side views constituting of three parts: the semi-infinite left (L) and right (R) electrodes and the scattering region for monolayer carbon phosphide. Adapted with the permission from Royal Society of Chemistry [109].

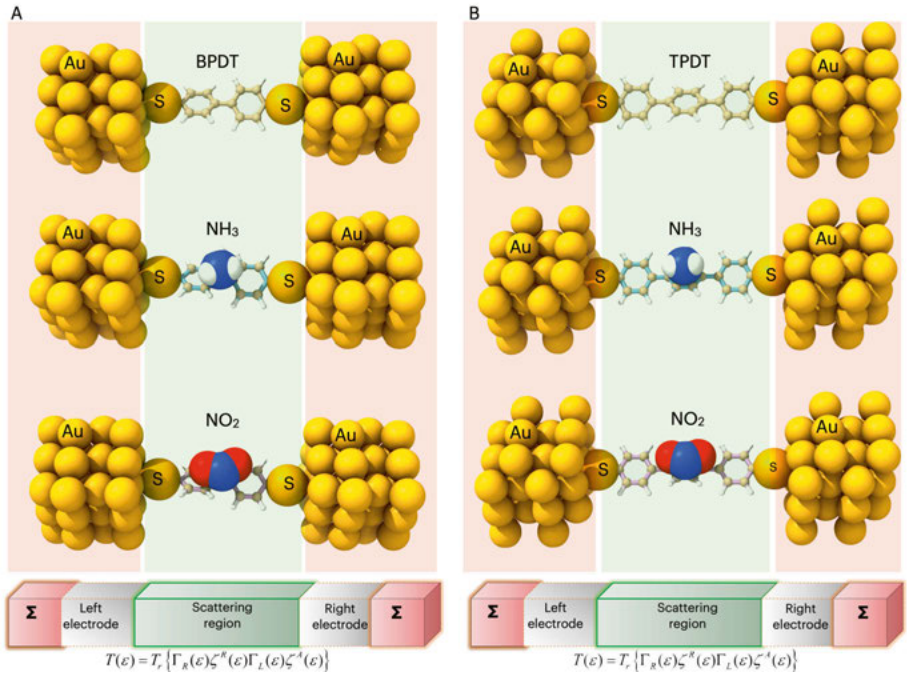

Figure 2.6: Top and side views of the schematic presentation of a nanoMoED device to measure IV characteristics when adsorbed with the NH_3 and NO_2gas molecules (a) BPDT as sensing molecule (b) TPDT as sensing molecule. The left and right boxes (pink shaded area) present semi-infinite electrodes and the central part (green shaded) where the gas molecules are adsorbed presents the scattering region. (Adapted from Paper IV)

2.7 Molecular docking from a viewpoint of nanomaterials and macromolecules

Molecular docking is a computational approach that uses the initial, unbound structures of a macromolecule (obtained from MD simulations, homology modeling, etc.) and a small molecule (ligand or nanomaterials) to predict their noncovalent interaction. Predicting bound conformations and binding affinities is the objective. Predicting how chemicals will bind to proteins is useful in the pharmaceutical industry since it can be used to screen large virtual libraries quickly and cheaply for potential new drug candidates. Even when experimental structures are not available, docking may be utilized to attempt to predict the bound conformation of known binders[66].

In this thesis, I have used two conventional programs, Autodock 4 [63] and Autodock Vina, in which the implementation of scoring functions is the same,

but the algorithms are different. A general framework of the scoring functions used in both cases has been shown here:

While performing docking simulations, AutoDock 4.2 evaluates conformations using a semi-empirical free energy force field. Many protein-inhibitor complexes with known structures and *Ki* values were used to calibrate the force field. There are two phases to the binding evaluation performed by the force field. At the outset, the ligand and protein are in an unbound state. The first step is to calculate the intramolecular energetics of changing from the unbound state of the ligand and protein to the bound state conformations. Afterwards, the bound conformation of the ligand and protein are analyzed for their intermolecular energies.

The force field includes six pair-wise evaluations (V) and an estimate of the conformational entropy lost upon binding (ΔS_{conf}):

$$\Delta G = \left(V_{\text{bound}}^{L-L} - V_{\text{unbound}}^{L-L}\right) + \left(V_{\text{bound}}^{P-P} - V_{\text{unbbuund}}^{P-P}\right) + \left(V_{\text{bound}}^{P-L} - V_{\text{urrbound}}^{P-L} + \Delta S_{\text{conf}}\right) \quad (2.9)$$

When "L" is the "ligand" and "P" is the "protein" in a ligand-protein docking computation. Dispersion/repulsion, hydrogen bonding, electrostatics, and desolvation are all evaluated for each pair-wise energy term:

$$V = W_{\text{vaww}} \sum_{i,j} \left(\frac{A_{ij}}{r_{ij}^{12}} - \frac{B_{ij}}{r_{ij}^{6}}\right) + W_{\text{hhomd}} \sum_{i,j} E(t) \left(\frac{C_{ij}}{r_{ij}^{12}} - \frac{D_{ij}}{r_{ij}^{10}}\right) + W_{\text{elec}} \sum_{i,j} \frac{q_i q_j}{e(r_{ij}) r_{ij}} + W_{sol} \sum_{i,j} \left(S_i V_j + S_j V_i\right) e^{\left(-r_{ij}^2/2\sigma^2\right)} \quad (2.10)$$

Using a set of binding constants found experimentally, the weighting constants W have been tuned to calibrate the empirical free energy. The first term is a standard 6/12 dispersion/repulsion potential. Amber, a quantum field theory, serves as the basis for the parameters. The second is an H-bond term with a directional component based on a 10/12 potential. Hydrogen bonds with oxygen and nitrogen are allocated well depths of 5 kcal/mol at 1.9 and 1 kcal/mol at 2.5Å by adjusting parameters C and D. Hydrogen bonds with sulfur are assigned at well depth of 0 kcal/mol at 1.9 Å. The directionality provided by E(t) is derived from the angle t relative to the geometry of perfect H bonds. Third, an electrostatic screen is used to implement a screened Coulomb potential. A desolvation potential is the last component, and it is calculated as the volume of atoms (V) that protect a single atom from the solvent, scaled by the solvation parameter (S), plus an exponential term with a distance-weighting factor σ =3.5.

For systematic conformational search, the number of possible molecular conformations is represented by equation 2.11[110]:

$$Nconformations = \prod_{i=1}^{N} \prod_{j=1}^{N} \frac{360}{\theta ij} \quad (2.11)$$

However, AutoDock Vina (v1.2.0) (Vina)[65] [64] is one of the docking applications in the AutoDock Suite, with AutoDock4 (AD4), AutoDock-GPU, AutoDock-FR, and AutoDock-CrankPep. When compared to the other docking tools in the suite and elsewhere, Vina is notable for being both user-friendly and fast.

Generalized scoring function form with conformational dependence Vina, or Autodock Vina in this context, is intended to function with:

$$c = \sum_{i=j} f_{i_i t_j}(r_{ij}) \quad (2.12)$$

where all pairs of atoms that may move relative to one another are added together, with interactions between atoms separated by four consecutive covalent bonds typically disregarded. This number may be thought of as the total of the contributions from both outside and within the molecule:

$$c = c_{\text{inter}} + c_{\text{intra.}} \quad (2.13)$$

The next section describes an optimization technique that looks for the global minimum of c and other low-scoring conformations and ranks them. From the intermolecular portion of the least favorable conformation, we may anticipate the binding free energy, which is denoted by:

$$s_1 = g(c_1 - c_{\text{intra1}}) = g(c_{\text{inter 1}}) \quad (2.14)$$

where g is a function, and *f* may be any smooth strictly rising function, perhaps nonlinear. Other low-scoring conformations are also explicitly assigned *s* values in the final result; however, in order to maintain the ranking, cintra of the best binding mode is used.

$$s_i = g(c_i - c_{\text{intral}}) \quad (2.15)$$

For all the analyses in this thesis, I have used a conventional protocol as follows:

Each receptor protein underwent energy minimization in the Chimera program to better prepare it for molecular docking. DFT calculations, molecular modeling, and the Protein Data Bank database have all been used to determine the three-dimensional (3D) structures of macromolecules and 2D nanomaterials (obtained from DFT calculations). Grid spacing was set to 1 Å, and the dimensions of the grid were 126 X 126 X 126 (usually referred to as blind docking). For the docking runs, we employed a Lamarckian genetic algorithm with a population size of 150, a maximum of 2,500,000 evaluations, and maximum generations. Autodock4 analyze program was used to do the post-docking analysis, which included conformations and clustering, and the results were shown in both Chimera and the Discovery Studio Visualizer.

2.8 Molecular dynamics simulations

Potential energy, denoted by the symbol V, may be described in a number of different ways, two of which are molecular mechanics (MM) and quantum mechanics (QM). In contrast to QM, however, MM pays no attention to the motion or electronic state of electrons. The system's energy is determined only by the locations of its nucleons. A number of assumptions, including the Born-Oppenheimer approximation, enable MM to operate in this fashion. However, in some circumstances, MM may provide forecasts as excellent as QM at a fraction of the computer time. However, it cannot offer information on scenarios dependent on the electron distribution, such as chemical reactions, proton transfer, etc., since it just approximates and ignores the electron distribution.

Molecular dynamics, or MD, is a kind of N-body computer simulation in which the potential energy, V, is numerically integrated in accordance with Newton's equations of motion to provide a series of configurations for the simulated system. If we solve these Newtonian equations for each time step, we get a trajectory that specifies the location and velocity of every atom in the system at that instant. Therefore, the trajectory defines the 6N-dimensional phase space, with N amount of particles, in terms of the 3 spatial coordinates (x, y, z) and 3 momentum vectors. Empirical MM computations and what are popularly referred to as Force Fields are the basis for most Molecular Dynamics simulations. Considering explicit water molecules and more precise force fields, MD is more physically correct than docking. Here, though, MD compromises speed for physical precision.

Traditional MD simulations use empirical force fields that are parameterized based on measurements of tiny molecules taken by spectroscopy and calculations of quantum chemistry to describe interactions between atoms and

particles[111]. The Born-Oppenheimer approximation and treating nuclei as classical particles are two approximations that go into this condensed depiction of molecular interactions. The forces on each atom are computed according to the specifications provided by these force fields in each integration step of the equations of motion. Bonded interactions (bonds, bends, and improper bonds) are typically approximated in simulations of soft materials and biological systems by harmonics and torsions approximated by simple periodic functions. Non-bonded interactions are treated as pairwise interactions and are primarily represented by the Lennard-Jones (LJ) potential, while electrostatic interactions are described by Coulomb's law for each pair of charged atoms. The following equation will represent the typical force fields: (equation is adapted from ref. [112]

$$U = \sum_{\text{bonds}} k_b(b-b_0)^2 + \sum_{\text{bends}} k_\theta(\theta-\theta_0)^2 + \sum_{\text{dihedrals}} k_\phi(1+\cos(n\phi-\delta)) + \sum_{\text{improper}} k_w(w-w_0)^2 + \sum_{\text{nonbonded}} \varepsilon\left[\left(\frac{Rmin_{ij}}{r_{ij}}\right)^{12} - \left(\frac{Rmin_{ij}}{r_{ij}}\right)^{6}\right] + \frac{q_i q_j}{\varepsilon_2 r_{ij}} \quad (2.16)$$

where U represent total potential energy, force constants for a given bond, bend, improper angle or dihedral angle *are represented by* k_b, k_θ, k_w and k_ϕ , b_0, θ_0, w_0 are equilibrium value of the corresponding bond length, bend angle, and improper angle, respectively, ϕ is the multiplicity of the given dihedral angle and δ is the phase shift. In the nonbonded term, ε is the energy scale of the LJ potential, Rmin is the interatomic distance where LJ energy is zero, r_{ij} is the distance between two interacting nonbonded atoms, ε_2 (conventionally, ε is used, here ε_2 is used simply to distinguish it from the LJ energy scale ε) in the last term is the dielectric constant, q_i and q_j are the charge of atom i and j, respectively. Other than the LJ potential, another popular form of representing van der Waals interaction between atom types i and j is $A_{ij}\exp(-r_{ij}B_{ij}) - C_{ij}r_{ij}^{-6}$, the exponential function is quite expensive computationally and is usually approximated by splines.

Initial system setting are required for MD simulation setup. Accordingly, it is necessary to provide the positions (x, y, and z) and starting velocities of each atom in the system. For the most part, the initial velocities are drawn from the Maxwell-Boltzmann distribution. Periodic boundary conditions allow the simulated particles to feel forces similar to those of a bulk fluid, despite the very low number of particles used in the simulation. This is accomplished by repeatedly copying a cell of a given form (such as a cubic or an octahedron) in all directions. If a particle leaves a cell via one of its borders, an identical particle enters via the opposite boundary to maintain a constant total number of particles. Using PBCs has the advantage of simulating a bulk fluid more accurately since the solute of interest is shielded from solvent-free surface effects (condition is that the cell dimension has to be large enough). Since MD simulation is itself a vast subject and can only be used to write a thesis as well,

I am giving here references for the programs that I have used i.e., GROMACS [67][68]–[71]and LAMMPS[72]. However, a general protocol for macromolecular and nanomaterials simulation is shown below.

For all the analyses in this thesis, MD simulation using GROMACS v.2019.2 has been performed for the macromolecules, nanomaterials, and also complex molecules (drug bound proteins). The topologies for all the organic molecules were obtained from the PRODRG database [113]. Topologies for nanomaterials have been obtained using CHARMM-GUI[114]. The force fields used for simulating macromolecules and nanomaterials were GROMOS96 54a7[115] and CHARMM36[114], [116]. The whole system was put within a periodic cubic box that was solvated with straightforward solvent molecules with point charges. The particle mesh Ewald approach was used to account for the long-range electrostatic interactions under periodic boundary conditions with a 15 Å limit for nonbonded interactions. To achieve equilibrium, the system was neutralized using Na^+/Cl^-counterions. Every 10 steps, neighbor searching was carried out. With a cut-off of 1.2 nm, the PME technique was applied to electrostatic interactions. Fourth order B-spline interpolation was utilized using a reciprocal grid of 40 40 40 cells.Three phases of energy reduction and equilibration were completed: Using a steepest-descent method, we minimize the entire system, including the ions, solvent, protein, and ligand, for up to 50,000 steps. (ii) Using NVT (number of atoms, volume, temperature) ensemble with a leapfrog integrator and linear constraint solver for holonomic constraints, constraints were introduced to the protein and the ligand dimer for 100 ps during heating. (iii) For the second phase of equilibration, an NPT ensemble was utilized with a time step of 2 fs and constant pressure (1 bar) and temperature (300 K) for 100 ps. Hydrogen to heavy atom bonds were constrained using the SHAKE method. With a time step of 2 fs, the MD production phase for each system has been simulated for various timepoints.

Furthermore, to analyze the adsorption of molecules on nanomaterials, I have used LAMMPS[117] package, which focuses on material modeling using a classical dynamics approach. OVITO[118]and VMD (Visual Molecular Dynamics) [119]were used to visualize the MD trajectories of various structural configurations. The parameters for structural minimization coupled NVT, which is a combination of Langevin thermostat & Nose-Hoover [120] simulations were considered using Dreiding forcefield [121] for both molecules and nanomaterials. The input and data files for the systems were generated using the lammps_interface program [122]. The simulation was performed for varied time scales with a timestep of 1 fs.

Moreover, we have also implemented *ab-initio* molecular dynamics (AIMD) simulation; a method used in computational chemistry and physics to study the behavior of molecules and materials. It is based on first-principles

quantum mechanics calculations and does not rely on any empirical parameters. AIMD simulations are performed by solving the Schrödinger equation for the entire system at each time step, which allows for the calculation of forces and the prediction of molecular motion. These simulations can be used to study a wide range of properties, such as structural, thermodynamic, and electronic properties of molecular systems. To improve computational efficiency, various algorithmic techniques such as Car-Parrinello molecular dynamics, Born-Oppenheimer molecular dynamics, and time-dependent density functional theory are employed in AIMD simulations [123].

3 Chapter 1: Electronic transport at the nanoscale

The design of future nano-scale electronic devices relies heavily on our current understanding of the electronic structure and transport characteristics of nano-scale materials. Materials on the nanoscale range from individual molecules to clusters of molecules, nanotubes, semiconducting quantum dots, and even biomolecules. The science of molecular electronics has made considerable strides in the past few decades, and organic molecules are among the most promising of these alternatives. As the behavior of electrons at this scale is heavily impacted by quantum physics, material properties, and environmental factors, this is a complicated and fast expanding field of research. Nanoscale electronics, energy storage devices, and sensors will greatly benefit from a deeper understanding of electrical transport at the nanoscale. The study of electrical transport at the nanoscale will play a pivotal role in influencing future technology as the desire for smaller, more efficient devices emerges. In this chapter, I have discussed the possibilities of delineating the intrinsic atomistic interactions between biomolecules and materials in devising molecular devices and biosensors for varied applications. The investigation of the physical mechanisms of electron transport, charge transfer mechanisms, and physio-chemical processes at bio-inorganic interfaces has advanced biomedicine and sensing technologies significantly.

A summary of the results obtained through theoretical calculations of electronic transport in the nanoscale regime has been depicted in **Figure 3.1**. I have additionally measured the I-V characteristics of different 2D materials for the DNA nucleobases using nanopore sequencing technology. Because Guanine is an organic compound belonging to the purine group, a class of compounds with a characteristic two-ringed structure composed of carbon and nitrogen atoms, the results I obtained were mostly oriented towards Guanine sensing in the case of DNA. A purine is a heterocyclic aromatic organic compound, consisting of a pyrimidine ring fused to an imidazole ring. It contains two carbon-nitrogen rings and four nitrogen atoms, followed by Thyamine which is a Pyrimidine heterocyclic aromatic organic compound similar to benzene and pyridine, containing two nitrogen atoms at positions 1 and 3 of the six-member ring.

In case of Amino acid sensing, the categories in which amino acids are characterized are non-polar, polar, +charge and -ve charge AA. Amino acids can be classified into four general groups based on the properties of the "R" group in each amino acid. Amino acids can be polar, nonpolar, positively charged, or negatively charged. Polar amino acids have "R" groups that are hydrophilic, meaning that they seek contact with aqueous solutions. Nonpolar amino acids are the opposite (hydrophobic) in that they avoid contact with liquids. These interactions play a major role in protein folding and give proteins their 3-D structure. The nonpolar amino acids are hydrophobic, while the remaining groups are hydrophilic. Likewise in gas sensing mechanisms, most of the materials taken for study have selective sensing performance towards NO_2. Substituents with pi bonds to electronegative atoms (e.g. -C=O, -NO_2) adjacent to the pi system are electron withdrawing groups (EWG); they deactivate the aromatic ring by decreasing the electron density on the ring through a resonance withdrawing effect.

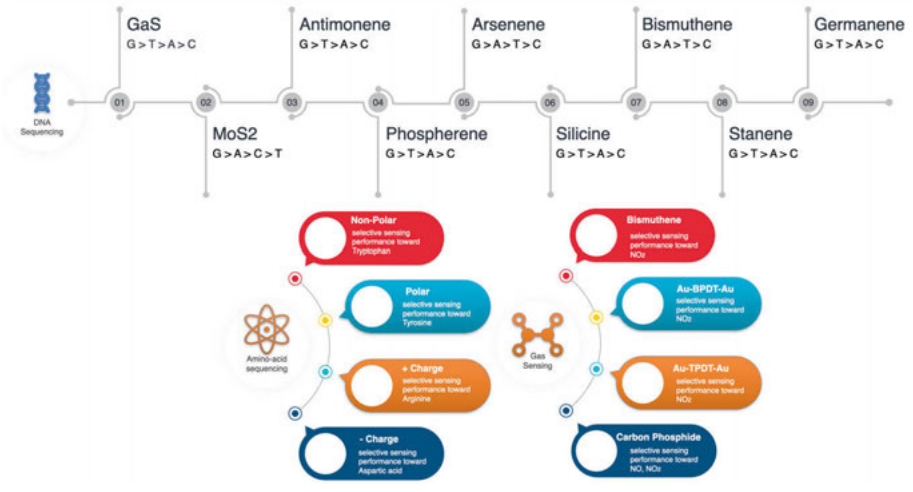

Figure 3.1: Summary of the results obtained in Chapter 1 for different 2D materials which are based on DNA nucleobases, amino acids, and gas molecules.

3.1 Amino acid sequencing in g-C_3N_4

The **Paper 1** discusses g-C_3N_4 , an allotrope of carbon nitride that shares structural similarities with graphene but is made up of heptazine units connected by amino groups. This material has received a lot of attention in the field of materials science because of its resemblance to graphene and its impressive properties (high chemical and thermal resistance, super hardness, low density, wear resistance, biocompatibility, surface modification, water resistivity, an emitting device that produces light, and photocatalysis, to name a few).A metal-free and non-toxic photocatalyst with a visible-light reaction, it is widely regarded as the most stable allotrope in its natural environment. The use of functionalized g-C_3N_4-based materials for photocatalytic hydrogen evolution, CO_2 reduction, pollutant removal, organic synthesis, and disinfection, among other environmental applications, has been the subject of research.

The NEGF method is used to characterize the typical characteristics in terms of transport transmission and current-voltage relationship before and after the amino acid (AA) adsorption, which is then used to illustrate the performance of g-C_3N_4 as a DNA sensor. As entropy generation is generally thought to be a hallmark of resistance, NEGF provides a perturbation theory to characterize these processes as they unfold throughout the channel. The results from the experiment can be used to determine which sensor materials have the required sensitivity. In this case, the probe system is meant to imitate a g-C_3N_4 field-effect transistor, where the central scattering zone is in contact with semi-

infinite sections of the left and right electrodes. Each electrode is represented by a 6 x 1 supercell, and center scattering is considered for 6 x 6 supercells with and without AA located in the center scattering region interacting with three N2 atoms. **Figure 3.2** shows the predicted transmission spectra with no gate bias voltage, separated into five groups based on the amount of AA adsorption, including the spectrum for an undoped g-C_3N_4 monolayer. An asymmetric resistance effect along the [1 0 0] direction can be seen in the transmission at zero bias by observing the variable response to varying bias energies. Near-zero transmission occurs between 1.5 and 0.7 eV, with transmission levels ranging from 10^{-18} G/G_0 to 10^{-16} G/G0, in accordance with the characteristics of semiconductor materials. This transmission appears to be more receptive to the constructive force of the electronic application's left-to-right presentation. Adsorption of AA molecules on the g-C_3N_4 monolayer causes a little change in the energy levels of the absorbed molecules, indicating that the transmission resistance of the monolayer is increased. This is shown in the high order transmission on negative energy and the low order transmission on positive energy. Meanwhile, the g-C_3N_4 system's response to zero bias energy is the slowest for functional groups that interact with the benzene ring, such as Phe. This indicates that the resistance impact of systems will be amplified due to the substantial structural deformation generated by strong repulsive interactions. On the positive energy from 1.5 eV to 2.0 eV, the area is an essential attribute of device transport to produce an available conductance channel by adjusting the energy signals.

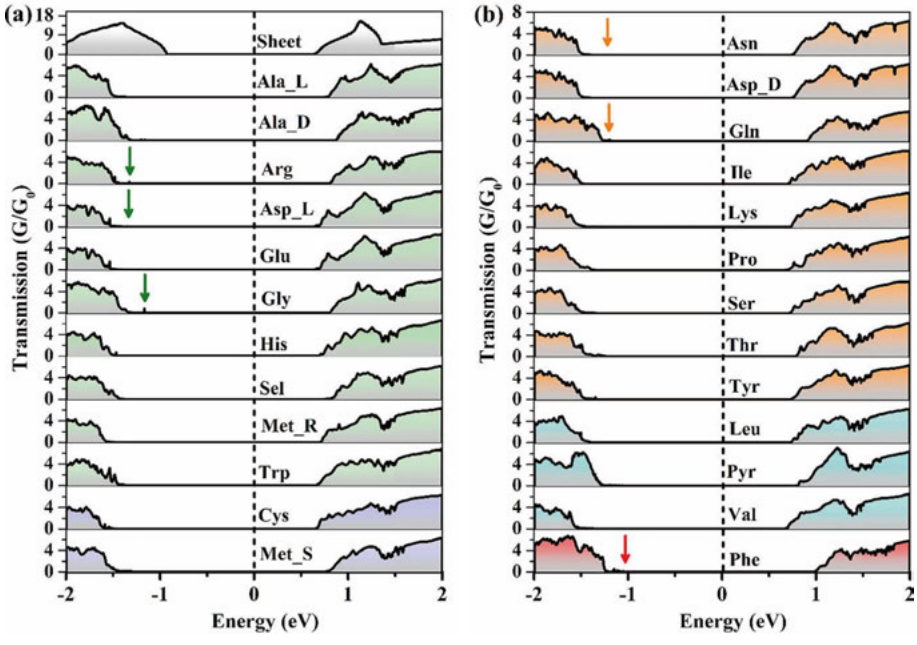

Figure 3.2: Zero-bias transmission spectra for g-C_3N_4 monolayer with and without amino acids. The grey area shows the DOS of pristine g-C_3N_4, the light green area shows the NH_2@amino acids, the light blue area shows COOH@amino acids, the light-yellow area shows the CH_2R@amino acids, the forest green area line shows the CH_3@amino acids, and the light red area shows the benzene ring @amino acids. (Adapted from Paper I)[106]

Figure 3.3 sequentially displays the obtained V-I curves for g-C_3N_4 monolayers with and without AA adsorption at voltages ranging from 1.5 V to 3 V. These results are highly consistent with the analysis of zero-bias transmission's findings, which were made after observing the strong transmission peaks that locate in positive energy after 1.5 eV. Keep in mind that for pristine g-C_3N_4 monolayers with a resistance constant of 3×10^8 Ω, the current increases linearly with voltage from 2.0 V to 3.0 V. However, due to the structural distortion of g-C_3N_4 and the asymmetric distribution of AA molecules, the pristine resistance effect of g- C_3N_4 was broken by interacting with AA molecules. With the exception of the Arg, Ser, and Pyr systems, the current through the pristine g-C_3N_4 monolayer is 10 nA under a bias of 3.0 V, however it somewhat decreases from the pristine condition. In contrast to the current of the Pyr molecule, which is 600 nA, the current for 22 different types of AA molecules ranges from 5 nA to 10 nA. Additionally, we see that the length of the R chain, as in a g-C_3N_4 monolayer with a Pyr molecule, is crucial in reducing the resistance impact of the system. Importantly, the current signal has been seen after 2 V with magnitudes greater than 1 nA (ppb), which can be

recognized by various experimental tests with a sensitivity of nanotube sensor. The g-C_3N_4 monolayer has a lot of unique qualities that make it a potential material for use as a biosensor.

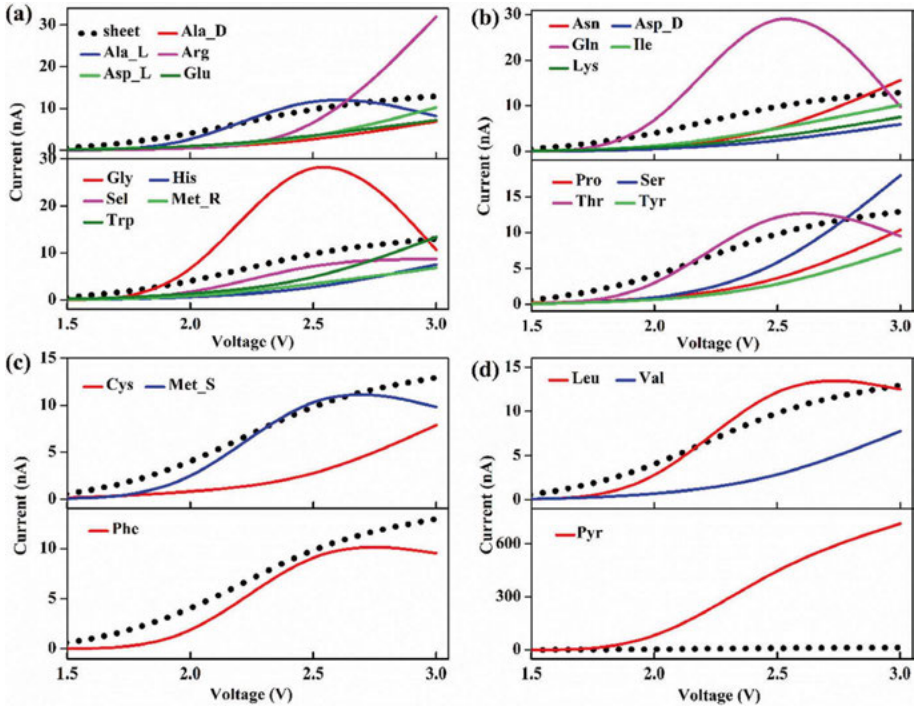

Figure 3.3: Voltage-Current (V-I) characteristics for g-C_3N_4 monolayer with and without adsorbing amino acids. (Adapted from Paper I)[106]

The metal-free semiconductor g-C_3N_4 monolayer was used in this work to create a field-effect transistor. All g-C_3N_4/amino-acids have been found to have strong interactions (covalent or electrostatic hydrogen bonds), which are influenced by the single-pair N2 atom electrons in g-C_3N_4. In addition, through interacting with the NH2 and CH2R functional groups, the g-C_3N_4 monolayer is more likely to adsorb AA. The measured adsorption energy is in the range of 2.232 eV to 1.016 eV, with the following adsorption trend: Trp > Tyr > Asp D > Arg > Asp L > Lys > Gln > Pyr > Met R > Ala D > Ile > Ala L > Met S > His > Phe > Val > Glu > Pro > Asn > Thr > Leu > Sel > Ser > Gly > Cys. With a charge transfer of less than 0.025e, the g-C_3N_4 monolayer can act as an electron donor or acceptor. While all systems preserve their semi-conductor properties, AA adsorbed on g-C_3N_4 monolayer can push the fermi level shifting to a lower energy level throughout the physisorption process. The transmission spectra at the zero bias gate voltage region also show a consistent line on the positive energy from 1.5 eV to 2.0 eV, demonstrating a conductance

channel that is open for use by varying the energy signals. Additionally, the profiles of V-I curves show that after a voltage of more than 2 V, a stable current signal with magnitudes larger than 1 nA Parts per billion (ppb) can be achieved.

3.2 DNA sequencing on single-layer gallium sulfide

Strategies for customized medicine and biomedical applications have been reenergized by the elimination of dependency on the biological regime that it is contemplated or imagined as a conceivable, desirable future occurrence for many researchers. This is because DNA self-assembles from 2D materials through molecular recognition. There have been several 2D materials suggested for theoretical studies that concentrate more on the physisorption of nucleobases. The main obstacle, however, is the nucleobase detection's sensitivity and specificity. Group-III monochalcogenides (MX, where M = Ga, In; X = S) are a promising class of 2D topological insulators and layered semiconductors that have been intensively researched because of their unusual electrical characteristics. An efficient method for modifying the characteristics of 2D materials to cause a variety of phenomena, including physisorption, chemisorption, and numerous biological regimes, is functionalization. Nucleobase physical adsorption hasn't been studied before utilizing a GaS monolayer. The findings of our first-principles investigation into how nucleobases interact with a GaS monolayer surface may provide insight into how single stranded (ss)DNA interacts with the GaS monolayer. GaS monolayer has been examined in prior research and exhibits intriguing anisotropic features, programable optical properties, carrier mobility of 0.6 $cm^2 V^{-1} s^{-1}$, and tunable electronic properties by external electric fields and stresses. It is also a superior photocatalyst for water splitting.

GaS monolayer has been synthesized experimentally, opening up a stable class of 2D metal dichalcogenides (MD) materials and creating a new class of materials that are appealing for optoelectronic applications. Because of these intriguing properties, monolayer GaS is an excellent choice for constructing single-sheet based field-effect transistors, making it suitable for use in high-performance photodetectors on both traditional silicon and flexible substrates (field effect transistor, or FET).

The zero-bias transmission spectra with and without the adsorption of DNA nucleobase pairs AT and GC have been calculated in order to better understand the impact of these molecules on the GaS monolayer. The transmission spectra of the GaS monolayer with and without various gas adsorptions at zero-bias are shown in **Figure 3.4**. The adsorption of the DNA nucleobase pairs AT and GC is dramatically impacted by the zero-bias transmission

spectrum. Attraction of DNA molecules with the nucleobase pairs AT and GC results in a decreased transmission spectra, which can be attributed to backscattering, which limits the number of conduction channels available. A step-like characteristic in the transmission spectra, which is derived from the available conductance channels of distinct energy bands, appears to be a region of zero-bias transmission near and beyond the Fermi level. It is evident that the AT molecule only slightly affects transmission spectra, whereas the GC molecule significantly affects transmission spectra. As seen in **Figure 3.5**, the channels with reduced conductance represent a decrease in passing current.

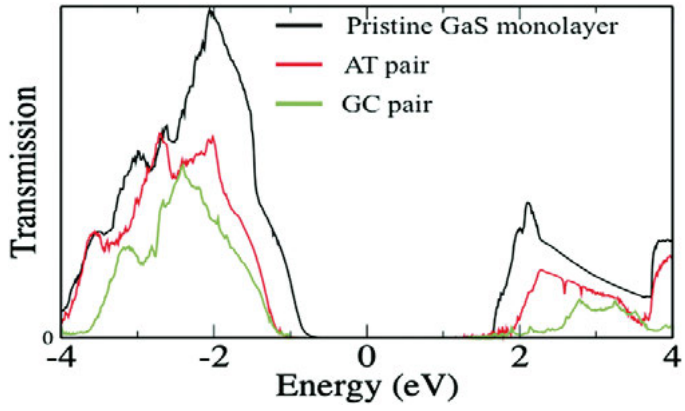

Figure 3.4: *Zero-bias transmission spectra of the pristine GaS monolayer (black line), DNA nucleobase pair molecules AT (red line), and GC (green line) adsorbed on the GaS monolayer. (Adapted from Paper II)*[107]

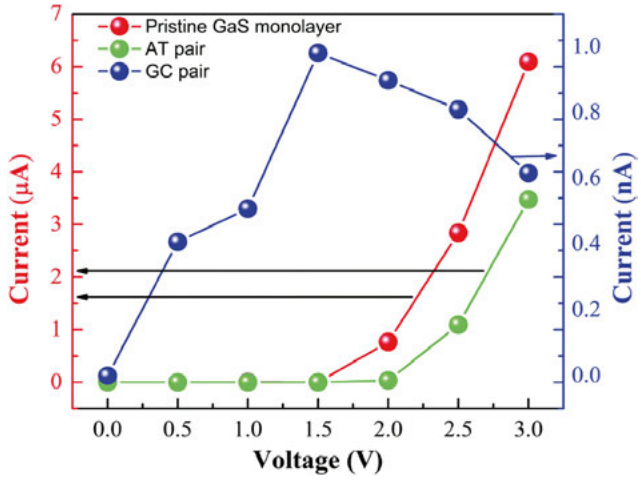

Figure 3.5: *Current–voltage characteristics of (a) pristine GaS monolayer (Red-line), AT pair molecules of DNA nucleobase adsorbed on the GaS monolayer (green line) presented on the* y*-axis with red color (left-side) and GC pair molecules of the DNA nucleobase absorb on the GaS monolayer (blue line) presented on the* y*-axis with blue color (right-side). (Adapted from Paper II)*[107]

The DNA nucleobase pairs AT and GC detections may now be realized via the appropriate current-voltage (I-V) relations, which is advantageous to simulating the I-V curves. The GaS system and its DNA nucleobase sensing features have been carefully constructed. I-V characteristics for the AT and GC pair with the GaS sheet. Due to the presence of semiconducting behavior, the pristine GaS system exhibits almost no Ohmic behaviours through the current characteristics in which current passes through the centre scattering region, which exhibited increasing behavior when the bias voltage was applied with an interval of 0.5 V. The I-V curves for pristine as well as AT and GC pairings with variations up to 3.0 V are shown in **Figure 3.5.** In contrast to the pristine GaS monolayer, the current is decreased when the DNA nucleobase pairs AT and GC engage with the GaS surface. Because AT and GC molecules will increase the resistance of the GaS monolayer by contact with DNA nucleobase pairs, this explains why the current in DNA nucleobase pairs AT and GC that interact with the GaS sheet abruptly becomes reduced. Because there is less binding energy and charge transfer between the GaS sheet and the AT pair, the current increases linearly for the AT pair over 2.0 V. On the other hand, a GC pair exhibits nonlinear behavior in the I-V characteristics because it has strong binding energy and increased charge transfer, which causes it to increase resistance in the GaS sheet and decrease current compared to pure GaS. Surprisingly, it is discovered that the current decreases at particular bias voltage levels, which correspond to the negative differential resistance (NDR). NDR is a crucial characteristic for nanodevices to switch quickly. It is possible to distinguish between DNA nucleobase pairs AT and GC for the purpose of

detection. DNA nucleobase pairs AT and GC appear to have differing resistance and are recognizable from one another. The ON and OFF states of this device can be distinguished by the distinct current signals that are clearly displayed with and without the DNA nucleobase pairs AT and GC. On the basis of the significant differences in current signals caused by the DNA nucleobase pair AT and GC adsorption characteristics, a more popular GaS-based detecting device with higher sensitivity can be built. It is crucial to highlight the behavior of several other 2D materials in this relationship, such as graphene, where the current rapidly decreases with an increase in bias voltage for DNA nucleobase detection beyond 0.4 V. This implies that the properties of a 2D GaS monolayer are superior for modeling and detecting sensing nanodevices.

3.3 Gas sensing using 2D-materials

Designing effective nanosensors for environmentally harmful gases requires a thorough grasp of the practical sensing mechanisms of two-dimensional (2D) materials. The environment may be exposed to several contaminants, such as gases with nitrogen (NO_2, NH_3) and sulfur (H_2S, SO_2) bases, as a result of an unintentional release or maliciously flawed planning. While NO_2 poisoning is detrimental to all forms of life because it can cause heart failure when inhaled, NH_3 poisoning can cause olfactory tiredness even when exposure occurs at low concentrations. H_2S, on the other hand, is a deadly molecule that suffocates and can harm a person's health permanently. H_2S can harm the eyes at relatively modest exposure levels (50 ppm), and at higher doses (1000 ppm), it can even be fatal. Due to its extreme corrosiveness, even short-term exposures to the noxious gas SO_2 have a devastating long-term effect on the lungs. The aforementioned gases are mostly colorless, combustible, and heavier than air, making it difficult to detect them at lower quantities. In this case, depending on the kind and concentration of gases, a highly stable and sensitive gas sensor can produce distinct electric signals. New materials for gas sensors that are clearly selective, stable, reversible, and have quick recovery times are always being sought after.

Next-generation gas sensors are being developed using two-dimensional (2D) nanomaterials because they have a high surface-to-volume ratio, excellent carrier mobility, rich surface chemistry, and low electrical noise. In general, depending on the charge transfer mechanism, target gas molecules adsorbed on a 2D monolayer can either act as electron donors or acceptors, which can change the band structure of the monolayer. Upon the adsorption of specific gas molecules, even the electrical resistance of the 2D monolayers changes noticeably. Similar concentrations of charge carriers brought on by target gas molecule adsorption affect the electrical resistivity of the host 2D material.

We have constructed a nanodevice with two electrodes and a scattering zone to study the transport characteristics of the buckled honeycomb Bismuthene (bBi) nanosheet (Refer **Figure 2.4**).

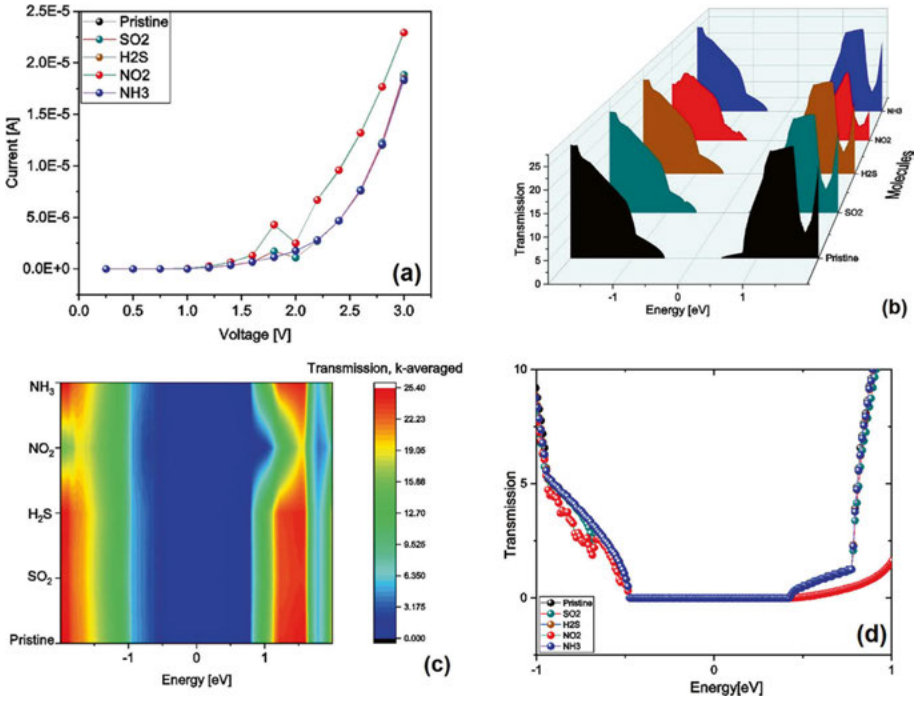

Figure 3.6: (a) I–V characterizes measurements for the bBi sheet and gas-adsorbed sheets, bBi-X_g (Xg: SO_2, H_2S, NO_2, and NH_3). (b) 3D surface map depicting zero-bias transmission with pristine and adsorbed gas molecules. (c) Extended heatmap illustrating the k-averaged transmission plot where red color depicts transmission and blue color depicts transmission at the fermi level. (d) Close-up view of the zero-bias transmission plot at around the fermi level to illustrate the semiconducting behavior of the bBi sheet. Reproduced with permission from American Chemical Society[108]

As gas detection can be accomplished from the corresponding I-V difference with and without gas molecules in a nanodevice, the current-voltage characteristic is a crucial criterion to comprehend the effectiveness of the nanoscale device. **Figure 3.6a**. displays the I-V curves for sheets with and without gas molecule adsorption at various voltages up to 3.0 V. The bias was raised in a periodic order by 0.5 V every step, and self-consistent calculations were carried out at each step to obtain the I-V curve. Due to its semiconducting nature, which was determined by calculations of the electronic structure, the pure bBi monolayer almost exhibits the nonlinear curve in I-V characteristics. The

study clearly shows that when the bBi nanodevice is exposed to harmful gases, the current decreases due to the obstructed conduction pathways given by the gas molecules in the sheet, resulting in resistance in the device. Figure 5a represents the I-V trends up to 1.5 V.

These findings support the electrical structure and charge transport properties previously mentioned. Even though the I-V trends for the SO_2, H_2S, and NH_3 gas instances are similar, they are comparable to those of pristine sheets, and the current variance is sufficiently substantial in comparison to that of most 2D sheets. Under 3.0 V bias, the value of current for pure bBi can reach up to 2.0×10^{-5} A, however. it can decrease to 2.0×10^{-5} A following gas molecule adsorption, which is a meaningful quantity to detect in studies. Additionally, when using a paramagnetic gas, such as NO_2, the device's current can reach up to 2.0×10^{-5} A. The extra unpaired electrons in NO_2 that are shared by the surface and the molecules that have been adsorbed cause a significant decrease in current. This localization of the electron distribution near the site of adsorption blocks the transport channel and raises the resistivity of the device when it is biased. It is suitable for sensing these harmful gas molecules because of the substantial decreases in current. The current is lower than it would be with clean bBi when the gas molecules interact with the surface. The I-V characteristic fluctuates linearly or nonlinearly as a result of the contact or adsorption of gas molecules on the bBi sheet due to its resistance. Because NO_2's binding energy is higher than that of the other gas molecules, the current is suppressed in all gas molecules other than NO_2, for this reason. Since there is less binding energy and charge transfer between bBi and the gas molecules in the cases of SO_2, H_2S, and NH_3, the current drops linearly above 1.5 V. Contrarily, NO_2 exhibits nonlinear behavior in the I-V characteristics and causes greater resistance in the bBi sheet due to its high binding energy and increased charge transfer, which reduces current compared to pure bBi. Surprisingly, it is discovered that the current decreases at particular bias voltage levels, which correspond to the negative differential resistance (NDR). NDR is a crucial characteristic for nanodevices to switch quickly. A different distinction can be made for the detection of gas molecules. **Figure 3.6 (b-d)** shows the zero-bias transmission (zbt) graphs for the bBi sheet and the bBi-Xg (Xg/SO_2, H_2S, NO_2, and NH_3) gas-adsorbed sheets. The zbt plot displays the pure bBi sheet's semiconducting properties. While all the other gases only showed slight alterations, the observed transmission function for NO_2 gas molecules indicated significant decreases. Compared to other adsorbed gas molecules, NO_2 exhibits a greater change in the transmission function around the Fermi level.

Similarly, we have also investigated gas sensing mechanism on monolayered carbon phosphide (CP) (not included in the thesis papers), with semi-metallic electrical conductivity and graphene-like Dirac cone responses **(Figure 3.7)**.

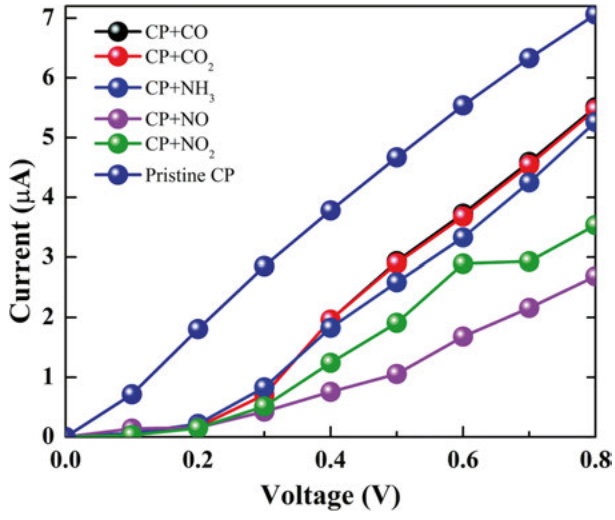

Figure 3.7: The I–V curves for pristine CP, and the CP monolayer with the CO, CO_2, NO, NO_2 and NH_3 adsorption. Adapted from ref. [107]

In conclusion, the study described here carefully examines the structural, electrical, and transport characteristics of a pure CP monolayer as well as the adsorption of CO, CO2, NO, and NH_3 on the CP surface. The CP monolayer's electrical characteristics exhibit semi-metallic behavior, with Dirac cones showing that this behavior is extremely anisotropic (semi-metallic behavior in the x-direction and a finite band gap in the y-direction). The γ -CP monolayer has better carrier mobility because it contains Dirac cones. Each molecule has been examined and has demonstrated physisorption interactions on the CP surface as we have analyzed the interactions of the hazardous gas molecules with the CP monolayer. These findings demonstrate that, in contrast to other hazardous gases, the toxic gases NO and NO_2 include nitrogen and interact strongly with the CP monolayer. The more sensitive CP surface is thought to be responsible for these two gases' noticeable differences in the electronic DOS and charge transfer mechanisms. According to the transport estimates, the reduction in current signals caused by gas molecule adsorption on the CP surface may be readily observed through experimental testing. It has been noted that the different current signals for the gas molecules NH_3, NO, and NO_2 show considerable variations in conduction channels above 0.2 V. These changes could also be seen in zero-bias transmission spectra. The scientific importance of this transport behavior in the CP monolayer makes the gas molecules relatively simple to recognize and classify. The study therefore shows that the CP monolayer material may be a better choice for superior gas sensors by offering sensitivity and selectivity.

3.4 Gas sensing in nano-molecular electronics devices: NanoMoED platform

Chemiresistors are a great option for miniaturizing gas sensors since they have a size range of nanometers to microns and feature an electrical connection to the transducer unit that makes it simple to integrate them with other electrical components. Metals, metal oxides, or polymers make up traditional chemiresistor sensors. Metals are mostly utilized for the selective detection of a small number of gases, such as H_2, whereas metal oxides and polymers are sensitive to a wide range of gases. The disadvantage of metal oxide thin film-based sensors is their low gas selectivity. They also have to deal with the discomfort of functioning at high temperatures between 100°C and 300°C. Polymer-based sensors have the potential to be more precise and work just as well at room temperature. The sensors do, however, have a limited lifespan because gases permeate the polymer and bond to the molecular chains. Thus, the sensor response of a polymer-based gas sensor depends on modifications to the polymer's electrical structure as well as swelling after contact with gases. As a result, it might be more challenging to understand the response of the polymer sensor than the response of a metal oxide-based sensor. When analyte gases interact with free-standing conjugates, conducting molecules that are in touch with metallic nanoelectrodes, as in a more straightforward situation, can be produced. In this instance, the NO_2 gas sensor response may be directly explained by the alteration in the sensor molecule's transmission function and density of states as a result of the analyte gas's adhesion to the sensor molecule. Since the single conjugate molecule is directly exposed to the gas surface and no diffusion through the material is required, adhesion and desorption should be simpler to interpret than in the case of the polymer thin film. As a result, one would anticipate that the selectivity of such a nano gas sensor would be similar to that of a polymer sensor.

These nano-molecular electronic devices (nanoMoEDs), in which the electrical current passes through three to four junctions between nanoelectrodes, were used for the gas sensing tests. A gold nanoparticle (AuNP) and at least one molecule can be found at each junction. The change in electrical resistance is caused by the alteration of the conduction channels following the physisorption of the analyte gas at such a molecule-AuNP junction. The effectiveness of the physisorption, as determined by the adsorption energy and the subsequent change in the density of states of the sensor molecule, will therefore be the key determinant of the gas sensor response in these devices.

In this study, we employ a streamlined procedure to manufacture the AuNPs and analyze the NO_2 gas sensor response in such nanoMoED devices made from those functionalized AuNPs and by using 1,8-biphenyl-dithiol (BPDT) as the sensor molecule. Triphenyldithiol (TPDT) is also used to study the

sensor response in the nanoMoED gap. The devices are subjected to NH_3 as well as varied ethanol concentrations to examine the selectivity of this sensor. Both the response as a function of concentration and the response times are compared. The outcomes are contrasted with transmission functions derived from density functional theory (DFT) simulations. The transmission spectrum denotes the probability for an electron with incident energy *E* to transfer from the left semi-infinite electrode to the right electrode.

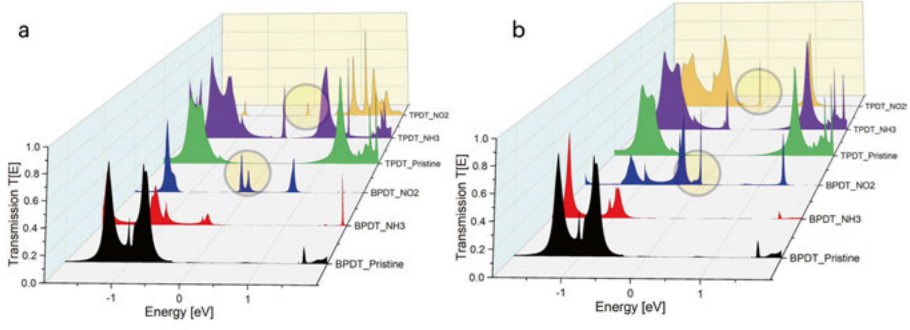

Figure 3.8: Transmission spectra of the nanoMoED system with NH_3, NO_2 adsorbed on BPDT and TPDT molecules. (a) chemisorbed (b) physiosorbed state, respectively.

The transmission function under zero-bias for the pristine and gas-adsorbed systems were shown in **Figure 3.8** and witnessed an observable effect for particular gases e.g., NO_2. At the Fermi level, the influence of gas molecules adsorption decreases the transmission function. This decrease in transmission function is attributed to back scattering, which inhibits the available conduction channels. It was observed that, there is a region of zero-bias transmission near and beyond the Fermi level which is attributed to step-like feature in transmission spectra is from the available conduction channels of various energy bands. It was evident that NO_2 induces substantial effect in the transmission spectra while NH_3 have smaller effect overall in both the BPDT and TPDT cases. This is because of the reflection of reduced conduction channels on passing current and the decrease in conduction channels in both the gas molecules NH_3 and NO_2 which depicts interaction and charge transfer with BPDT and TPDT molecules. To comprehend the scenarios of chemisorption and physisorption, we have depicted the cases individually in the below section.

The zero-bias transmission functions for BPDT pristine and adsorbed gas molecules shown reduction in conduction channels, which arises from the backscattering that inhibits the conduction channels. In the case of NH_3, the reduced intensity of transmission spectra denotes that there is smaller

interaction with the surface (BPDT) and less charge transfer. NH_3 in this case gains electrons from the surface of BPDT which in turn increases the current flow intensity in comparison to pristine BPDT. BPDT is an aromatic organic compound and have π orbitals that makes them appropriate candidate for fast switching of nanodevices. However, there has been less interaction of NH_3 with BPDT in chemisorption state followed by gain of electrons from the surface of BPDT. So, the current flow has not been affected by the negative differential resistance (NDR) and in turn shows increased current under different voltage bias. NDR is an essential property for fast switching of the nanodevices. In the case of physisorption of NH_3 with BPDT, a peculiar observation has been depicted where the current intensity has been substantially decreased as compared to the pristine BPDT. This has also been observed in the transmission spectra where there is a substantial decrease conduction channels after the adsorption. While in the case of NO_2, the NO_2 loses electrons to the surface of BPDT that means more charge transfer to the surface. This is due to the sharing of unpaired electrons in NO_2 molecules. The charge transfer between the NO_2 and BPDT surface is substantially higher than NH_3 and is observed from the zero-bias transmission spectra where there is a peculiar peak near the Fermi level when the gas is adsorbed.

Also, when looking into the interaction profile, NO_2 in both chemisorbed and physiosorbed state shows π interaction with the aromatic ring of BPDT which can be attributed to the re-arrangements in energy levels of π-electrons in BPDT. This peculiar interaction and re-arrangements in energy levels was also seen in the transmission spectra where there is maximum of electrical conductance in negative potential as compared to BPDT. Comparing BPDT and TPDT in terms of molecular length also have significant effect in conduction channels (transmission spectra). The adsorbed NO_2 gas molecule interacts significantly in chemisorbed and physiosorbed state via π orbitals where charge transfer has been occurred between the Oxygen atom and the BPDT. This in turn increases the current flow as more charges have been accumulated on the surface. It is a well-known fact that when there is a strong binding energy, it induces more charge transfer and resistance. This resistance is called the negative differential resistance (NDR) which is an essential property for fast switching of the nanodevices. In our case, NO_2 adsorption, the NDR is less because of the rearrangement of in energy levels of π-electrons. This in turn increase the current where the current flow path is attributed to the surface which is why we have observed increased I-V characteristics in BPDT. In the case of TPDT, the adsorption of NO_2 in chemisorption state formed an unstable complex which resulted in positive binding energy, which is also reflected in the transmission function and IV characteristics, where there is a reduction of the transmission spectra near the Fermi level **(Figure 3.9).** This can also be attributed to increased NDR and reduced current when compared to NH_3.

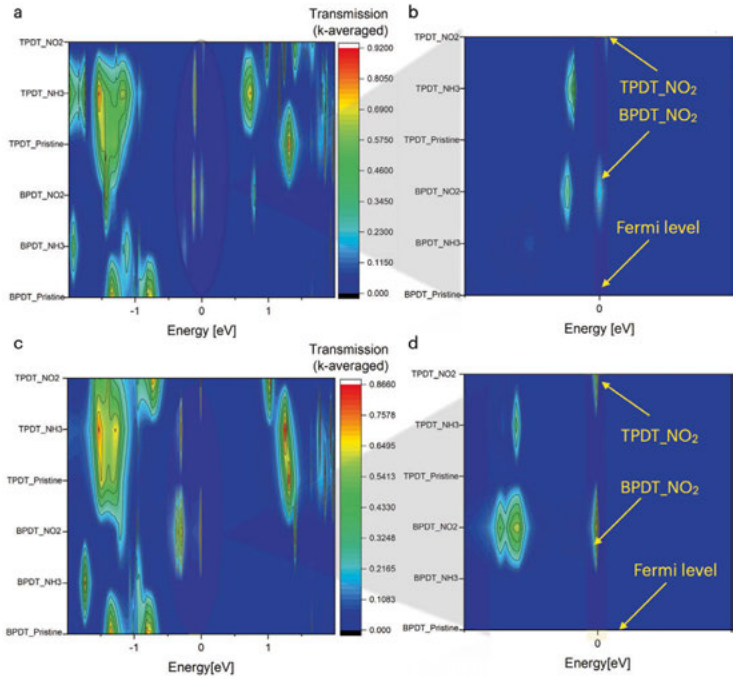

Figure 3.9: Heatmap of the transmission spectra of the nanoMoED system with NH_3, NO_2adsorbed on BPDT and TPDT molecules. (a-b) chemisorbed (c-d) physio-sorbed state.

One essential specification to understand the efficiency of the nanoscale device is the current–voltage characteristic, as gas detection can be achieved from the corresponding *I–V* difference with and without gas molecules in a nanodevice. To get the *I–V* curve, the bias was increased in periodic order by 0.2 V per step, and self-consistent calculation were performed at each step. *I–V* traces for the gas adsorbed system with the pristine system is shown Figure 3.4.3. The figure represents the *I–V* trends up to 1.0 volt, and it is evident from the study that, when the BPDT is exposed to the gas molecules, current drops due to the inhibited conduction channels offered by the NH_3 in the sheet, which results in resistance in the device. In the case of TPDT, an increased trend of *I–V* characteristics has been observed for NH_3. These observations are implicative of the electronic structure and charge transfer characteristics discussed antecedently.

In the case of para-magnetic gas i.e., NO2, the I-V characteristics showed a negative trend in TPDT and an increased trend in BPDT. This significant drop (negative trend) in current comes from the extra unpaired electrons in these two molecules shared between the surface and the adsorbed molecules, which somehow localize the electron distribution around the adsorption site, which consequently blocks the transport channel and increases the resistivity of the

device under bias. These significant drops in current make it suitable for sensing these gas molecules. In BPDT, the increased trend in current comes from the rearrangement of π orbitals and the stable interaction between the NO_2 and surface. Overall, the response of TPDT (0.7 μA to 1.0 μA) is lower than BPDT (1.0 μA to 3.5 μA). The trend has been also experimentally verified.

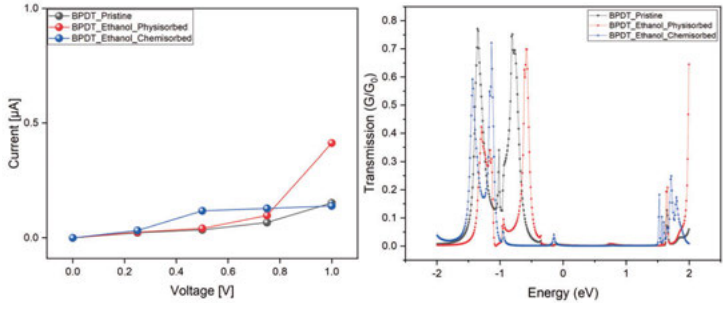

Figure 3.10 : *I-V characteristics for the nanomolecular setup using BPDT with Ethanol.*

When ethanol has been adsorbed on the surface of BPDT, we see low response of I-V characteristics (current)as compared to NH_3 and NO_2 gases. **(Refer to Figure 3.10).** Furthermore, the CI-NEB method was used to explore the gas molecules NH3 and NO2 diffusion paths with their corresponding minimum-energy profiles (MEPs) scattered on the surfaces of the BPDT and TPDT devices to confirm the states, favourable positions of the gas molecules, and predict the transition states. The position of the gas molecules was taken from the VASP optimised calculations. We have observed that all the molecules that were placed close to the substrate molecules were moved faster away from their respective position. That means, the molecules are favourable only in their physiosorbed state but not in chemisorbed state. This has been reflected on the MEP which are depicted in Paper IV. For NH_3 physiosorbed on BPDT and TPDT, the minimum energy barrier path (saddle points) is assessed to be -0.35 eV and -0.5 eV respectively, whereas for NO_2, -0.5 eV and -0.7 eV respectively. In other words, extra energy is required to dissociate NO_2 from the two surfaces aforementioned. Different types of devices functionalised with BPDT and TPDT showed a good, though different, sensor response to NO_2 . The sensor response to NO_2, NH_3, and ethanol is significantly different, which sets the basis for the use of nanoMoED sensor devices as gas sensors operating at room temperature and with good selectivity. We could affirm from our DFT simulations that the gas adhesion and sensor response depend on the direct interaction between the analyte and sensor molecules.

4 Chapter 2: Contact electrification: Interface mechanism

In materials science, the term interface mechanism refers to the study of the interactions and phenomena occurring at the boundary between two different materials. The interface plays a crucial role in determining the properties and behavior of a material and understanding the interface mechanism is crucial for the development of new materials and technologies. Researchers in materials science study the interface mechanism by analysing the atomic and molecular interactions, chemical reactions, and energy transfers that occur at the interface. They also examine the effect of external factors such as temperature, pressure, and electrical fields on the interface and its properties. The knowledge gained from the study of interface mechanisms is applied in various fields, including electronics, energy storage, and biomedicine, to create new and improved materials with enhanced performance and functionality.

One such phenomenon is Contact Electrification, in which electric charges are transferred between two objects that are brought into direct contact and then separated. This process can result in the creation of static electricity, which can have various effects, such as producing sparks, attracting, or repelling objects, or interfering with the proper functioning of electronic devices. Contact electrification is a fundamental concept in physics and has important implications in various fields, including electronics, material science, and tribology.

Some of the major conclusions have been illustrated in this chapter from the perspective of the solid-liquid interface. Adsorbed water on surfaces, where H^+ and OH^- ions may transmit charges to the surface of the materials, is a well-studied example of the triboelectric effect. However, the concept of charge transfer from liquid to solid contact is still debatable, unlike solid-to-solid contact. The solid-liquid interface is therefore the main challenge for the researchers in investigating the effect of ions on the surface of the materials. On the other hand, CE between two metals or between metals and semiconductors is caused via electron transfer, which has been extensively researched in the past. The fluidity and dispersibility of liquids, as well as the adsorption of molecules and ions on surfaces, make it challenging to accurately describe the processes at the solid-liquid interface.

Many hypotheses have been put forth in the past proposing that physiochemical reactions, experimentally verifiable phenomenological characteristics, such as the wettability of materials by water and relative humidity, and ion adsorption, are the basis for electrification or charge transfer. The impact of electrified solid and fluid interfaces on the interfacial transfer of charges reveals how well energy transformation and storage systems like batteries, fuel cells, and electrolyzers operate. The pace at which an ion is moved from a liquid to a solid phase determines intercalation, a crucial process in Li-ion and Na-ion batteries, and it depends on both the bulk electrode's (or electrolyte's) properties as well as those of the interface.

Numerous processes and phenomena, including electron transfer, ion transport, and material transfer, have been used in research on solid-solid CE to define distinct types of triboelectricity (interfacial charge transfer for a wide variety of materials). It is now thought that the primary cause of many innovations and physical-chemical phenomena, including liquid-solid triboelectric nanogenerators (TENGs), electric double-layers (EDL), and hydrophobic and hydrophilic surfaces, is liquid and solid CE. One example of this is the charging of moving water inside a pipe. But since there is so little information on liquid-solid CE and because interfacial charge transfer has been poorly understood for decades, there is still some debate over the identity of the charge carriers (ions and electrons) in solid-solid CE. With no reference to an ion transfer mechanism, Wang et al. [29] recently characterized the charge carriers that have been recognized as solid-solid CE electrons based on photoexcitation and temperature-dependent effects on charged surfaces.

4.1 Mechanistic viewpoint on solid-liquid interface

Triboelectrification, also known as contact electrification, has been a common occurrence for more than 2600 years. The phrase contact electrification suggests a complex phenomenon involving mechanical contact or sliding of two materials involving numerous physico-chemical processes, therefore the scientific knowledge of this phenomenon is not yet fully developed. In contrast to the conventional view of ion adsorption, recent experimental evidence reveals that electron transfer occurs in contact electrification between solids and liquids. In order to explain the phenomenon of interfacial charge transfer, we have used the Density Functional Theory formalism, which is based on a first-principles theory combined with temperature-dependent *ab initio* molecular dynamics. The model captures the kinetics of charge transfer following the adsorption of various ions and molecules on AlN (001), GaN (001), and Si (001) surfaces, revealing the role of interfacial charge transfer and predicting charge transfer discrepancies between materials. When various ions that contribute to physiological pH changes in aqueous solutions, for example, HCl

for an acidic pH and NaOH for an alkaline pH—are adsorbed on the surfaces, we have shown the significant differential in charge transfer between fluids and solids. Additionally, a precise picture based on the electron localization function has been offered as proof of contact electrification, which could provide insight into solid-liquid interfaces.

On three different surfaces, the effects of theoretical computations using combinatorial DFT, and traditional molecular dynamics simulation techniques have been thoroughly studied. The fundamental knowledge of this study can be attributed to the physiological pH effect, which can modify the interfacial charge transfer mechanisms (HCl is acidic, NaOH is basic, and NaCl is neutral). In other words, using this method, contact electrification, has nearly contributed to the physical meaning of the term. We have investigated the atomic scale analysis utilizing a first principles theory based on the DFT formalism, in contrast to earlier research that merely considered the adsorption energy of various molecules and gases on solid surfaces **(Figure 4.1).** The investigation uncovered some fascinating facts, such as the correlation between the work function, binding energies and the basic tenets of physics. The interfacial charge transfer does appear to be driven by coordination chemistry in some situations, such as NaCl and NaOH. Nevertheless, many achievements in the real world can be attributed to a paradigm shift in the realm of power generation and storage. Thus, an effort is made to comprehend some of the fundamental ideas, and more intriguingly, theoretical ideas like the DFT formalism can be used to simulate the practicality seen in everyday life.

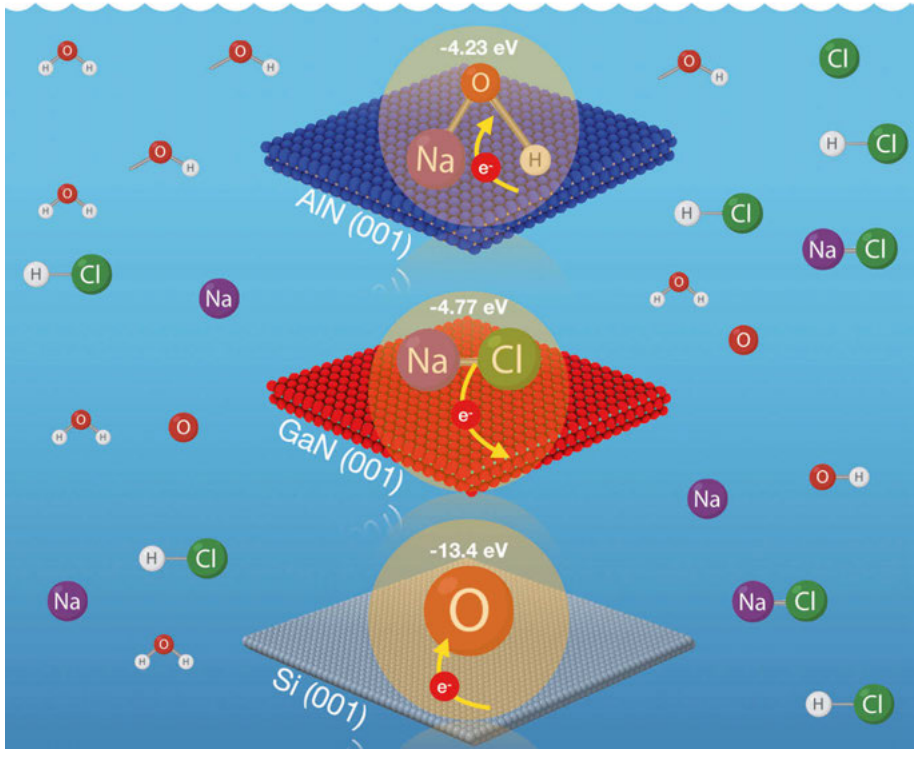

Figure 4.1: *The binding energies of the molecules and ions adsorbed on the surface of AlN (001), GaN (001), and Si (001). (Adapted from Paper V ref.* [124]

The negative adsorption/binding energy (Eb) denotes exothermic adsorption in accordance with the binding energy formula discussed in section 2.4. The binding energies for ions and molecules on various surfaces are shown in **Figure 4.2** and range from 13.4 eV to 0.09 eV. As previously mentioned, Si (001) surfaces have greater ion and molecule binding energies than GaN (001) and AlN (001) surfaces. AlN, GaN, and Si are the order in which the binding stability rises. Furthermore, with AlN but not with the other two surfaces, the OH ion tends to be in the range of positive binding energy. The singlet O atom on the surface of Si has contributed the most efficient binding energy, followed by NaCl > Cl > H > H2O > NaOH > Na.

The comprehensive analysis explains the mechanisms of adsorption or binding, with Si (001) surface typically having the highest adsorption energies followed by GaN and AlN. Additionally, as depicted in **Figure 4.2b**, there has been a negligible inherent effect of vdW forces on the adsorption energies. The molecule's contribution to the adsorption potential of van der Waals forces increases with molecule size. Van der Waals forces, which are often weak forces, impact electrostatic attraction between otherwise non-attracting atoms and molecules when they do not naturally attract one another. Similar

findings were drawn from the potentials for adsorption, where vdW forces have comparatively lower adsorption energies.

The investigation indicated above showed the impact of ions and molecules on various surfaces as well as the strength of their binding. In other words, pH modulation based on ionic concentrations was the main focus of our research. H_2O behaves as both an acid and a base because of its amphoteric character, which includes the presence of H atoms that can donate H+ ions and lone-pair electrons that can embrace H+ ions. Similar to NaOH, which breaks down into Na^+ and OH^- ions when dissolved, HCl is categorized as an acid because it transfers H^+ ions to the solvent (water) when dissolved. NaCl, a salt created by the reaction of NaOH + HCl = NaCl + H_2O, strongly bonds to all surfaces out of all the binding energies shown, with the exception of the singlet oxygen ion. This covalent bond is discussed in more detail in the following sections. Analysis of NaCl, which is a mixture of a strong acid (HCl) and base, can be used to show the strength of acids and bases' binding to all surfaces (NaOH). Additionally, the strength of both the physical and chemical bonding to the surfaces can be determined by the charge transfer between the various ions and molecules. The singlet O atom prefers to behave as an acceptor while Na always acts as a donor among all molecules and ions. Depending on the electronegativity of the elements, certain ions, and molecules, including NaOH, H_2, H_2O, HCl, and NaCl, tend to lose or gain electrons. According to **Figure 4.3**, while other molecules like NaCl and NaOH transfer electrons to the surface, H_2, H_2O, and HCl act as electron acceptors. Apart from that, all of the ions—Cl, H, O, and OH—gained electrons from the surface due to the stronger electronegativity of these elements, with the exception of Na ions. **Figure 4.3** displays the specific charge transfer values in detail.

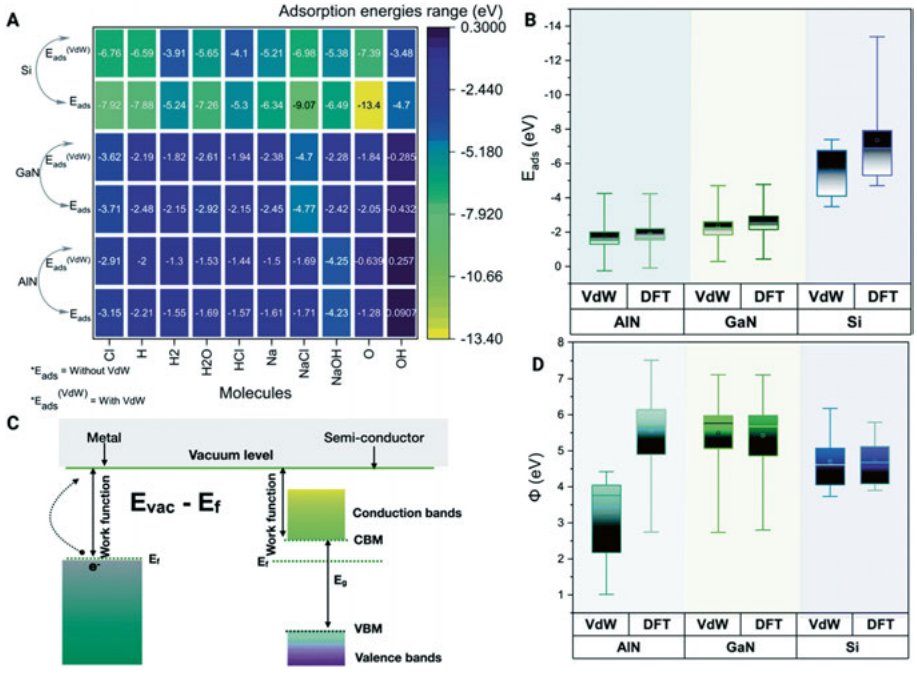

Figure 4.2: *(A) Heat map depicting the binding energies of the molecules and ions adsorbed on the surface of AlN (001), GaN (001), and Si (001) with and without the effect of vdW forces. (B) Box plot illustrating the overall effect with and without vdW forces (DFT) on binding or adsorption energies. (C) Schematic of the work function Φ in the case of (A) metals and (B) semiconductors. (D) Box plot depicting the work function relation (eV). All the box plots are depicted with 25% to 75% percentile and minimum and maximum points with median energies (eV). (Adapted from Paper V ref.* [124]

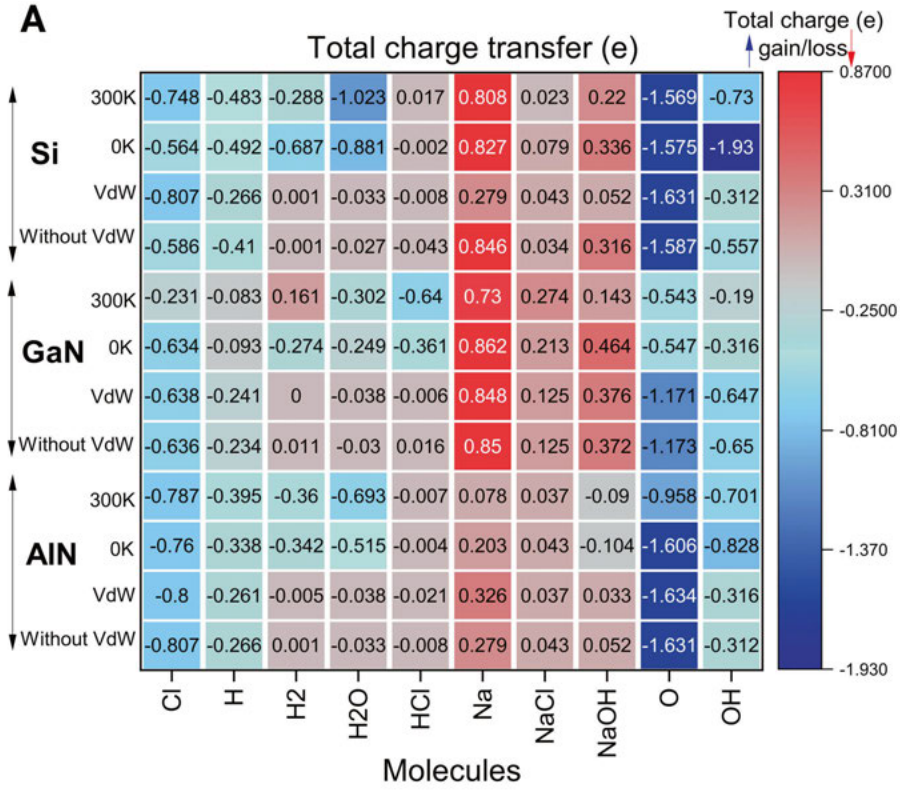

Figure 4.3: *(A) Charge transfer between the adsorbed ions/molecules on the three different 001 surfaces (AlN, GaN and Si) analyzed through Bader charge analysis during the relaxation of the complex system with and without vdW forces and at 0 K and 300 K. (Adapted from Paper V ref.* [124])

5 Chapter 3: Nanomaterials with complex architectures

Complex shaped nano and microstructures from metal oxides/nitrides offer multifunctional applications because of their extra-ordinary nanoscale size (*i.e.*, high surface to volume ratio) and shape dependent physical and chemical features. Because of their intriguing electrical, optical, and chemical properties, these nanoscale structures have enormous application potential in a wide range of advanced technologies, including modern devices ranging from energy harvesting to sophisticated bioelectronic devices. In fact, all the nanostructures exhibit interesting properties. However, when it comes to utilizing those features, their very short lifespans entail a lot of integration complexities. Therefore different shapes (0D, 1D, 2D, 3D) and sizes of these nanostructures in different forms have been of significant interest with respect to various applications. A particular shape of nanostructure, for example one dimensional (1D) nano- rod/nanowire, enable simple handling steps. Simultaneously, the nanoscale-shape dependent properties are used, as in the case of a nanowire-based electronic device for gas sensing, photodetection, energy harvesting, and so on. The shape of the nanostructures indeed exhibits very important role in context of better utilization of their nanoscale properties. Various nano- and micro- structures (simple and complex shaped) from different metal oxides (ZnO, SNO_2, etc.) and metal nitrides (GaN, AlN, *etc.*) have been synthesized and accordingly utilized for various applications.

Nanomaterials with complex architectures are gaining significant research interest over an interdisciplinary community as they offer lot of flexibilities ranging from their simple and efficient utilizations to hybridize their surface with desired functional organic/biomolecules. These nano- and microscale structures' unique properties make them suitable for a wide range of interesting technological applications, particularly in the field of green energy, such as bioelectronics, biofuel cells, and so on.The main goal here is to investigate the unique potentials of tailored interfaces using new nanomaterials with programmable operations in response to structural morphologies. Novel hybrid materials with such functionalities will be aimed for bioelectronics and biofuel cell applications. The responsiveness of our “smart” architecture of the tunable electro biocatalytic interfaces can pave the way for bioelectronics through a ‘built-in’ program of unique physical, structural, or morphological features

of hybrid nanomaterials. At a given stimulus, these properties can provide changes in physical insights related to volume-phase transitions, electrical conductivity, zeta potential, dielectric constant, mechanical flexibility, permeability, wettability, and viscoelasticity. These complex architectures, such as 0D, 2D or 3D nanomaterials, have been investigated using nano-informatics approach through the use of molecular modeling and docking to elucidate the interaction mechanisms.

5.1 Molecular interaction of 2D nanomaterials with macromolecules

The visible-light responsive element g-C_3N_4 with a bandgap of 2.7 eV and the capacity to resist heat, strong acid, and strong alkaline conditions are shown in paper I. Because of the benefits mentioned above, it has been used more efficiently and effectively in water splitting, CO_2 photoreduction, organic pollutants purification, organic synthesis, and other applications. Utilizing bioinformatics techniques, one application, such as the antibacterial capabilities of g-C_3N_4, has been demonstrated. **Figure 5.1.1** provides a schematic illustration of the combination of DFT and in-silico methods for water disinfection and microbiological control. The molecular docking method has been used to show how g-C_3N_4 inhibits the assembly of the outer membrane protein of E. coli, bamA. Beta-barrel proteins were assembled and inserted into the E. coli outer membrane with the assistance of the bamA protein. Membrane depolarization caused by g-C_3N_4- bacterial surface contacts set off the generation of ROS, which damages cellular macromolecules like protein, DNA, and lipids. The role of proteins like dnaK, sodA, sodB, sodC, and soxR was shown to channel the induction of oxidative stress in E. coli. The molecular interaction of the g-C_3N_4 monolayer with the bacterial proteins of E. coli is shown in **Figure 5.1.**

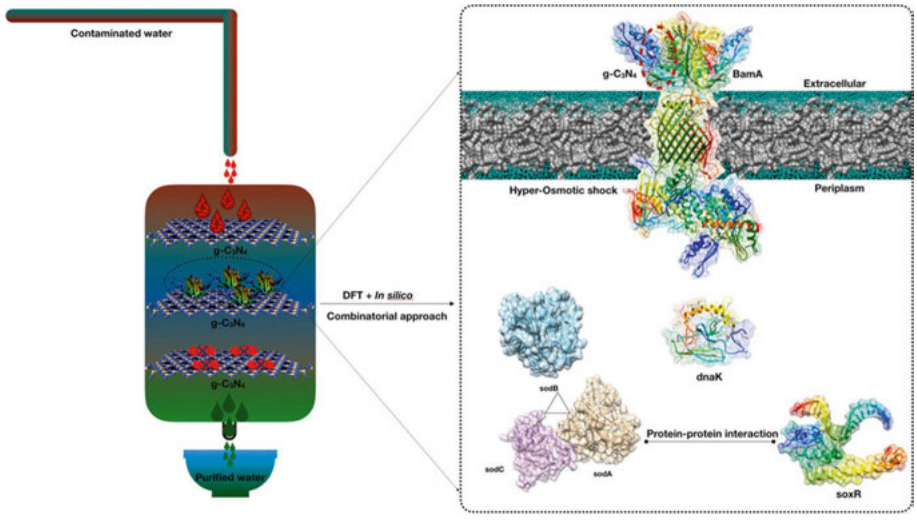

Figure 5.1: *Schematic illustration of the Combinatorial approach (DFT + In silico) used in Paper 1. Adapted from Paper I ref.)*[106]

Numerous investigations have shown that g- C_3N_4 has antibacterial properties. The creation of more ROS, primarily hydroxyl radicals and singlet oxygens, as well as the build-up of g-C_3N_4 on bacterial surfaces, which cause disruption of cellular function and membrane disorganization, are the likely mechanisms that may be pictured in this context. Additionally, in order to illustrate the effectiveness of binding and sensing functions, we examined the binding affinities of each amino acid (AA) on the surface of g-C_3N_4. We have demonstrated one potential use for the previously demonstrated water disinfection technology, g-C_3N_4, which has AA sensing capabilities. However, the inherent molecular interactions have not yet been investigated. In light of this, we explicitly illustrated the intricate chemical mechanism of the interaction between the gram-negative bacteria E. coli related proteins and the g-C_3N_4 monolayer, which results in the rupture of cell membranes and, ultimately, microbial control **(Figure 5.2).**

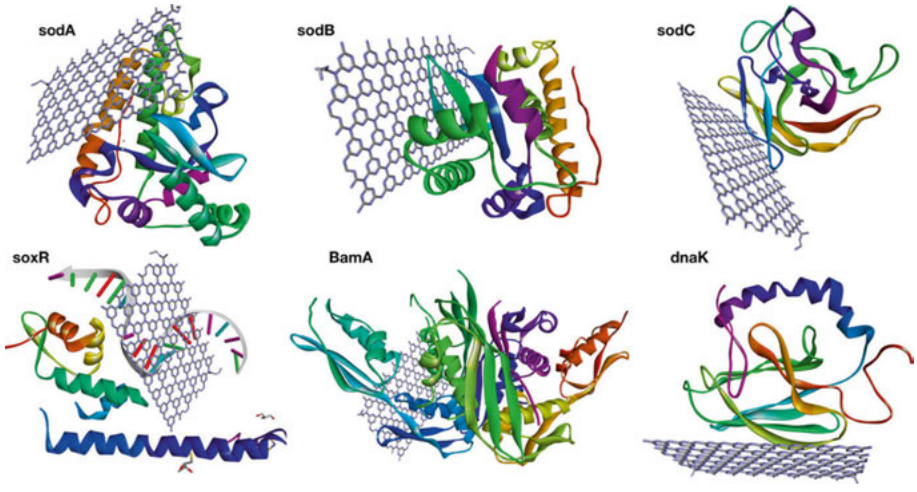

Figure 5.2: *Molecular interaction of g- C_3N_4 with gram-negative E. coli bacterial proteins. (Adapted from Paper I ref* [106])

5.2 Atomistic interaction of 0D nanomaterials with macromolecules

Because of the rapid evolution of nanotechnology, there are greater risks of exposure to both humans and the environment from created nanomaterials. Colloidal and dynamic forces have an impact on the numerous biological interfaces that nanoparticles come into contact with, including DNA, proteins, membranes, and cell organelles. As a result, the resulting nano-bio interface is dynamic, includes a wide range of cellular absorption processes, different biocatalytic activities, and biocompatibility, all of which require further research. In order to address the problem, the work presents a unique method to study the interaction mechanism of antibacterial silver nanoparticles (AgNPs) and from the viewpoint from the mechanistic in vivo biocompatibility of AgNPs at the cellular and molecular levels. Understanding nanotechnology has allowed for a wide range of applications. It contains in-depth analyses and explorations of several nanoparticle types, including both organic and inorganic nanoparticles. Scientists have been fascinated by the unusual chemical and physical characteristics of inorganic nanoparticles. Silver (Ag), gold (Au), CuO, ZnO, and titanium dioxide (TiO2) nanoparticles are some of the most prevalent metallic nanoparticles that have been studied for their many applications. For various biological and chemical uses, such as their use as antibacterial agents, catalytic agents, or in food packaging, silver nanoparticles (AgNPs) are among the most researched and used materials. To clarify the mechanism resulting from abnormal physiological metabolism in oxidative stress and neutral lipid metabolism due to dose-dependent interactions with

proteins such as he1a, sod1, PEX protein family, and tp53 involving amino acids such as arginine, glutamine, and leucine that lead to improper apoptosis, we performed a theoretical investigation with a combinatorial approach. With a novel combinatorial technique based on first-principles density functional theory and in silico analyses, the research provided a complete understanding of the role of various AgNPs-protein interactions, opening up a new avenue for understanding their inherent characteristics and applications.

The interaction between the specific lipid membrane, i.e., DPPC, and the specific protein, namely AgNPs, was first predicted using the HEX docking program before digging into the real mechanism of how these molecules infiltrate the phospholipid bilayer membrane. The three solutions with the highest binding energies—154.14 kcal mol^{-1}, 153 kcal mol^{-1}, and 152.10 kcal mol^{-1}—were chosen out of 3000 solutions that were modeled, as shown in **Figure 5.3**. Since rigid docking was carried out in a vacuum, the effects of the interaction were examined by considering the interacting molecules using the DFT formalism. When dynamics were run for 2000 steps, the total energy variation was noticeably high. The simulation resulted in a significant change to the interaction's starting condition, as illustrated in **Section 5.4**. In the final state, the AgNPs cluster was dissociated, but the association with the lipid molecules was not lost. The same has been examined through uptake analysis in in vivo tests (experimental section of the paper VI). It was proposed that the exposed AgNPs (G-AgNPs and C-AgNPs) displayed biotoxicity via a pathway of cellular processes started by the aggregation at the surface and subsequent uptake of nanoparticles.

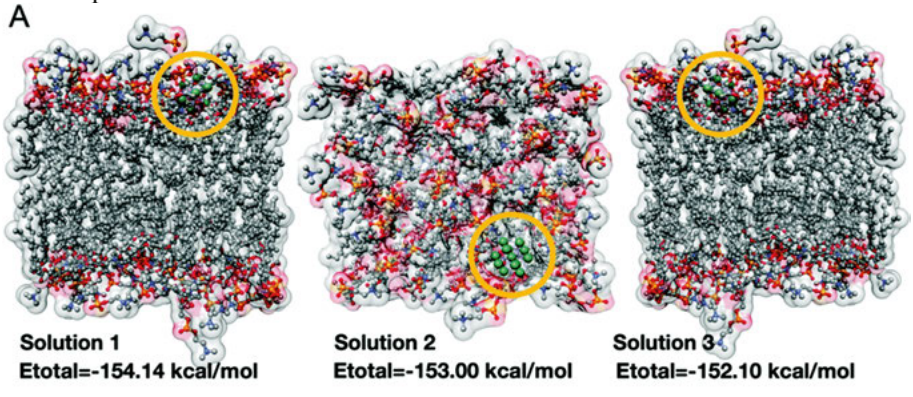

Figure 5.3: In silico *and* in vivo *analysis of AgNPs activity; (A) Three best conformations obtained from AgNPs docking with DPPC using HEX docking program. (Adapted from Paper VI, ref.*[125] *)*

AgNPs were discovered to interact with He1a via amino acid residues such as glutamine (GLN), tyrosine (TYR), and isoleucine (ILE) because of their metal donor and metal acceptor qualities, as shown in **Figure 5.4**. This interaction

may be related to He1a's structural and functional dysfunctionality, which results in irregular and late chorion hardening and abnormal hatching rates.

Numerous protein receptor molecules have been reported in the past to have a function in translocation at the cell membrane's surface. In order to gain insight into the molecular mechanisms of matrix-protein import, we focused on those aspects of peroxisomal-matrix-protein import for which the biochemical data are most reliable, beginning with the recognition of PTS1-containing enzymes by PEX5, the step-in import that has received the most thorough biochemical analysis. It has been suggested that the peroxisomal biogenesis receptor protein family (PEX) is crucial for the transfer of proteins and other molecules for metabolic activities, including oxidation. As a result, it was assumed that the PEX family of proteins was also crucial for the transport of nanoparticles through the membrane. The interaction of AgNPs with the PEX protein family was examined in silico using a molecular docking approach in order to understand the mechanism. The PEX5 protein, along with other PEX family members like PEX and PEX4, was thought to be engaging with AgNPs and assisting in the translocation of nanoparticles both directly across the membrane and indirectly through a channelized interaction with PEX14 **(Figure 5.4A)**. The docking study revealed that AgNPs interacted with PEX5 via the amino acids' arginine (ARG290, ARG595) and leucine (LEU533), causing metal acceptor and donor effects, as illustrated in **Figure 5.4.B**. The transport mechanism has been associated with the PEX5-PEX14 complex as deciphered in the mechanism. Only PEX14 from the PEX5-PEX14 complex was shown to interact strongly with AgNPs via the amino acids' glutamine (GLN170, GLN177), threonine (THR165), and lysine (LYS178). The computational data shed light on the PEX protein family's role in the absorption of nanoparticles.

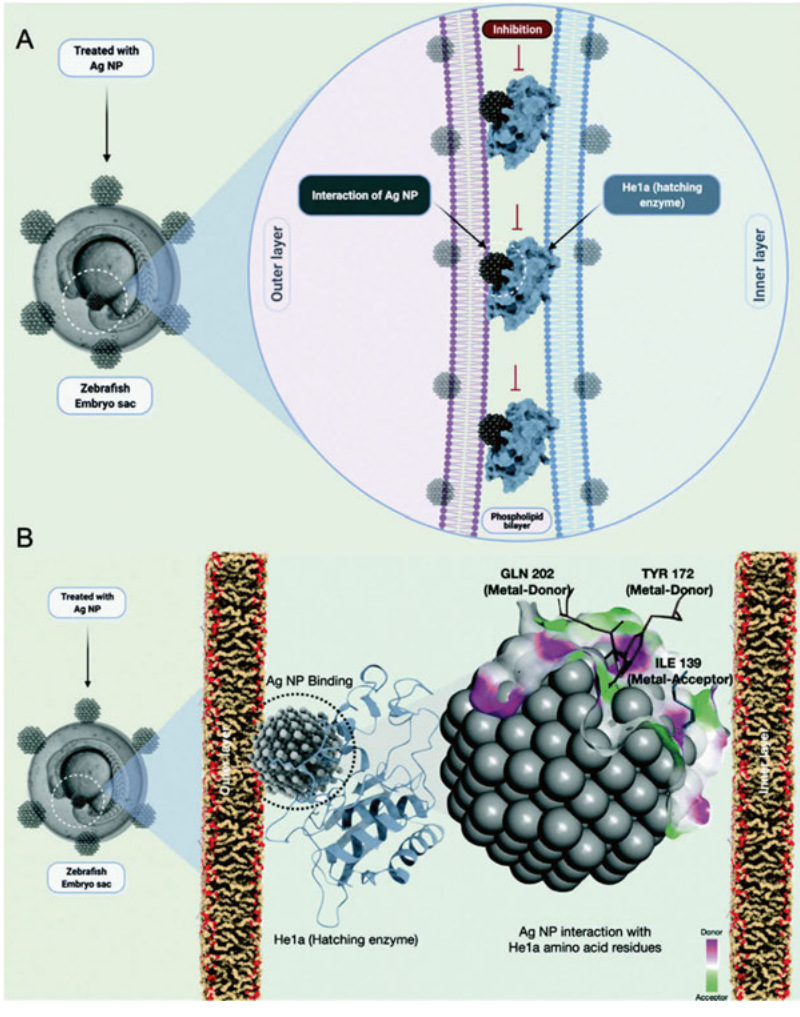

Figure 5.4: *Schematic presentation of G-AgNPs-He1a enzyme interaction for their impact on the hatching rate of zebrafish embryos. The elucidation is based on* in silico *analysis by molecular docking program HEX, which was used to study the interaction with AgNPs as a ligand with He1a of zebrafish as receptor proteins. Visualization and post-docking analysis were performed with the help of conformational clustering, using Chimera and Discovery Studio Visualizer. (Adapted from Paper VI, ref.*[125] *)*

The impact of internalized AgNPs on neutral lipid modification and cell death brought on by ROS generation was validated by the experimental study, but unravelling the molecular mechanism is still necessary. Computational docking analysis was used to investigate the interactions with several proteins involved in ROS formation, steatosis, and apoptosis in order to uncover the molecular process **(Figure 5.5A)**. The crucial role that superoxide dismutase (sod1) plays in oxidative stress is well understood. As seen in **Figure 5.5B**,

molecular docking studies of sod1 with AgNPs revealed contact via the hydrogen bond with an average energy of 309.55 kcal/mol and via the amino acids lysine (LYS43, LYS97), glutamic acid (GLU101), and threonine (THR89). Apolipoproteins (apoa1a) are believed to be produced by the yolk syncytial layer during embryonic development. From yolk lipids, these apolipoproteins further produce very-low-density lipid droplets (VLDL) and cytoplasmic LDL, which travel through the circulatory system and distribute lipids to various tissues. Microsomal triglyceride transfer protein (MTTP) controls the transfer of VLDLs and LDs by forming an MTTP-apoa1a complex.

AgNPs and the MTTP-apoa1a complex interacted via H-bonding with an energy of 12.21 kcal/mol through interactions with the amino acids lysine (LYS193), glutamic acid (GLU316), threonine (THR192), and proline (PRO195). Numerous proteins, including tp53 and caspase, have been discovered to control the apoptotic activity in cells. tp53 was docked with AgNPs for our investigation in order to comprehend their interaction. With an average value of 393.82 kcal/mol, **Figure 5.6** depicts the interaction of tp53 with AgNPs via glutamic acid (GLU 316) and lysine (LYS320). According to the investigation, the AgNPs were impacting the sod1, mttp-apoa1a complex, and tp53 proteins' structural and functional activity, which in turn affected the processes of ROS production, neutral lipid buildup, and apoptosis. Sod1 and Tp53 have both been demonstrated to be impacted by AgNPs in earlier investigations. As a result, it may be inferred from the experimental findings and the literature that AgNPs cause their lethal effect by disrupting cellular metabolism at the molecular level.

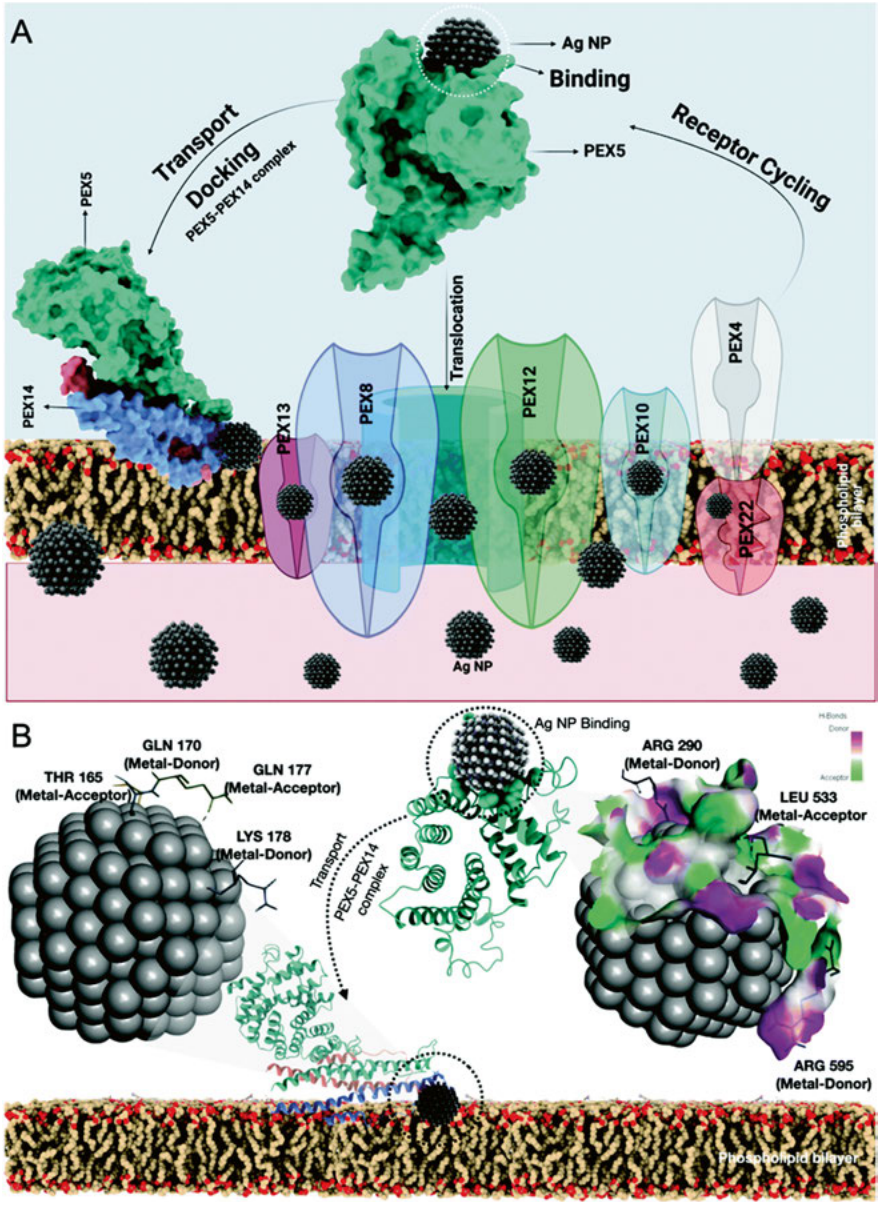

Figure 5.5: Schematic presentation of the mechanism of AgNPs uptake in embryonic cells through PEX-AgNPs interaction. The elucidation is based on the in silico *analysis determined by molecular docking. HEX docking program was used to study the interaction of AgNPs as a ligand with PEX5 and PEX14 of zebrafish as receptor proteins. (Adapted from Paper VI, ref.*[125] *)*

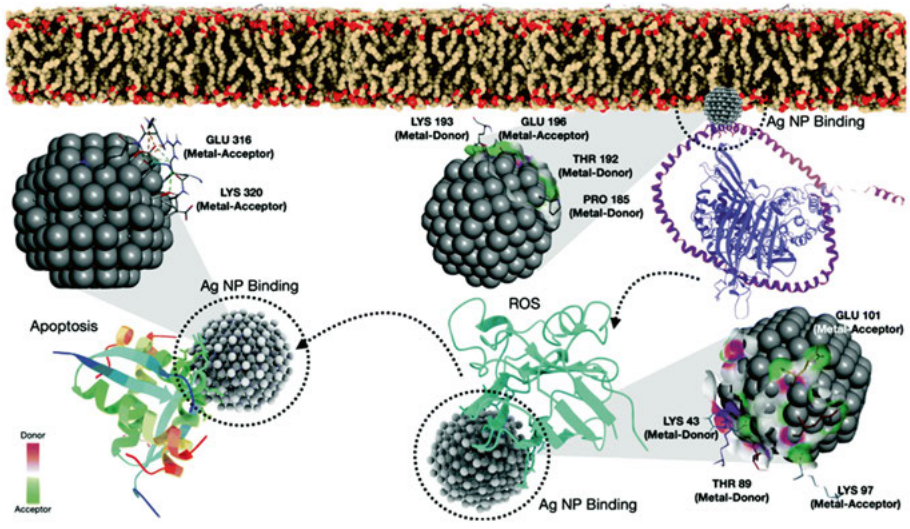

Figure 5.6: Schematic presentation of in vivo *biocompatibility of AgNPs determined by computational analysis through molecular docking. The interaction was studied for AgNPs as a ligand with mttp-apoa1, sod1 and tp53 of zebrafish as receptor proteins for estimation of AgNP effect on steatosis, oxidative stress induction and apoptosis. HEX was used for the docking analysis. Visualization and post-docking analysis were performed with the help of conformational clustering using Chimera and Discovery Studio Visualizer. (Adapted from Paper VI, ref.*[125] *)*

The following can be used to summarize the experimental and computational findings about the process underlying G-AgNPs' biocompatibility: When AgNPs are exposed to zebrafish embryos, they accumulate at the chorion's surface, blocking pores and delaying chorion hardening due to the suppression of the he1a enzyme. The interaction with AgNPs may be responsible for the dysfunctionality. The molecular imbalance leads to anomalies in the embryos' hatching rate. Furthermore, the obstruction of chorion pores causes hypoxia in embryos, which causes aberrant ROS generation to offset hypoxia. In the embryos, some of the accumulating nanoparticles internalize and have an impact on both early and late developmental processes. The nanoparticles enter the cellular cytosol after interacting with receptor proteins like PEX5 and PEX14. Additionally, the internalized nanoparticles affect the structural and functional integrity of antioxidant and metabolic proteins such tp53, sod1, and the apoa1-mttp complex.

Oxidative stress results from an impact on SOD1. The ROS generated as a result of the over-regulation of various cytochrome systems also has aberrant effects on the operation of other metabolic processes. Additionally, the ingested nanoparticles interfere with the apoa1-mttp protein complex's ability to generate VLDL and LDL, impairing their transport throughout the body and altering the metabolism of steatosis (**Figure. 5.7**). Additionally, AgNPs

interact with tp53 proteins to impair the controlled program of cell death (apoptosis), coupled with other elements including faulty apoa1-mttp function and ROS generation. Therefore, cellular death accelerates with concentration-dependent exposure to AgNPs, resulting in their cytotoxicity, as a combinatorial impact of these metabolic anomalies. As a result, the study described the biocompatibility of AgNPs' molecular interactions and determined how G-AgNPs and C-AgNPs' biocompatibilities varied from one another. Additionally, it promotes and suggests a green method to create silver nanoparticles that are more biocompatible and environmentally friendly for use in biomedical and ecological applications.

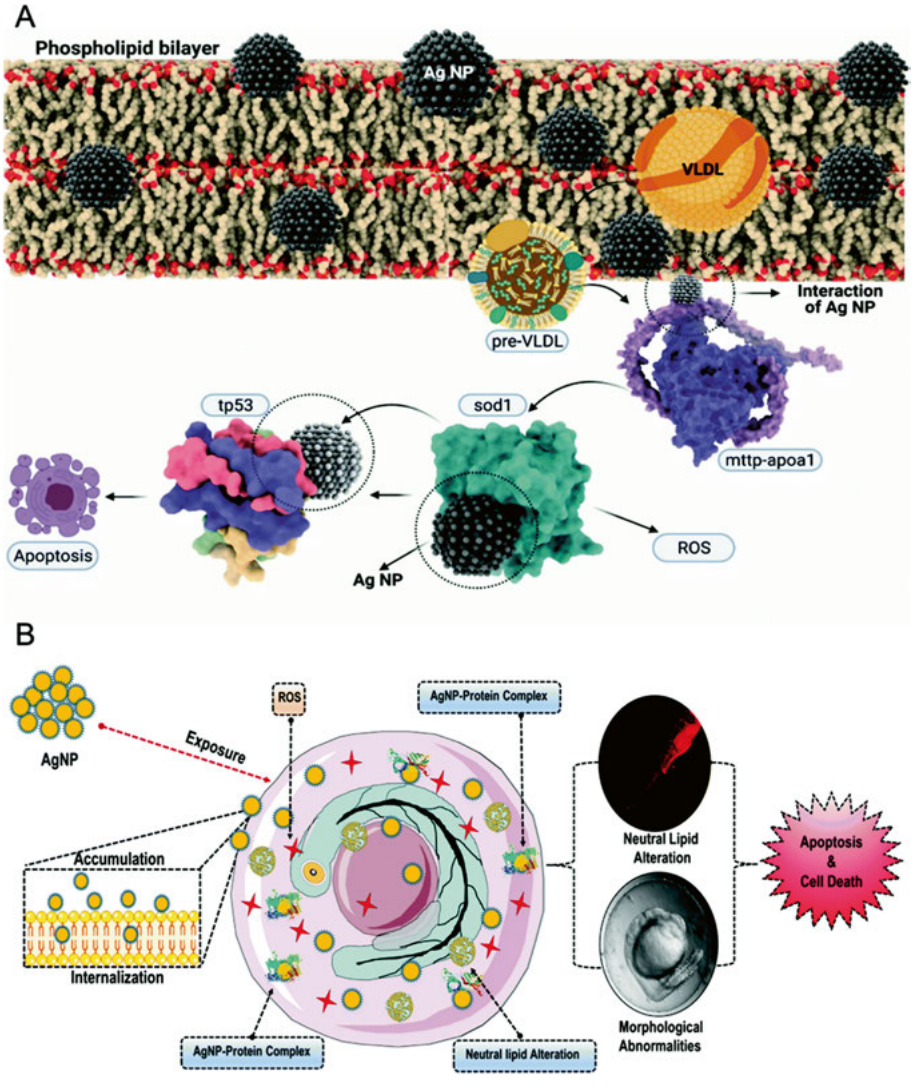

Figure 5.7: Schematic presentation of mechanisms of in vivo *interactions bio-compatibility of AgNPs with zebrafish embryos. AgNPs are internalized through PEX family support, which further impacts the function of mttp-apoa1, sod1 and tp53 to influence oxidative stress, steatosis, and apoptosis. Adapted from Paper VI, ref.*[125]

5.3 Atomistic interaction of 3D complex nanomaterials with macromolecules

In the past, nanoparticles have been utilized to decrease viral attachment through competitive inhibition and to offer antiviral advantages by lowering

viral adhesion to cell surfaces and obstructing viral entry and multiplication. Their capacity to imitate heparan sulfate's (HS) negative charge density offers one potential route. Cell surface HS proteoglycans are utilized by a variety of microorganisms (bacteria and viruses) as cell attachment receptors to infect humans. For the infection of herpesviruses, papillomaviruses, flaviviruses, rhinoviruses, coronaviruses, and the human immunodeficiency virus (HIV), HS proteoglycans are widely expressed on the surface of all cell types. The highly contagious pathogen Herpes simplex virus (HSV), for example, relies heavily on HS for cell attachment and entry. HSV can cause a wide range of clinical diseases, from oral, face, and vaginal sores to serious infections of the central nervous system. According to WHO estimates, 3.7 billion people, or 67% of the global population, have HSV-1. Additionally, by making contact between HS and the receptor binding domain of its spike protein, the severe acute respiratory syndrome-related coronavirus 2 (SARS-CoV-2) infection, which is the root of the current worldwide epidemic and unparalleled public health concern, is made possible. Despite the prevalence of these viruses, existing antivirals have significant efficacy and side effect issues. The prevention of the spread of these viruses and the development of viable therapeutic approaches have immediate global significance. In order to achieve this, tetrapod-like zinc oxide microparticles (ZOTEN) were created to mimic the HS's manufactured oxygen vacancies' negative charge density. Microbivac is a brand-new idea in immunotherapy that ZOTEN has defined due to its distinct features. It has the ability to capture viral particles and encourage the presentation of bound virions to mucosal antigen-presenting cells, which starts and strengthens adaptive immunity.

In this study, we test the drug adjuvant benefits of our nanostructured microparticles against viral infections. For improved activity and safe administration, we functionalized ZOTEN with gold nanoparticles (ANZOT)[126]. We found that this hybrid material performed better than the independent administration of either gold nanoparticles (GNP) or ZOTEN. We also tested ANZOT in a drug adjuvant approach to enhance the efficacy of acyclovir, a guanosine analog clinically used to treat HSV, and small molecule inhibitor BX795 (N-[3-[[5-iodo-4-[[3-[(2-thienylcarbonyl)amino]propyl]amino]-2-pyrimidinyl]amino]phenyl]-1-Pyrrolidinecarboxamide hydrochloride), a promising preclinical drug with strong activity against multiple strains of HSV in several disease models[127]. We show that ANZOT as a drug adjuvant significantly lowers the threshold concentration of acyclovir or BX795 and eliminates drug-associated toxicity. We also demonstrate that BX795 limits the nuclear release of virions through inhibition of protein kinase C isoform α and ζ expression and intracellular localization. Taken together, we show that use of nanoparticles as drug adjuvants has the potential to revolutionize the antiviral drug field.

We have retrieved the crystal protein structures of the Pleckstrin Homology Domain of Protein Kinase B/Akt (PDB ID 1UNQ), PKC alpha (PDB ID: 3IW4), C2 Domain of PKC (PDB ID: 1YRK), Protein Kinase C iota (PDB ID: 1WMH), and glycoprotein B from Herpes Simplex Virus type I (PDB ID: 5V2S) from the Protein Data Bank (PDB) and were subjected to initial target receptor preparation for molecular docking analyses. The ligand small molecules i.e. Acyclovir and BX795 were retrieved from PubChem database and were refined using Marvin sketch. The molecules i.e. ZOTEN and Au@ZOTEN were constructed using Atomic Simulation Environment (ASE) and structural minimizations have been performed based on first principles density functional theory using the Vienna Ab initio Simulation Package (VASP) software **(Figure 5.8)**

In addition, computational molecular docking was used to investigate the likely interaction of small molecules, ZOTEN and Au@ZOTEN, with target receptors in order to elucidate the likely binding mechanisms. To understand the interaction at the molecular level, experimental analyses are used to impart the atomic reaction needed to understand the interaction mechanism. An in silico molecular docking approach was efficiently used to know the preferred binding orientations of the ligand that confer minimum binding energy to determine the binding efficacy of the ligands and the target receptors. Molecular docking analysis has been performed using both Autodock Vina and Autodock tool as the metal ions e.g., Au do not have the AutoDock (AD4) element type in the Autodock Vina tool. Therefore Au@ZOTEN binding interaction with target receptors has been performed using Autodock software. We have used UCSF Chimera, Discovery Studio Visualizer, and LigPlot^{+} to visualize, analyze and depict 2D plots of the interactions.

The results inferred from molecular docking analyses depicts the probable interaction mechanism of ZOTEN and Au@ZOTEN with the ecto domain of HSV-1 gB receptor. ZOTEN has a higher binding efficacy (-12.9 kcal/mol) than Au@ZOTEN (-8.97 kcal/mol) towards the HSV-1 gB receptor. Both the molecules bind to the ecto domain of the HSV-1 glycoprotein with a slightly different orientation. The difference in the conferred orientations of the two molecules affects the binding efficacy. ZOTEN and Au@ZOTEN tend to bind similar residues but with different preferred binding orientations as shown in Fig. ZOTEN has high a number of hydrophobic interactions as compared to Au@ZOTEN. Similarly, conventional bonds (green color) tend to form with oxygen atoms in both cases with different bonding patterns and distances. ZOTEN forms conventional bonding patterns with a lesser distance between the O atom and corresponding Zn atoms, whereas the Au@ZOTEN has a higher range in terms of bonding patterns **(refer to Figure 5.9).** Furthermore, the AuZOTEN has more hydrophilic binding residues (solvent accessible), whereas the ZOTEN has more hydrophobic residues in the vicinity of binding,

increasing the binding efficacy of ZOTEN. A clear viewpoint can be drawn from different aspects of binding orientations, per say. The nine poses of binding orientations derived from the Autodock tools have a high range of binding affinities in case of ZOTEN as compared to Au@ZOTEN.

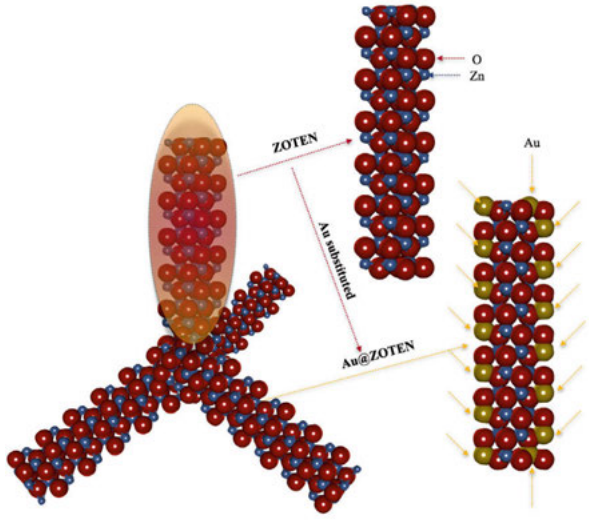

Figure 5.8: ANZOT: functionalized tetrapod-like zinc oxide microparticles (ZOTEN) with gold nanoparticles.

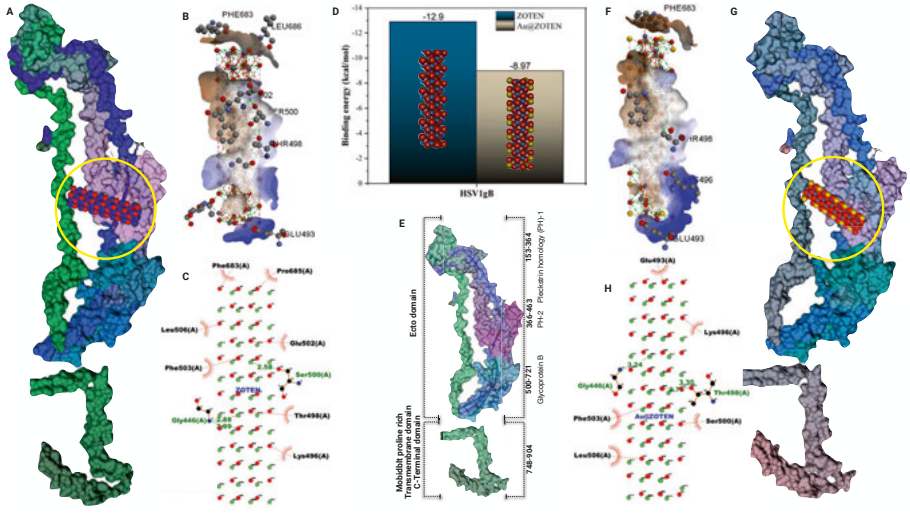

Figure 5.9: Interaction mechanism of ZOTEN and Au@ZOTEN with the ecto domain of HSV-1 gB receptor. A & G. With ZOTEN and ANZOT, respectively. B & F. Hydrogen bond analysis of interaction of ZOTEN with HSV1. C & H . LigPlot analysis of the interaction profile. E. Schematic of ecto-domain of HSV1.

The ligand molecules that were screened for protein kinases also showed higher binding affinity towards ZOTEN and Au@ZOTEN in comparison to the small molecules i.e. Acyclovir and BX795. However, when comparing small molecules, the binding affinity of BX795 for all protein kinases was significantly higher than that of Acyclovir. PKC-delta has the lowest affinity for both small molecules of any protein kinase. In the case of ZOTEN and Au@ZOTEN, the PKC-delta's binding affinity was substantially increased, i.e. -12 kcal/mol and -12.9 kcal/mol. **(Figure 5.10)**

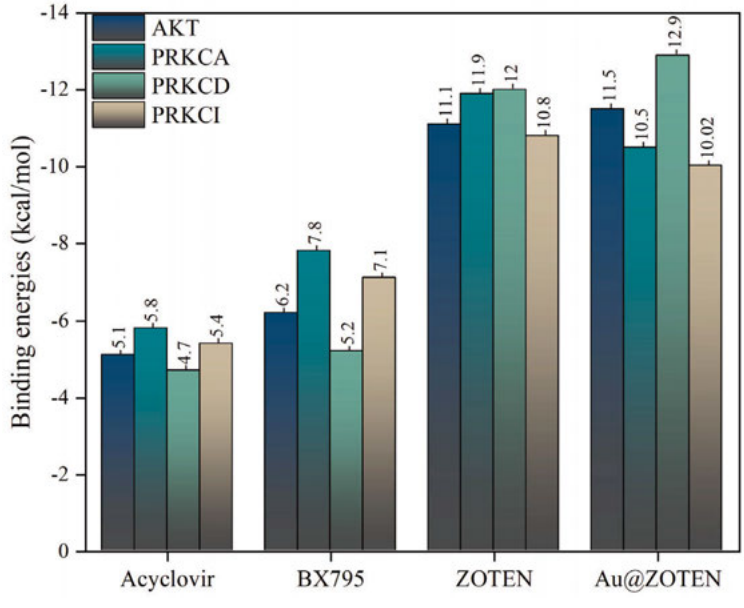

Figure 5.10: Binding affinities of ligand molecules (Acyclovir, BX795, ZOTEN and Au@ZOTEN(ANZOT) that were screened for protein kinases.

5.4 Biophysics of nanomaterials

Simulation is an approximate representation of how a process or system works, and it can disclose the underlying mechanics of physiological phenomena with atomic-level accuracy. It is the most effective method for studying the dynamics of the nano-bio interface, which consists of nanomaterials and biological components. Diverse simulation techniques have been developed and used based on various research goals. In this section, I want to emphasize the all-atom molecular dynamics part, where I have noticed a measurable difference in comparison to the static interactions from molecular docking or from the DFT formalism.

For instance, in **Paper I**, the optimized structures (g-C_3N_4 with individual AA) produced from DFT were put through a molecular dynamics simulation using LAMMPS as a crude example of AA adsorption to a g-C_3N_4 monolayer. Some fascinating findings from the post-analysis are then contrasted with DFT findings to gain a better understanding of the physisorption process of AA on the g-C_3N_4 monolayer. When comparing DFT adsorption energies, it can be shown that DFT yields Asn with the highest adsorption energy, followed by Tyr and Asp. Different energies associated with each unique AA upon adsorption on a g-C_3N_4 monolayer have been examined. When the NVT ensemble and structural minimization are applied to molecular dynamics simulations to gain insight into the binding effectiveness and change in total energies when adsorbed on the g-C_3N_4 surface, similar results are obtained **(Figure 5.11**).

Similar to this, in **Paper V**, we used classical dynamics to explain the adsorption of ions and molecules at the surface of the solid-liquid interface **(Figure 5.12A-F)**. The first layer of water is more apparent near the GaN contact, as seen by the density profiles in **Figure 5.12A**. On the other hand, the initial layer's position is the same for all three schemes. In contrast to the AlN and Si surfaces, **Figure 5.12E** demonstrates that the Cl atoms are strongly attracted to the GaN surface. The image of the final arrangement in **Figure 5.12B** makes it easy to see this dense layer of Cl atoms at the GaN contact. On the other hand, the Cl atoms are randomly dispersed, as shown in the snapshots of the AlN and Si systems. Na atoms do not appear to have a clear preference for any of the three materials, as seen in **Figure 5.12F**. Understanding the behavior of ion and molecule distribution and their binding mechanisms on various surfaces in a confined environment (in this case, the solvent environment) can be gained via this approach.

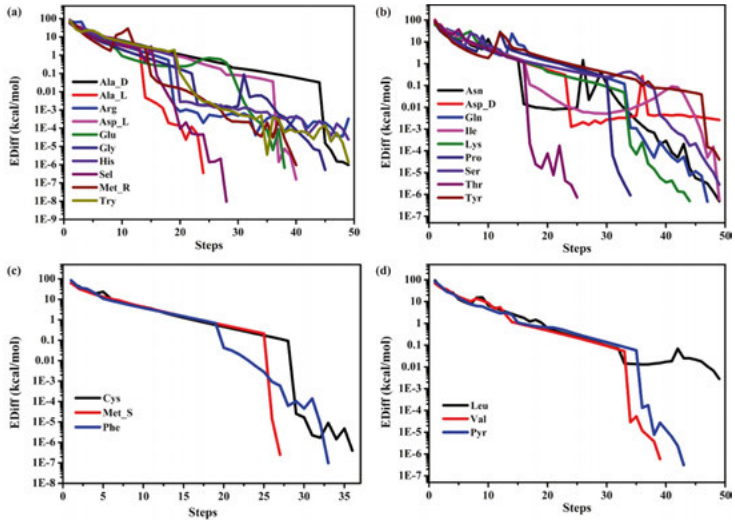

Figure 5.11: Total Energy difference in kcal/mol obtained from structural minimization using conjugate-gradient algorithm used in LAMMPS. Adapted from Paper I, ref.[106]

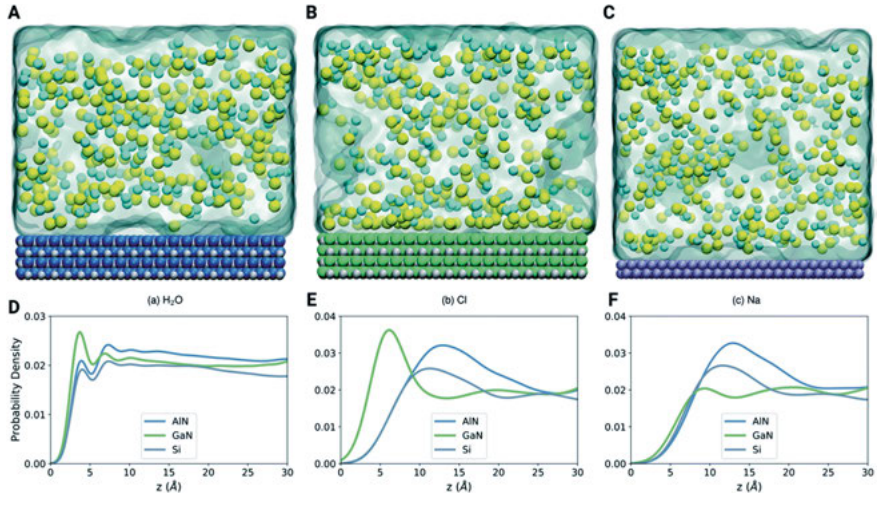

Figure 5.12: LAMMPS based classical molecular dynamics simulations comprising three systems, (A) AlN, (B) GaN and (C) Si surfaces, embedded in a solvent box with different ions and molecules. (D–F) Density profiles of the three complex systems depicting the probability density of H_2O, Cl and Na. (Adapted from Paper V ref. [124])

Even though there has been a lot of research on nanoparticles and their applications in industry, medicine, and other fields, it is difficult to observe and analyze in real time the physical processes that underlie many of the unique qualities of different nanoparticles. Molecular dynamics (MD) simulations,

along with other computational methods, occupy an increasingly significant niche in this rapidly evolving and expanding field because of the quick development of computational algorithms, the accessibility of computational resources to scientific researchers, and the relatively small sizes of nanoparticles. Therefore, along with experimental verifications, we have employed ab-initio and classical dynamics to understand how nanoparticles behave in different conditions, such as vacuum and solvent medium.

In paper VI, using the DFT formalism and combinatorial molecular dynamics modeling methods, AgNPs were modelled in both a solvated medium and a vacuum, respectively. Classical mechanics evaluation of the 10 ns simulated AgNPs (**Figure 5.13A)** in the solvent medium revealed no significant changes in the geometry of the structure. As shown in **Figure 5.13B,** the influence of the solvent medium had a modest negative impact on the structure's compactness, causing a divergence of 0.76–0.70 nm in the radius of gyration (*Rg*). The root mean square deviation (RMSD), which ranged from 0.44 to 0.45 nm, also displayed a same trend. In order to demonstrate the effect of vacuum on AgNPs with DFT formalism, we first evaluated the influence of solvent on AgNPs. Using a novel approach, we investigated the total energy fluctuation of each Ag atom as it was isolated sequentially from the AgNPs cluster. The structural arrangements of the aforementioned technique and the overall energy fluctuation are shown in the plot **(Figure 5.13C).** As seen in the plot, the total energy of the AgNPs cluster was 24 eV and decreased sequentially by 2 eV until all Ag atoms were taken out of the cluster. This indicates that each Ag atom has 2 eV because its valence is +2. Additionally, the DFT formalism in a vacuum has been used to evaluate the cluster's dynamics **(Figure 5.13D)**. According to **Figure 5.13E,** the cluster in a vacuum environment has been significantly impacted by the total energy variation. The native shape of the cluster has been significantly altered, and it is not present.

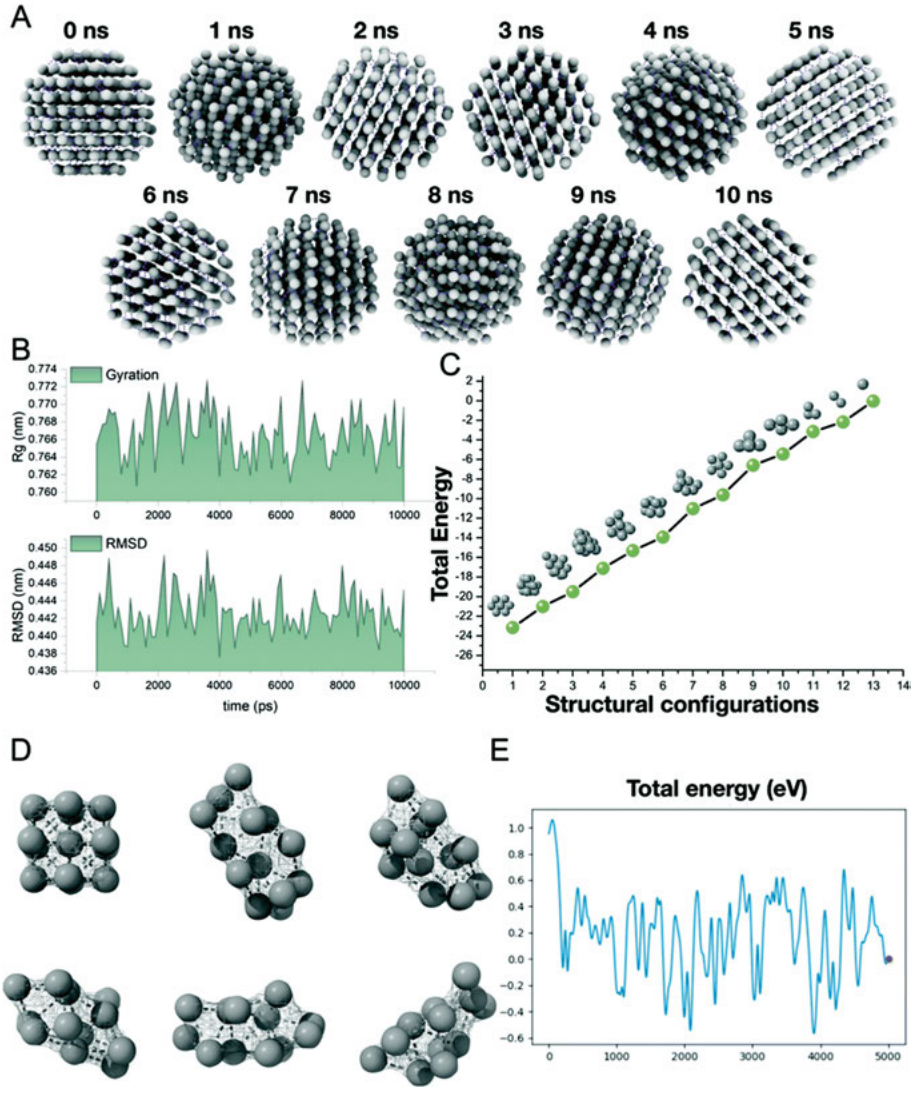

Figure 5.13: In silico *analysis of AgNPs activity; (A) Structural conformations of AgNPs during the course of 10 ns molecular dynamics simulation in the solvated environment. (B) The radius of gyration and Root Mean Square Deviation plots depict the compactness and structural deviations during the 10 ns dynamics study. (C) The structural configurations and the total energy obtained from DFT formalism for the AgNPs cluster. (D)* Ab initio *molecular dynamics simulation of AgNPs cluster. (E) Total energy (eV) was obtained during the course of* ab initio *molecular dynamics. (Adapted from Paper VI, ref.*[125] *)*

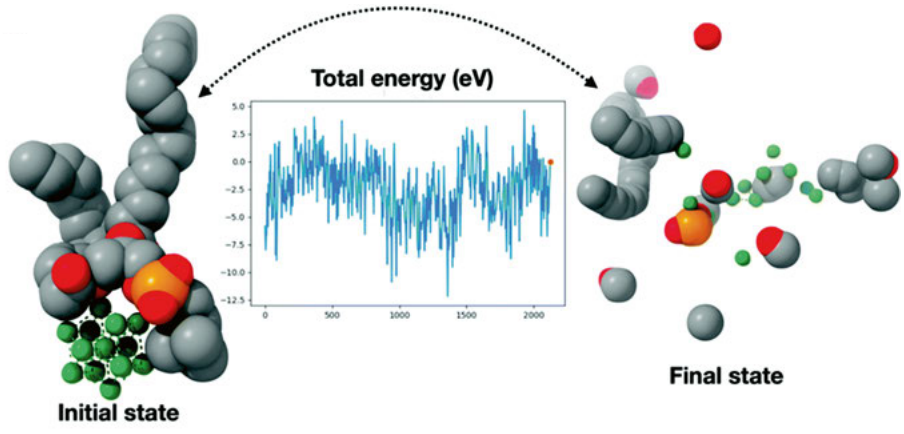

Figure 5.14: Ab initio *molecular dynamics simulation of the interaction of AgNPs cluster with lipid biomolecules obtained from HEX molecular docking. The combinatorial approach illustrated shed light upon the dynamic stability of the AgNPs cluster when interacting with lipid molecules.(Adapted from Paper VI, ref.*[125] *)*

Through a molecular dynamics simulation, we have also demonstrated the channelized interaction mechanism of AgNPs with lipid molecules. It can be shown that when dynamics were run for 2000 steps, the total energy variation was quite large. The simulation resulted in a significant change to the interaction's initial condition, as depicted in **Figure 5.14**. In the final state, the AgNPs cluster was dissociated, but the association with the lipid molecules remains intact.

In **paper VII**, the dynamics of 3D nanomaterials was a daunting task. It was a first-of-its kind simulation strategy we employed to understand the complexity of ZnO tetrapod architecture. The LAMMPS package has been used to understand the structural complexity of the nanomaterial. **Figure 5.15** depicts the structural architecture of a ZnO tetrapod.

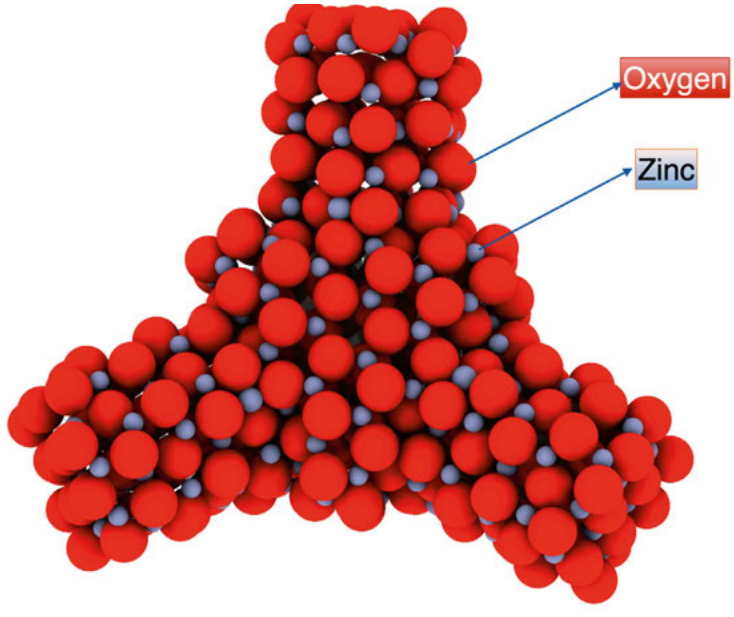

Figure 5.15: The structure of ZnO tetrapods with four arms and a tetrahedral core at the center.

Our group, along with a collaboration from India, studies the different nanomaterials exposed to in-vivo embryonic zebrafish to check their biocompatibility and cytotoxicity. In **Figure 5.16**, the zebrafish embryos were exposed to ZnO-tetrapods at different concentrations. We observed that ZnO-tetrapods were accumulated at the interface of outer cell membrane in two phases: (i). whole ZnO-tetrapod shape, and (ii). broken arms from the tetrapods. We were curios to study the dynamics of ZnO-tetrapods in solvent environment to understand how the arms of the tetrapods behave. As shown in **Figure 5.17**, we used the strategy to see if an individual arm prefers to remain separate from the initial configuration or if it prefers to merge with the original tetrapod configuration. The initial configuration and the final configuration of the ZnO-tetrapods (one, two and three legs) after simulation showed promising results that, in the case of one leg simulation, the relative distance after ~5 ns tends to come closer to the initial configuration. Likewise, in legs two and three, the relative distance is higher but tends to come closer if it is simulated for a longer time.

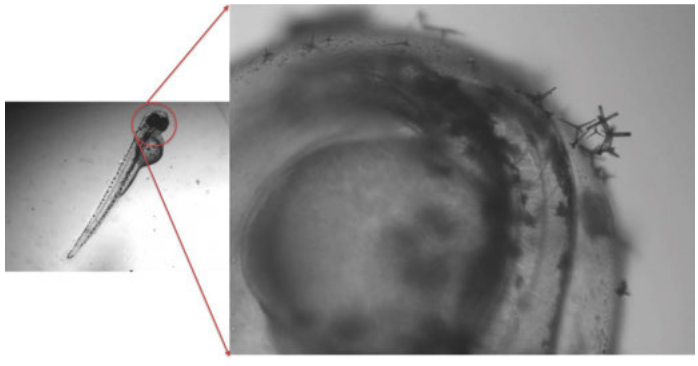

Figure 5.16: Bright-field microscopic image of zebrafish embryos with ZnO-Tetrapods. The embryos were maintained and exposed to the egg water.

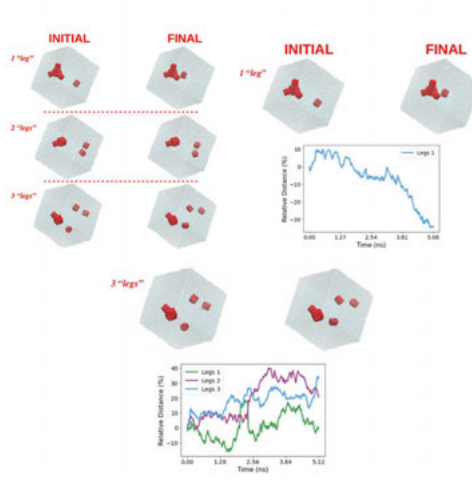

Figure 5.17: LAMMPS dynamics of ZnO tetrapods in solvent environment with tetrapodal arms separated from original conformations. The graph shows relative distance during the course of simulation.

Conclusion & Outlook

As healthcare is a fundamental human right, it is frequently the target of new technological advances. Technological innovation has considerably helped to the provision of high-quality, on-time, acceptable, and cheap healthcare. Advancements in nanoscience have led to the birth of a new generation of nanostructures. Their remarkable use can be attributed to the fact that each one possesses its own special set of characteristics. Better medical results have been a consistent byproduct of nanotechnology's pervasive influence on the healthcare industry ever since it was first developed. In the previous two decades, nanotechnology has made great strides toward global adoption, a trend that has been hastened by intensive study in several areas of medicine. Many advances have been made in illness prevention, diagnosis, and treatment since nanotechnology and its associated nanocarriers/nano systems were introduced to the medical field. Compared to traditional methods, many nano systems have proven to be superior options for theragnostic applications. One of the major research challenges for the coming decades will be to find sustainable methods of providing technological growth. Providing new functional nano materials is expected to be very important in this development since it has the potential to tune material properties to a previously unthinkable degree.

In the realms of optics, electronics, chemistry, and medicine, 2D materials constitute a promising new frontier. Researchers have been on the lookout for new 2D materials since they were inspired to do so by the desirable features of graphene due to its 2D structure. A wide variety of new applications are made possible by the special qualities of 2D structures, such as their high surface-to-volume ratio, form, surface charge, anisotropic nature, and the ability to be tuned for certain functionalities. Two-dimensional (2D) materials have made significant contributions to several fields, including material science, optoelectronics, engineering, and biomedical science. New 2D materials are being developed, and existing 2D materials are being functionalized to attain desirable qualities.

Furthermore, understanding the nano-bio interactions of manufactured nanomaterials is crucial to the field of nanomedicine. This is due to the fact that nano-bio interactions are linked to the rational development of risk-free and efficient nanomedicine, drug transport, pathological site targeting,

metabolism, and biocompatibility. From the vantage point of corona and redox processes, we examine current developments in nano-bio interactions of nanomaterials. These developments bode well for the potential of nanomaterials in biomedicine in the future, notably in the treatment of diseases. However, there are still numerous obstacles in the way of nano-bio interactions research; there is currently a paucity of knowledge regarding the catalytic processes of nanomaterials towards various diseases. To be truly useful as superior therapeutic and diagnostic techniques, however, a strategy for controlling the catalytic activity of nanomaterials must be established. The in vivo complexity must be considered in nano-bio interaction studies. In order to examine the nano-bio interactions precisely and thoroughly, theoretical simulations should be given more attention. As a result, more work needs to be put into studying nano-bio interactions.

The future outlook for nanomaterials is very promising, with continued growth and expansion in various fields such as medicine, energy, electronics, and materials science. Nanomaterials have unique properties due to their small size, and they have the potential to revolutionize the way we approach a wide range of applications. In medicine, nanomaterials are being used to develop new therapies, such as targeted drug delivery, and to improve diagnostic methods. In energy, nanomaterials are being used to improve the efficiency of energy production and storage, as well as to develop new materials for clean energy applications. In electronics, nanomaterials are being used to develop new types of devices with improved performance, such as flexible electronics and nanoscale sensors. However, there are also concerns about the potential toxic effects of nanomaterials, as well as the need for further research to fully understand their behavior and impact on the environment. As a result, the development and regulation of nanomaterials will likely continue to evolve in the coming years, with a focus on ensuring their safe and responsible use.

In this thesis, we study new applications for nanomaterials ranging from 0D to 3D and tune their properties through functionalization, creating new hybrid nanomaterials for multifunctional applications. We have employed a combinatorial approach to decipher the role of nanomaterials, focusing on biosensing, contact electrification, and nano-bio interactions. We have tried our best to address and depict properties of nanomaterials in varied applications, however, we also need to focus on some key challenges as described in chapters 1 to 3, both experimentally and theoretically.

i. **Computational cost:** The high computational cost of DFT and other quantum mechanical simulations is a significant challenge in interface science. This can make it difficult to perform simulations on large-scale or complex systems, and can limit the scope of the simulations that can be performed.

ii. **Modeling accuracy:** Accurately modeling the behavior of interfaces is challenging due to the complex interplay of chemical, electronic, and structural factors. Ensuring that the models used in DFT, and computational simulations accurately reflect the behavior of real-world interfaces is a major challenge in interface science.

iii. **Interfacial properties:** The properties of interfaces, such as electronic structure, charge transfer, and reactivity, can be difficult to quantify and predict. Developing methods for accurately characterizing and predicting these properties is a major challenge in interface science.

iv. **Interfacial dynamics:** Understanding the dynamic behavior of interfaces, such as the kinetics of reactions and the transport of charge and energy, is critical to their study. However, capturing this behavior using DFT and computational simulations can be challenging due to the complexity of the processes involved.

v. **Validation:** Validating the results of DFT and computational simulations against experimental data can be difficult due to the complex nature of interfaces and the limited availability of experimental data. Developing methods for validating the results of simulations is a major challenge in interface science.

vi. **Selectivity and sensitivity:** One of the main challenges in biosensing is to ensure that the sensor is selective and sensitive to the target analyte, while being insensitive to other interfering substances. This can be especially difficult when using 2D materials, as their small size and high surface-to-volume ratio can lead to interference from the environment.

vii. **Surface modification:** 2D materials often have poor biocompatibility and low chemical stability, which can limit their ability to interact with biomolecules such as DNA, gases, and amino acids. To overcome this, it is necessary to modify the surface of the 2D material to improve its biocompatibility and stability.

viii. **Integration with electronics:** Biosensors must be integrated with electronics in order to detect and quantify the target analyte. The integration of 2D materials with electronic devices can be challenging and requires the development of new and innovative fabrication methods.

ix. **Stability:** The stability of 2D materials in biological environments can also be a challenge, as they can be prone to degradation and corrosion. This can limit the lifespan of the biosensor and impact its performance over time.

x. **Cost:** The cost of 2D materials can also be a challenge, as they are often more expensive than other materials used in biosensors. This can make it difficult to commercialize 2D material-based biosensors and bring them to market.

xi. **Material quality:** The quality and uniformity of 2D materials is critical to their use in contact electrification, as even small defects or variations in the material can affect its performance. Ensuring the quality and consistency of 2D materials is a significant challenge.

xii. **Interfacial behavior:** The behavior of 2D materials at interfaces, such as the interface between the 2D material and the electrode, is critical to the success of contact electrification. Understanding and controlling the interfacial behavior is a major challenge in the development of contact electrification using 2D materials.

xiii. **Contact area:** The size and shape of the contact area between the 2D material and the electrode can significantly impact the performance of the contact electrification. It is important to understand the relationship between the contact area and the resulting electrification, and to develop methods to optimize the contact area.

xiv. **Environmental stability:** The stability of 2D materials in various environments, such as high humidity and high temperature, is critical to their use in contact electrification. Ensuring that 2D materials remain stable and functional under these conditions is a significant challenge.

xv. **Scale-up:** The challenge of scaling up the production of 2D materials and integrating them into contact electrification systems is a significant barrier to commercializing the technology.

xvi. **Material biocompatibility:** The biocompatibility of nanomaterials is critical to their use in biological systems, as their small size and high surface-to-volume ratio can lead to toxicological effects. Ensuring that nanomaterials are biocompatible and do not cause adverse effects in living systems is a major challenge.

xvii. **Material stability:** The stability of nanomaterials in biological environments, such as high humidity, high temperature, and exposure to biological fluids, can be a challenge. Ensuring that nanomaterials remain stable and functional under these conditions is critical to their use in biological systems.

xviii. **Interfacial behavior:** The behavior of nanomaterials at interfaces, such as the interface between the nanomaterial and biological tissues, is critical to their success in nano-bio interactions. Understanding and controlling the interfacial behavior is a major challenge in the development of nano-bio interactions.

xix. **Cellular uptake and localization:** The ability of nanomaterials to enter cells and reach specific target sites is critical to their use in biological systems. Understanding the mechanisms of cellular uptake and localization is a major challenge in the development of nano-biointeractions.

xx. **Dosage and toxicity:** The challenge of determining the appropriate dosage and toxicity of nanomaterials is a significant barrier to their use in biological systems. Ensuring that nanomaterials are safe and effective at the appropriate doses is a major challenge in nano-bio interactions.

Despite these limitations, nanoparticles' usage in the aforementioned applications holds much promise because of their exceptional characteristics. Health care, environmental monitoring, food safety, energy storage, tribology, sensing, drug delivery, diagnostics, and regenerative medicine are just some of the fields that stand to benefit from the continuous development of 2D materials. In the future, research of the properties and uses of nanomaterials in numerous domains of science may benefit from the methodologies used to develop the insights described in this thesis. Because of their potential to provide a molecular-level insight, computational tools in interface science hold enormous promise in helping us achieve our aim of comprehending the interface between nanomaterials and biological components. New discoveries and developments in interface science are anticipated with the continuous development of these methods.

The chapters depict the aforementioned topics while keeping in mind the key scientific challenges. They are fascinating in the real world, but assuming there is a theoretical basis is a difficult challenge. That's why I use a variety of computational methods, ranging from DFT (which works with a few atoms) to classical dynamics (which works with billions of atoms). To bridge the concepts of biophysics and quantum physics, the topic **GENOME2QUNOME** has been integrated to impersonate the real-world scenarios.

Interface science based on nanomaterials holds the key to unlocking a wealth of potential applications, from advanced electronics to innovative medical therapies. By studying the behavior of nanomaterials at the interface between different materials and systems, we can gain a deeper understanding of the fundamental properties and processes that govern their behavior and unlock new possibilities for their use.

"The aim of science is to seek the simplest explanations of complex facts. We are apt to fall into the error of thinking that the facts are simple because simplicity is the goal of our quest." - Richard Feynman

Sammanfattning pa Svenska

Som hälsovård är en grundläggande mänsklig rättighet är det ofta målet för nya tekniska framsteg. Teknologisk innovation har bidragit till en stor utsträckning till tillgången till högkvalitativ, tidsenlig, acceptabel och billig hälsovård. Framsteg inom nanovetenskap har ledt till födelse av en ny generation av nanostrukturer. Deras utmärkta användning kan hänföras till det faktum att var och en har sin egen särskilda uppsättning av egenskaper. Bättre medicinska resultat har varit en konsekvent bieffekt av nanoteknologins genomgripande inverkan på hälso- och sjukvårdsindustrin sedan den först utvecklades. De senaste två decennierna har nanoteknologin gjort stora framsteg mot global adoption, en trend som har främjats av intensiv forskning inom flera områden inom medicin. Många framsteg har gjorts inom sjukdomsprevention, diagnostik och behandling sedan nanoteknologi och dess associerade nanobärare/nano-system introducerades inom medicinfältet. Jämfört med traditionella metoder har många nano-system visat sig vara överlägsna alternativ för teragnostiska tillämpningar. Att hitta hållbara sätt att tillhandahålla en teknologisk tillväxt är en av de främsta forskningsutmaningarna för de kommande decennierna. Att tillhandahålla nya funktionsmässiga nano-material förväntas vara mycket viktigt i denna utveckling eftersom det har potentialen att justera materialegenskaper till en tidigare oöverstiglig grad.

I den världen av optik, elektronik, kemi och medicin utgör 2D-material en lovande nya fronter. Forskare har letat efter nya 2D-material sedan de inspirerades att göra det av den önskvärda egenskapen hos grafen på grund av dess 2D-struktur. En mängd nya tillämpningar görs möjliga genom de speciella egenskaperna hos 2D-strukturer, såsom deras höga yt-till-volymförhållande, form, yteladdning, anisotropa natur och förmåga att stämmas för vissa funktioner. Tvådimensionella (2D) material har gjort viktiga bidrag till flera områden, inklusive materialvetenskap, optoelektronik, teknik och biomedicinsk vetenskap. Nya 2D-material utvecklas och befintliga 2D-material funktionaliseras för att uppnå önskvärda egenskaper.

Dessutom är förståelse av nanobio-interaktioner mellan tillverkade nanomaterial avgörande för nanomedicinområdet. Detta beror på det faktum att nano-bio-interaktioner är kopplade till en rationell utveckling av riskfri och effektiv nanomedicin, läkemedelstransport, patologisk platsinriktning,

metabolism och biokompatibilitet. Från utsiktspunkten för korona- och redox-processer undersöker vi den aktuella utvecklingen i nanobio-interaktioner mellan nanomaterial. Denna utveckling förbättrar väl potentialen för nanomaterial i biomedicin i framtiden, särskilt vid behandling av sjukdomar. Det finns emellertid fortfarande många hinder i vägen för nanobio-interaktionsforskning; det finns för närvarande en mängd kunskap om de katalytiska processerna för nanomaterial mot olika sjukdomar. För att vara verkligt användbar som överlägsna terapeutiska och diagnostiska tekniker måste emellertid en strategi för att kontrollera den katalytiska aktiviteten hos nanomaterial fastställas. In vivo-komplexiteten måste beaktas i nano-bio-interaktionsstudier. För att exakt och noggrant undersöka nano-bio-interaktioner bör teoretisk simulering ägnas mer uppmärksamhet. Som ett resultat måste mer arbete läggas på att studera nano-bio-interaktioner.

Framtidsutsikterna för nanomaterial är mycket lovande, med fortsatt tillväxt och expansion inom olika områden som medicin, energi, elektronik och materialvetenskap. Nanomaterial har unika egenskaper på grund av deras lilla storlek, och de har potential att revolutionera hur vi närmar oss ett brett spektrum av applikationer. Inom medicinen används nanomaterial för att utveckla nya terapier, såsom riktad läkemedelsleverans, och för att förbättra diagnostiska metoder. När det gäller energi används nanomaterial för att förbättra effektiviteten i energiproduktion och lagring, samt för att utveckla nya material för ren energiapplikationer. Inom elektronik används nanomaterial för att utveckla nya typer av enheter med förbättrad prestanda, såsom flexibel elektronik och nanoskala sensorer. Det finns emellertid också oro över de potentiella toxiska effekterna av nanomaterial, liksom behovet av ytterligare forskning för att fullt ut förstå deras beteende och miljöpåverkan. Som ett resultat kommer utvecklingen och regleringen av nanomaterial troligen att fortsätta utvecklas under de kommande åren, med fokus på att säkerställa deras säkra och ansvarsfulla användning.

I denna avhandling studerar vi nya applikationer för nanomaterial som sträcker sig från 0D till 3D och om att ställa in deras egenskaper med funktionalisering, skapa nya hybrid nanomaterial för multifunktionella applikationer. Vi har använt kombinatorisk strategi för att dechiffrera rollen som nanomaterial med fokus på biosensering, kontaktelektrifiering och nanobio-interaktioner. Vi har försökt vårt bästa för att adressera och skildra egenskaper hos nanomaterial i olika applikationer. De nämnda ämnena som visas i kapitlen, med tanke på de viktigaste vetenskapliga utmaningarna är fascinerande i den verkliga världen men att anta att det finns en svår utmaning. Det är därför jag har en kombination av olika beräkningsmetoologier från DFT som handlar om få atomer till klassisk dynamik (som hanterar miljarder atomer). För att överbrygga begreppen biofysik och kvantfysik har ämnet GENOME2QUNOME interagerats för att efterge sig de verkliga scenarierna.

"Gränssnittsvetenskap baserad på nanomaterial har nyckeln till att låsa upp en mängd potentiella applikationer, från avancerad elektronik till innovativa medicinska terapier. Genom att studera nanomaterials beteende vid gränssnittet mellan olika material och system, vi kan få en djupare förståelse av de grundläggande egenskaperna och processerna som styr deras beteende och låsa upp nya möjligheter för deras användning."

Acknowledgments

This Ph.D. thesis is based on theoretical studies that is part of a broader research approach that seeks to comprehend the properties, behavior, and uses of nanomaterials in the context of real-world scenarios. In order to establish a clear narrative for the thesis, data that is ancillary to the primary theme has been omitted, and projects have been explained in sufficient detail. Thus, a substantial portion of the Ph.D.-level work I performed is not recounted here, and a few components of the work provided incorporate contributions from joint collaborations; these latter contributions must, however, be fully acknowledged. This distinction between my contributions and those of others will be reiterated throughout the thesis, and all facts that are not exclusively my own will be clearly labeled as such and cited in the text. I expect that the final product will be a coherent paper in which my thoughts are solely supported where necessary to offer a logical argument. In addition to these specific contributions, I would like to thank everyone who contributed general input and assistance during the duration of this prolonged project. The subsequent chapters detail my transition from bench bioinformatician to materials scientist.

I owe a great deal of gratitude to many people for making my time as a doctoral student at Uppsala University an exciting one. They all deserve my sincere acknowledgement, and I did my best to include them all on this list. I sincerely apologize if I accidentally dropped any of them, but it's possible that I did. I was able to conduct research and finish my thesis in a relaxed setting thanks to my group members and colleagues in the Materials Theory Division. Additionally, I would like to express my gratitude to Uppsala University for providing me the opportunity to work and collaborate with scientists, researchers, industries, and grant agencies that allowed me to successfully complete my doctoral thesis in Sweden. I would like to convey my overwhelming thanks to **Prof. Susanne Mirbt, Prof. Biplab Sanyal**, and **Prof. Göran Ericsson**, who always manage an excellent working environment and are ready to provide support. Furthermore, I would also like to thank the **Swedish Research Council** (VR grant no. 2016-06014) and the **Swedish National Infrastructure for Computing** (SNIC) for providing financial assistance and computational resources, respectively, during my Ph.D.

My supervisor, **Prof. Rajeev Ahuja**, played a pivotal role in guiding me through this journey. He not only acquainted me with the theoretical nitty-gritty of materials science, but also exposed me to novel computational techniques for dealing with it. **Prof. Yogendra Kumar Mishra**, whose unparalleled knowledge of nanoscience provided a sure footing in this new domain and who served as a hub for scientific debate, philosophical musings, shared and introduced the nanobiotechnology field, provided prompt assistance whenever it was required, and whose insightful and critical comments led to lively discussions about every aspect of my work, has my deepest gratitude. Without his meticulous scrutiny, scientific direction, and assistance, I couldn't have completed this scientific endeavor. To **Dr. Anton Grigoriev**, who has helped me understand the concept of DFT. I owe a significant portion of my acknowledgment to **Prof. Johan Frostegård**, who introduced me to the fantastic world of clinical research. You have always believed in me to pursue my ideas in terms of research and also towards entrepreneurial activities. I am immensely grateful to **Prof. Zhong Lin Wang, Prof. Deepak Shukla, Prof. Klaus Leifer, Prof. Ajeet Kaushik, Prof. Rodney Ruoff, Prof. Marcin Wlodarski, Prof. Mrutyunjay Suar, Dr. Sushree Sahoo, Dr. Ravi Prakash, Dr. Wei Luo**, who helped to frame innovative ideas which has resulted in high impact publications and sharing their critical feedback and finding time for numerous discussions on research works. I am indebted to **Dr. Bikash Ranjan Sahoo** for brainstorming discussions and who has enriched me with his scientific views, and experiences that resulted in impactful research outcomes.

I would like to extend my heartfelt gratitude to my mentors, colleagues and friends for their guidance and support throughout my Ph.D. journey. Their wisdom and experience have been invaluable in shaping my skills and helping me grow both professionally and personally. I am truly grateful to **Dr. Suresh K. Verma** for the time you took to mentor me and for always being there to offer a listening ear and sage advice. Your encouragement and belief in me have given me the confidence to pursue my goals and dreams. Your impact on my life will never be forgotten. **Dr. Deobrat Singh and Dr. Nisha Singh**, who has been a constant inspiration and guided me throughout my Ph.D., thank you so much for being always there for me whenever needed. Special thanks to **Dr. Vivekananda Shukla** who has helped me in deciphering the electronic transport code. I would also like to thank my office/corridor mates and friends **Dr. Syeda Rabab Naqvi, Dr. Amitava Banerjee, Dr. Nabil Khossossi, Dr. Xiaoyong Yang, Dr. XiaoFeng Zhao, Dr. Mateus Kohler** for always cooperating with me, sharing knowledge with me, and making my time memorable at Uppsala University. **Dr. Pushpamita Panigrahi**, thanks for positive outlook, inspiration, continuous support and for providing critical feedback on my publications. I owe a debt of gratitude to my exceptional

friends **Mr. Abhay Patil, Dr. Ronak Shah, and Mr. Naman Ashar** for the stress-busting discussions and words of support they have given me.

Dr. Shailesh Kumar Samal has been a constant source of encouragement to me as a result of his remarkable communication abilities; I owe him a great debt of gratitude for our many late-night conversations, business endeavors, grant and patent proposals, and publications. In both my professional and personal life, I am lucky to have a colleague who is always there for me.

I want to express my deepest appreciation to **Dr. Nishant Saini** for always being there for me, offering amazing recipes and meals with unlimited gossips and late-night discussions. Grateful to be a part of small Odia family here in Sweden; **Smt. Punya Pallabi Mishra, Dr. Smruti Ranjan Panigrahi, Dr. Narendra Padhan, Dr. Sujata Bhoi, Mr. Mruganka Bedbak, Mrs. Swagatika Panigrahi, Mr. Himanshu Nayak, Mrs. Priyanka Priyadarshini, Dr. Sulena Pradhan, and Dr. Kalicharan Patra**. I am happy to have such people in my life.

I take this opportunity to express my sincerest gratitude for all the love and support my mother **Smt. Minakhi Tripathy** have given me throughout my life. Your unwavering encouragement has been a source of strength and motivation for me. You have been a constant source of comfort and inspiration, and I am grateful for all the sacrifices you have made for me. Your kindness, generosity, and understanding have no bounds, and I am honored to have you in my life. Your selflessness, devotion, and care have been instrumental in shaping who I am today. Your love has been a guiding light, and I will always cherish it.

I want to take a moment to express my heartfelt gratitude to my wife **Mrs. Suman Mishra**. Your unwavering love, support, and encouragement have been a source of strength and comfort for me. I am grateful for the way you have stood by my side, through thick and thin, and for always being there for me. Your kindness, patience, and understanding have been a shining light in my life, and I am so lucky to have you as my wife. I am in awe of your strength, determination, and resilience, and I admire the way you always put others before yourself. Your selflessness and devotion inspire me to be a better person, and I am grateful for all the sacrifices you have made for me and our family. I am thankful for the love and laughter we share, and for all the precious memories we have created together. You are my rock, my partner, and my best friend, and I am so grateful for you. I love you more than words can express, and I promise to always be here for you, to support you, and to cherish you, for as long as I live.

To all my family members, my late grandmother Smt. **Priyambada Tripathy, Shri. Lalit K. Tripathy, Smt. Purabi Tripathy, Shri. Shyam Sundar Mishra, Smt. Sanhita Das, Mrs. Supriya Mishra, Mr. Mayank Dwivedi, Mr. Prabhudutta Mishra, Mr. Samay Chakra Pradhan, Ms. Subhashree Pradhan**; thank you for your love, support, and guidance. I am grateful for each and every one of you and for the unique role you play in my life. I am blessed to have such an amazing family, and I will always strive to make you proud. Since everyone in my life has played some role in my success, and earning my Ph.D., I could go on forever naming my gratitude, but there just isn't enough room. All of you have my undying appreciation.

Lastly, I want to thank **me** for believing in me, doing all this hard work and for never quitting.

Pritam Kumar Panda
Uppsala
March 2023.

Bibliography

[1] P. K. Panda, A. Grigoriev, Y. K. Mishra, and R. Ahuja, "Progress in supercapacitors: Roles of two dimensional nanotubular materials," *Nanoscale Adv*, vol. 2, no. 1, 2020, doi: 10.1039/c9na00307j.

[2] R. Yuksel *et al.*, "Necklace-like Nitrogen-Doped Tubular Carbon 3D Frameworks for Electrochemical Energy Storage," *Adv Funct Mater*, vol. 30, no. 10, 2020, doi: 10.1002/adfm.201909725.

[3] X. Zhao *et al.*, "Strain-Engineered Metal-Free h-B<inf>2</inf>O Monolayer as a Mechanocatalyst for Photocatalysis and Improved Hydrogen Evolution Reaction," *Journal of Physical Chemistry C*, vol. 124, no. 14, 2020, doi: 10.1021/acs.jpcc.0c00834.

[4] D. Singh, P. K. Panda, N. Khossossi, Y. K. Mishra, A. Ainane, and R. Ahuja, "Impact of edge structures on interfacial interactions and efficient visible-light photocatalytic activity of metal-semiconductor hybrid 2D materials," *Catal Sci Technol*, vol. 10, no. 10, 2020, doi: 10.1039/d0cy00420k.

[5] S. Gahlot *et al.*, "Molecules versus Nanoparticles: Identifying a Reactive Molecular Intermediate in the Synthesis of Ternary Coinage Metal Chalcogenides," *Inorg Chem*, vol. 59, no. 11, 2020, doi: 10.1021/acs.inorgchem.0c00758.

[6] P. K. Panda *et al.*, "Structure-based drug designing and immunoinformatics approach for SARS-CoV-2," *Sci Adv*, vol. 6, no. 28, 2020, doi: 10.1126/sciadv.abb8097.

[7] N. Khossossi *et al.*, "Rational Design of 2D h-BAs Monolayer as Advanced Sulfur Host for High Energy Density Li-S Batteries," *ACS Appl Energy Mater*, vol. 3, no. 8, 2020, doi: 10.1021/acsaem.0c00492.

[8] N. Khossossi *et al.*, "Hydrogen storage characteristics of Li and Na decorated 2D boron phosphide," *Sustain Energy Fuels*, vol. 4, no. 9, 2020, doi: 10.1039/d0se00709a.

[9] R. Kumar *et al.*, "Core-shell nanostructures: perspectives towards drug delivery applications," *J Mater Chem B*, vol. 8, no. 39, 2020, doi: 10.1039/d0tb01559h.

[10] S. K. Verma *et al.*, "Determining factors for the nano-biocompatibility of cobalt oxide nanoparticles: proximal discrepancy in intrinsic atomic interactions at differential vicinage," *Green Chemistry*, vol. 23, no. 9, 2021, doi: 10.1039/d1gc00571e.

[11] B. R. Sahoo, P. K. Panda, W. Liang, W.-J. Tang, R. Ahuja, and A. Ramamoorthy, "Degradation of Alzheimer's Amyloid-β by a Catalytically Inactive Insulin-Degrading Enzyme," *J Mol Biol*, vol. 433, no. 13, 2021, doi: 10.1016/j.jmb.2021.166993.

[12] S. S. Sahoo *et al.*, "Clinical evolution, genetic landscape and trajectories of clonal hematopoiesis in SAMD9/SAMD9L syndromes," *Nat Med*, vol. 27, no. 10, 2021, doi: 10.1038/s41591-021-01511-6.

[13] P. K. Panda, S. K. Verma, and M. Suar, "Nanoparticle-biological interactions: The renaissance of bionomics in the myriad nanomedical technologies," *Nanomedicine*, vol. 16, no. 25, 2021, doi: 10.2217/nnm-2021-0174.

[14] S. K. Samal *et al.*, "Antibodies Against Phosphorylcholine Among 60-Year-Olds: Clinical Role and Simulated Interactions," *Front Cardiovasc Med*, vol. 9, 2022, doi: 10.3389/fcvm.2022.809007.

[15] N. R. Alluri *et al.*, "Crystallinity modulation originates ferroelectricity like nature in piezoelectric selenium," *Nano Energy*, vol. 95, 2022, doi: 10.1016/j.nanoen.2022.107008.

[16] S. Gupta, P. K. Panda, W. Luo, R. F. Hashimoto, and R. Ahuja, "Network Analysis Reveals Tumor Suppressor lncRNA GAS5 Acts as a Double-edged Sword in Gastric Cancer," *ResearchSquare*. 2022. doi: 10.21203/rs.3.rs-1599866.

[17] O. Sher *et al.*, "Analysis of molecular ligand functionalization process in nano-molecular electronic devices containing densely packed nano-particle functionalization shells," *Nanotechnology*, vol. 33, no. 25, 2022, doi: 10.1088/1361-6528/ac5cfc.

[18] H. Liu *et al.*, "Investigation of Nd^{3+} incorporation in Ce-rhabdophane: Insight from structural flexibility and occupation mechanism," *Journal of the American Ceramic Society*, vol. 105, no. 7, 2022, doi: 10.1111/jace.18438.

[19] S. Gupta *et al.*, "Dynamical modeling of miR-34a, miR-449a, and miR-16 reveals numerous DDR signaling pathways regulating senescence, autophagy, and apoptosis in HeLa cells," *Sci Rep*, vol. 12, no. 1, 2022, doi: 10.1038/s41598-022-08900-y.

[20] R. K. Suryawanshi *et al.*, "Putative targeting by BX795 causes decrease in protein kinase C protein levels and inhibition of HSV1 infection," *Antiviral Res*, vol. 208, 2022, doi: 10.1016/j.antiviral.2022.105454.

[21] S. Gupta, P. K. Panda, W. Luo, R. F. Hashimoto, and R. Ahuja, "Network analysis reveals that the tumor suppressor lncRNA GAS5 acts as a double-edged sword in response to DNA damage in gastric cancer," *Sci Rep*, vol. 12, no. 1, 2022, doi: 10.1038/s41598-022-21492-x.

[22] H. Y. Alniss *et al.*, "Investigation of the factors that dictate the preferred orientation of lexitropsins in the minor groove of DNA," *J Med Chem*, 2019, doi: 10.1021/acs.jmedchem.9b01534.

[23] E. Jha *et al.*, "Intrinsic atomic interaction at molecular proximal vicinity infer cellular biocompatibility of antibacterial nanopepper," *Nanomedicine*, vol. 16, no. 4, 2021, doi: 10.2217/nnm-2020-0395.

[24] R. Ahuja, "Front Matter," in *Next-Generation Materials for Batteries*, AIP Publishing, 2021, pp. i–xx. doi: 10.1063/9780735421684_frontmatter.

[25] F. Mazzocchi, "Scientific research across and beyond disciplines," *EMBO Rep*, vol. 20, no. 6, Jun. 2019, doi: 10.15252/embr.201947682.

[26] R. W. Barker, "Is precision medicine the future of healthcare?," *Per Med*, vol. 14, no. 6, pp. 459–461, Nov. 2017, doi: 10.2217/pme-2017-0060.

[27] R. P. Feynman, "There's Plenty of Room at the Bottom, Engineering and Science 23," 1960.

[28] T. Ohshiro, "Nanodevices for Biological and Medical Applications: Development of Single-Molecule Electrical Measurement Method," *Applied Sciences*, vol. 12, no. 3, p. 1539, Jan. 2022, doi: 10.3390/app12031539.

[29] Z. L. Wang and A. C. Wang, "On the origin of contact-electrification," *Materials Today*, vol. 30, pp. 34–51, Nov. 2019, doi: 10.1016/j.mattod.2019.05.016.

[30] C. Filippi, D. J. Singh, and C. J. Umrigar, “All-electron local-density and generalized-gradient calculations of the structural properties of semiconductors,” *Phys. Rev.*, vol. 50, no. 20, p. 14947, 1994, doi: 10.1103/physrevb.50.14947.
[31] G. B. Bachelet and M. Schlüter, “Relativistic norm-conserving pseudopotentials,” *Phys. Rev.*, vol. 25, no. 4, p. 2103, 1982, doi: 10.1103/physrevb.25.2103.
[32] G. Lippert, J. Hutter, P. Ballone, and M. Parrinello, “Response Function Basis Sets: Application to Density Functional Calculations,” *J. Phys. Chem.*, vol. 100, no. 15, p. 6231, 1996, doi: 10.1021/jp9527766.
[33] D. Vanderbilt, “Soft self-consistent pseudopotentials in a generalized eigenvalue formalism,” *Phys. Rev.*, vol. 41, no. 11, p. 7892, 1990, doi: 10.1103/physrevb.41.7892.
[34] W. Kohn, “Analytic properties of Bloch waves and Wannier functions,” *Phys. Rev.*, vol. 115, no. 4, p. 809, 1959, doi: 10.1103/physrev.115.809.
[35] N. Troullier and J. L. Martins, “Efficient pseudopotentials for plane-wave calculations,” *Phys. Rev.*, vol. 43, no. 3, p. 1993, 1991, doi: 10.1103/physrevb.43.1993.
[36] K. Yabana and G. Bertsch, “Time-dependent local-density approximation in real time,” *Phys. Rev.*, vol. 54, no. 7, p. 4484, 1996, doi: 10.1103/physrevb.54.4484.
[37] G. Makov and M. C. Payne, “Periodic boundary conditions in ab initio calculations,” *Phys. Rev.*, vol. 51, no. 7, p. 4014, 1995, doi: 10.1103/physrevb.51.4014.
[38] L. Kleinman, “Relativistic norm-conserving pseudopotential,” *Phys. Rev.*, vol. 21, no. 6, p. 2630, 1980, doi: 10.1103/physrevb.21.2630.
[39] “The SIESTA method for ab initio order-N materials simulation - IOPscience.” https://iopscience.iop.org/article/10.1088/0953-8984/14/11/302 (accessed Feb. 06, 2023).
[40] P. E. Blöchl, “Generalized separable potentials for electronic-structure calculations,” *Phys. Rev.*, vol. 41, no. 8, p. 5414, 1990, doi: 10.1103/physrevb.41.5414.
[41] L. Kleinman and D. M. Bylander, “Efficacious form for model pseudopotentials,” *Phys. Rev. Lett.*, vol. 48, no. 20, p. 1425, 1982, doi: 10.1103/physrevlett.48.1425.
[42] J. P. Perdew, K. Burke, and M. Ernzerhof, “Generalized gradient approximation made simple,” *Phys. Rev. Lett.*, vol. 77, no. 18, p. 3865, 1996, doi: 10.1103/physrevlett.77.3865.
[43] G. B. Bachelet, D. R. Hamann, and M. Schl̈ter, “Pseudopotentials that work: From H to Pu,” *Phys. Rev.*, vol. 26, no. 8, p. 4199, 1982, doi: 10.1103/physrevb.26.4199.
[44] D. Vanderbilt, “Optimally smooth norm-conserving pseudopotentials,” *Phys. Rev.*, vol. 32, no. 12, p. 8412, 1985, doi: 10.1103/physrevb.32.8412.
[45] N. Ramer and A. Rappe, “Designed nonlocal pseudopotentials for enhanced transferability,” *Phys. Rev.*, vol. 59, no. 19, p. 12471, 1999, doi: 10.1103/physrevb.59.12471.
[46] P. Ordejón, E. Artacho, and J. M. Soler, “Self-consistent order density-functional calculations for very large systems,” *Phys. Rev.*, vol. 53, no. 16, p. R10441, 1996, doi: 10.1103/physrevb.53.r10441.
[47] P. Pulay, “Improved SCF convergence acceleration,” *J. Comput. Chem.*, vol. 3, no. 4, p. 556, 1982, doi: 10.1002/jcc.540030413.

[48] J. P. Perdew and A. Zunger, “Self-interaction correction to density-functional approximations for many-electron systems,” *Phys. Rev.*, vol. 23, no. 10, p. 5048, 1981, doi: 10.1103/physrevb.23.5048.
[49] S. G. Louie, S. Froyen, and M. L. Cohen, “Nonlinear ionic pseudopotentials in spin-density-functional calculations,” *Phys. Rev.*, vol. 26, no. 4, p. 1738, 1982, doi: 10.1103/physrevb.26.1738.
[50] E. Hernández and M. J. Gillan, “Self-consistent first-principles technique with linear scaling,” *Phys. Rev.*, vol. 51, no. 15, p. 10157, 1995, doi: 10.1103/physrevb.51.10157.
[51] W. Kohn and L. J. Sham, “Self-consistent equations including exchange and correlation effects,” *Phys. Rev.*, vol. 140, no. 4A, p. A1133, 1965, doi: 10.1103/physrev.140.a1133.
[52] P. Ordejon, D. A. Drabold, M. P. Grumbach, and R. M. Martin, “Unconstrained minimization approach for electronic computations that scales linearly with system size,” *Phys. Rev.*, vol. 48, no. 19, p. 14646, 1993, doi: 10.1103/physrevb.48.14646.
[53] D. R. Hamann, M. Schlüter, and C. Chiang, “Norm-Conserving Pseudopotentials,” *Phys. Rev. Lett.*, vol. 43, no. 20, p. 1494, 1979, doi: 10.1103/physrevlett.43.1494.
[54] L. Greengard, “Fast algorithms for classical physics,” *Science (1979)*, vol. 265, no. 5174, p. 909, 1994, doi: 10.1126/science.265.5174.909.
[55] S. Goedecker, “Linear scaling electronic structure methods,” *Rev. Mod. Phys.*, vol. 71, no. 4, p. 1085, 1999, doi: 10.1103/revmodphys.71.1085.
[56] K. Priskila Rahael *et al.*, “The SIESTA method for ab initio order-N materials simulation,” *Journal of Physics: Condensed Matter*, vol. 14, no. 11, p. 2745, Mar. 2002, doi: 10.1088/0953-8984/14/11/302.
[57] O. F. Sankey and D. J. Niklewski, “Ab initio multicenter tight-binding model for molecular-dynamics simulations and other applications in covalent systems,” *Phys. Rev.*, vol. 40, no. 6, p. 3979, 1989, doi: 10.1103/physrevb.40.3979.
[58] R. Car and M. Parrinello, “Unified approach for molecular dynamics and density-functional theory,” *Phys. Rev. Lett.*, vol. 55, no. 22, p. 2471, 1985, doi: 10.1103/physrevlett.55.2471.
[59] E. M. Godfrin, “A method to compute the inverse of an n-block tridiagonal quasi-Hermitian matrix,” *Journal of Physics: Condensed Matter*, vol. 3, no. 40, pp. 7843–7848, 1991, doi: 10.1088/0953-8984/3/40/005.
[60] J. Hafner and G. Kresse, “The Vienna AB-Initio Simulation Program VASP: An Efficient and Versatile Tool for Studying the Structural, Dynamic, and Electronic Properties of Materials,” *Properties of Complex Inorganic Solids*, pp. 69–82, 1997, doi: 10.1007/978-1-4615-5943-6_10.
[61] N. Papior, N. Lorente, T. Frederiksen, A. García, and M. Brandbyge, “Improvements on non-equilibrium and transport Green function techniques: The next-generation transiesta,” *Comput Phys Commun*, vol. 212, pp. 8–24, Mar. 2017, doi: 10.1016/J.CPC.2016.09.022.
[62] R. Li *et al.*, “A corrected NEGF + DFT approach for calculating electronic transport through molecular devices: Filling bound states and patching the non-equilibrium integration,” *Chem Phys*, vol. 336, no. 2–3, pp. 127–135, Jul. 2007, doi: 10.1016/j.chemphys.2007.06.011.
[63] G. M. Morris *et al.*, “AutoDock4 and AutoDockTools4: Automated docking with selective receptor flexibility,” *J Comput Chem*, vol. 30, no. 16, pp. 2785–2791, Dec. 2009, doi: 10.1002/jcc.21256.

[64] J. Eberhardt, D. Santos-Martins, A. F. Tillack, and S. Forli, “AutoDock Vina 1.2.0: New Docking Methods, Expanded Force Field, and Python Bindings,” *J Chem Inf Model*, vol. 61, no. 8, pp. 3891–3898, Aug. 2021, doi: 10.1021/acs.jcim.1c00203.

[65] O. Trott and A. J. Olson, “AutoDock Vina: Improving the speed and accuracy of docking with a new scoring function, efficient optimization, and multithreading,” *J Comput Chem*, p. NA-NA, 2009, doi: 10.1002/jcc.21334.

[66] S. Cosconati, S. Forli, A. L. Perryman, R. Harris, D. S. Goodsell, and A. J. Olson, “Virtual screening with AutoDock: theory and practice,” *Expert Opin Drug Discov*, vol. 5, no. 6, pp. 597–607, Jun. 2010, doi: 10.1517/17460441.2010.484460.

[67] P. Bauer, B. Hess, and E. Lindahl, “GROMACS 2022.5 Manual,” Feb. 2023, doi: 10.5281/ZENODO.7586765.

[68] D. van der Spoel, E. Lindahl, B. Hess, G. Groenhof, A. E. Mark, and H. J. C. Berendsen, “GROMACS: fast, flexible, and free,” *J Comput Chem*, vol. 26, no. 16, pp. 1701–1718, Dec. 2005, doi: 10.1002/JCC.20291.

[69] H. J. C. Berendsen, D. van der Spoel, and R. van Drunen, “GROMACS: A message-passing parallel molecular dynamics implementation,” *Comput Phys Commun*, vol. 91, no. 1–3, pp. 43–56, Sep. 1995, doi: 10.1016/0010-4655(95)00042-E.

[70] E. Lindahl, B. Hess, and D. van der Spoel, “GROMACS 3.0: A package for molecular simulation and trajectory analysis,” *J Mol Model*, vol. 7, no. 8, pp. 306–317, 2001, doi: 10.1007/S008940100045/METRICS.

[71] M. J. Abraham *et al.*, “GROMACS: High performance molecular simulations through multi-level parallelism from laptops to supercomputers,” *SoftwareX*, vol. 1–2, pp. 19–25, Sep. 2015, doi: 10.1016/J.SOFTX.2015.06.001.

[72] A. P. Thompson *et al.*, “LAMMPS - a flexible simulation tool for particle-based materials modeling at the atomic, meso, and continuum scales,” *Comput Phys Commun*, vol. 271, p. 108171, Feb. 2022, doi: 10.1016/J.CPC.2021.108171.

[73] J. Jumper *et al.*, “Highly accurate protein structure prediction with AlphaFold,” *Nature 2021 596:7873*, vol. 596, no. 7873, pp. 583–589, Jul. 2021, doi: 10.1038/s41586-021-03819-2.

[74] E. F. Pettersen *et al.*, “UCSF ChimeraX: Structure visualization for researchers, educators, and developers,” *Protein Sci*, vol. 30, no. 1, pp. 70–82, Jan. 2021, doi: 10.1002/PRO.3943.

[75] A. Dhar, “Heat transport in low-dimensional systems,” *Adv Phys*, vol. 57, no. 5, pp. 457–537, Sep. 2008, doi: 10.1080/00018730802538522.

[76] J. S. Wang, J. Wang, and J. T. Lü, “Quantum thermal transport in nanostructures,” *European Physical Journal B*, vol. 62, no. 4, pp. 381–404, Apr. 2008, doi: 10.1140/EPJB/E2008-00195-8.

[77] J. Taylor, H. Guo, and J. Wang, “Ab initio modeling of quantum transport properties of molecular electronic devices,” *Phys Rev B Condens Matter Mater Phys*, vol. 63, no. 24, 2001, doi: 10.1103/PHYSREVB.63.245407.

[78] B. Feldman, T. Seideman, O. Hod, and L. Kronik, “Real-space method for highly parallelizable electronic transport calculations,” *Phys Rev B Condens Matter Mater Phys*, vol. 90, no. 3, Jul. 2014, doi: 10.1103/PHYSREVB.90.035445.

[79] M. Otani and O. Sugino, “First-principles calculations of charged surfaces and interfaces: A plane-wave nonrepeated slab approach,” *Phys Rev B Condens Matter Mater Phys*, vol. 73, no. 11, 2006, doi: 10.1103/PHYSREVB.73.115407.

[80] O. Hod, J. E. Peralta, and G. E. Scuseria, “First-principles electronic transport calculations in finite elongated systems: A divide and conquer approach,” *Journal of Chemical Physics*, vol. 125, no. 11, 2006, doi: 10.1063/1.2349482.

[81] K. K. Saha, W. Lu, J. Bernholc, and V. Meunier, “First-principles methodology for quantum transport in multiterminal junctions,” *Journal of Chemical Physics*, vol. 131, no. 16, 2009, doi: 10.1063/1.3247880.

[82] A. Pecchia, G. Penazzi, L. Salvucci, and A. di Carlo, “Non-equilibrium Green’s functions in density functional tight binding: Method and applications,” *New J Phys*, vol. 10, Jun. 2008, doi: 10.1088/1367-2630/10/6/065022.

[83] M. di Ventra and T. N. Todorov, “Transport in nanoscale systems: The microcanonical versus grand-canonical picture,” *Journal of Physics Condensed Matter*, vol. 16, no. 45, pp. 8025–8034, Nov. 2004, doi: 10.1088/0953-8984/16/45/024.

[84] T. Ozaki, K. Nishio, and H. Kino, “Efficient implementation of the nonequilibrium Green function method for electronic transport calculations,” *Phys Rev B Condens Matter Mater Phys*, vol. 81, no. 3, Jan. 2010, doi: 10.1103/PHYSREVB.81.035116.

[85] P. Schmitteckert and F. Evers, “Exact ground state density-functional theory for impurity models coupled to external reservoirs and transport calculations,” *Phys Rev Lett*, vol. 100, no. 8, Feb. 2008, doi: 10.1103/PHYSREVLETT.100.086401.

[86] A. M. Bratkovsky and C. J. Lambert, “General green’s-function formalism for transport calculations with (formula presented) hamiltonians and giant magnetoresistance in co- and ni-based magnetic multilayers,” *Phys Rev B Condens Matter Mater Phys*, vol. 59, no. 18, pp. 11936–11948, 1999, doi: 10.1103/PHYSREVB.59.11936.

[87] G. Thorgilsson, G. Viktorsson, and S. I. Erlingsson, “Recursive Green’s function method for multi-terminal nanostructures,” *J Comput Phys*, vol. 261, pp. 256–266, Mar. 2014, doi: 10.1016/J.JCP.2013.12.054.

[88] M. Brandbyge, J. L. Mozos, P. Ordejón, J. Taylor, and K. Stokbro, “Density-functional method for nonequilibrium electron transport,” *Phys Rev B Condens Matter Mater Phys*, vol. 65, no. 16, pp. 1654011–16540117, Apr. 2002, doi: 10.1103/PHYSREVB.65.165401.

[89] H. Ness and L. K. Dash, “Many-body current formula and current conservation for non-equilibrium fully interacting nanojunctions,” *J Phys A Math Theor*, vol. 45, no. 19, May 2012, doi: 10.1088/1751-8113/45/19/195301.

[90] F. Mirjani and J. M. Thijssen, “Density functional theory based many-body analysis of electron transport through molecules,” *Phys Rev B Condens Matter Mater Phys*, vol. 83, no. 3, Jan. 2011, doi: 10.1103/PHYSREVB.83.035415.

[91] J. M. Soler *et al.*, “The SIESTA method for ab initio order-N materials simulation,” *Journal of Physics Condensed Matter*, vol. 14, no. 11, pp. 2745–2779, Mar. 2002, doi: 10.1088/0953-8984/14/11/302.

[92] H. Takahasi and M. Mori, “Double exponential formulas for numerical integration,” *Publications of the Research Institute for Mathematical Sciences*, vol. 9, no. 3, pp. 721–741, 1974, doi: 10.2977/PRIMS/1195192451.

[93] M. B̈ttiker, Y. Imry, R. Landauer, and S. Pinhas, “Generalized many-channel conductance formula with application to small rings,” *Phys Rev B*, vol. 31, no. 10, pp. 6207–6215, 1985, doi: 10.1103/PHYSREVB.31.6207.

[94] J. Chen, K. S. Thygesen, and K. W. Jacobsen, “Ab initio nonequilibrium quantum transport and forces with the real-space projector augmented wave method,” *Phys Rev B Condens Matter Mater Phys*, vol. 85, no. 15, Apr. 2012, doi: 10.1103/PHYSREVB.85.155140.

[95] H. Mera and Y. M. Niquet, “Are Kohn-Sham conductances accurate?,” *Phys Rev Lett*, vol. 105, no. 21, Nov. 2010, doi: 10.1103/PHYSREVLETT.105.216408.
[96] G. Stefanucci and S. Kurth, “Steady-State Density Functional Theory for Finite Bias Conductances,” *Nano Lett*, vol. 15, no. 12, pp. 8020–8025, Dec. 2015, doi: 10.1021/ACS.NANOLETT.5B03294.
[97] J. T. Falkenberg and M. Brandbyge, “Simple and efficient way of speeding up transmission calculations with k-point sampling,” *Beilstein Journal of Nanotechnology*, vol. 6, no. 1, pp. 1603–1608, May 2015, doi: 10.3762/BJNANO.6.164.
[98] G. Stefanucci and C. O. Almbladh, “Time-dependent quantum transport: An exact formulation based on TDDFT,” *Europhys Lett*, vol. 67, no. 1, pp. 14–20, Jul. 2004, doi: 10.1209/EPL/I2004-10043-7.
[99] S. Kurth and G. Stefanucci, “Dynamical correction to linear kohn-sham conductances from static density functional theory,” *Phys Rev Lett*, vol. 111, no. 3, Jul. 2013, doi: 10.1103/PHYSREVLETT.111.030601.
[100] A. Garcia-Lekue and L. W. Wang, “Elastic quantum transport calculations for molecular nanodevices using plane waves,” *Phys Rev B Condens Matter Mater Phys*, vol. 74, no. 24, 2006, doi: 10.1103/PHYSREVB.74.245404.
[101] P. Delaney and J. C. Greer, “Correlated electron transport in molecular electronics,” *Phys Rev Lett*, vol. 93, no. 3, Jul. 2004, doi: 10.1103/PHYSREVLETT.93.036805.
[102] P. Sautet and C. Joachim, “Electronic transmission coefficient for the single-impurity problem in the scattering-matrix approach,” *Phys Rev B*, vol. 38, no. 17, pp. 12238–12247, 1988, doi: 10.1103/PHYSREVB.38.12238.
[103] T. Yamamoto and K. Watanabe, “Nonequilibrium green’s function approach to phonon transport in defective carbon nanotubes,” *Phys Rev Lett*, vol. 96, no. 25, 2006, doi: 10.1103/PHYSREVLETT.96.255503.
[104] D. Wortmann, H. Ishida, and S. Blügel, “Ab initio Green-function formulation of the transfer matrix: Application to complex band structures,” *Phys Rev B Condens Matter Mater Phys*, vol. 65, no. 16, pp. 1–10, 2002, doi: 10.1103/PHYSREVB.65.165103.
[105] V. M. García-Suárez and C. J. Lambert, “First-principles scheme for spectral adjustment in nanoscale transport,” *New J Phys*, vol. 13, May 2011, doi: 10.1088/1367-2630/13/5/053026.
[106] X. Zhao, P. K. Panda, D. Singh, X. Yang, Y. K. Mishra, and R. Ahuja, “2D g-C_3N_4 monolayer for amino acids sequencing,” *Appl Surf Sci*, vol. 528, p. 146609, 2020.
[107] D. Singh, P. K. Panda, Y. K. Mishra, and R. Ahuja, “Van der Waals induced molecular recognition of canonical DNA nucleobases on a 2D GaS monolayer,” *Physical Chemistry Chemical Physics*, vol. 22, no. 12, pp. 6706–6715, 2020.
[108] P. Panigrahi *et al.*, “Two-dimensional bismuthene nanosheets for selective detection of toxic gases,” *ACS Appl Nano Mater*, vol. 5, no. 2, pp. 2984–2993, 2022.
[109] D. Singh, V. Shukla, P. K. Panda, Y. K. Mishra, H.-G. Rubahn, and R. Ahuja, “Carbon-phosphide monolayer with high carrier mobility and perceptible I–V response for superior gas sensing,” *New Journal of Chemistry*, vol. 44, no. 9, pp. 3777–3785, 2020.
[110] D. B. Kitchen, H. Decornez, J. R. Furr, and J. Bajorath, “Docking and scoring in virtual screening for drug discovery: methods and applications,” *Nat Rev Drug Discov*, vol. 3, no. 11, pp. 935–949, Nov. 2004, doi: 10.1038/nrd1549.

[111] P. Tian, “Molecular dynamics simulations of nanoparticles,” *Annual Reports Section “C” (Physical Chemistry)*, vol. 104, no. 0, pp. 142–164, Jun. 2008, doi: 10.1039/B703897F.
[112] P. Tian, “Molecular dynamics simulations of nanoparticles,” *Annual Reports Section “C” (Physical Chemistry)*, vol. 104, no. 0, pp. 142–164, Jun. 2008, doi: 10.1039/B703897F.
[113] A. W. Schüttelkopf and D. M. F. van Aalten, “PRODRG: a tool for high-throughput crystallography of protein-ligand complexes,” *Acta Crystallogr D Biol Crystallogr*, vol. 60, no. Pt 8, pp. 1355–1363, Aug. 2004, doi: 10.1107/S0907444904011679.
[114] S. Jo *et al.*, “CHARMM-GUI PDB manipulator for advanced modeling and simulations of proteins containing nonstandard residues,” *Adv Protein Chem Struct Biol*, vol. 96, pp. 235–265, 2014, doi: 10.1016/bs.apcsb.2014.06.002.
[115] N. Schmid *et al.*, “Definition and testing of the GROMOS force-field versions 54A7 and 54B7,” *Eur Biophys J*, vol. 40, no. 7, pp. 843–856, Jul. 2011, doi: 10.1007/S00249-011-0700-9.
[116] K. Vanommeslaeghe and A. D. Mackerell, “CHARMM additive and polarizable force fields for biophysics and computer-aided drug design,” *Biochim Biophys Acta Gen Subj*, vol. 1850, no. 5, pp. 861–871, 2015, doi: 10.1016/j.bbagen.2014.08.004.
[117] S. Plimpton, “Fast Parallel Algorithms for Short-Range Molecular Dynamics,” *J Comput Phys*, vol. 117, no. 1, pp. 1–19, Mar. 1995, doi: 10.1006/jcph.1995.1039.
[118] A. Stukowski, “Visualization and analysis of atomistic simulation data with OVITO–the Open Visualization Tool,” *Model Simul Mat Sci Eng*, vol. 18, no. 1, p. 015012, Jan. 2010, doi: 10.1088/0965-0393/18/1/015012.
[119] W. Humphrey, A. Dalke, and K. Schulten, “VMD: Visual molecular dynamics,” *J Mol Graph*, vol. 14, no. 1, pp. 33–38, Feb. 1996, doi: 10.1016/0263-7855(96)00018-5.
[120] D. S. Kleinerman, C. Czaplewski, A. Liwo, and H. A. Scheraga, “Implementations of Nosé–Hoover and Nosé–Poincaré thermostats in mesoscopic dynamic simulations with the united-residue model of a polypeptide chain,” *J Chem Phys*, vol. 128, no. 24, p. 245103, Jun. 2008, doi: 10.1063/1.2943146.
[121] S. L. Mayo, B. D. Olafson, and W. A. Goddard, “DREIDING: a generic force field for molecular simulations,” *J Phys Chem*, vol. 94, no. 26, pp. 8897–8909, Dec. 1990, doi: 10.1021/j100389a010.
[122] P. G. Boyd, S. M. Moosavi, M. Witman, and B. Smit, “Force-Field Prediction of Materials Properties in Metal-Organic Frameworks,” *J Phys Chem Lett*, vol. 8, no. 2, pp. 357–363, Jan. 2017, doi: 10.1021/acs.jpclett.6b02532.
[123] R. Iftimie, P. Minary, and M. E. Tuckerman, “Ab initio molecular dynamics: Concepts, recent developments, and future trends,” *Proc Natl Acad Sci U S A*, vol. 102, no. 19, pp. 6654–6659, May 2005, doi: 10.1073/PNAS.0500193102/SUPPL_FILE/00193FIG5.JPG.
[124] P. K. Panda, D. Singh, M. H. Köhler, D. D. de Vargas, Z. L. Wang, and R. Ahuja, “Contact electrification through interfacial charge transfer: a mechanistic viewpoint on solid–liquid interfaces,” *Nanoscale Adv*, vol. 4, no. 3, pp. 884–893, 2022.
[125] P. K. Panda *et al.*, “Molecular nanoinformatics approach assessing the biocompatibility of biogenic silver nanoparticles with channelized intrinsic steatosis and apoptosis,” *Green Chemistry*, 2021.

[126] J. Zhang, L. Mou, and X. Jiang, “Surface chemistry of gold nanoparticles for health-related applications,” *Chemical Science*. 2020. doi: 10.1039/c9sc06497d.
[127] R. K. Suryawanshi *et al.*, “Putative targeting by BX795 causes decrease in protein kinase C protein levels and inhibition of HSV1 infection,” *Antiviral Res*, vol. 208, p. 105454, Dec. 2022, doi: 10.1016/J.ANTIVIRAL.2022.105454.

Acta Universitatis Upsaliensis

Digital Comprehensive Summaries of Uppsala Dissertations from the Faculty of Science and Technology 2240

Editor: The Dean of the Faculty of Science and Technology

A doctoral dissertation from the Faculty of Science and Technology, Uppsala University, is usually a summary of a number of papers. A few copies of the complete dissertation are kept at major Swedish research libraries, while the summary alone is distributed internationally through the series Digital Comprehensive Summaries of Uppsala Dissertations from the Faculty of Science and Technology. (Prior to January, 2005, the series was published under the title "Comprehensive Summaries of Uppsala Dissertations from the Faculty of Science and Technology".)

Distribution: publications.uu.se
urn:nbn:se:uu:diva-496330

ACTA
UNIVERSITATIS
UPSALIENSIS
UPPSALA
2023